KTH Engineering Sciences

Phase transitions in novel superfluids and systems with correlated disorder

HANNES MEIER

Doctoral Thesis
Stockholm, Sweden 2015

TRITA-FYS 2015:09
ISSN 0280-316X
ISRN KTH/FYS/–15:09–SE
ISBN 978-91-7595-467-7

KTH Teoretisk fysik
AlbaNova universitetscentrum
SE-106 91 Stockholm Sweden

Akademisk avhandling som med tillstånd av Kungl Tekniska högskolan framlägges till offentlig granskning för avläggande av teknologie doktor i fysik den 27 Mars 2015 kl. 10:00 i sal FB42, AlbaNova Universitetscentrum.

© Hannes Meier, March 2015

Tryck: Universitetsservice US AB

Hannes Meier
Phase transitions in novel superfluids and systems with correlated disorder
Department of Theoretical Physics, Royal Institute of Technology (KTH)
ISBN 978-91-7595-467-7, ISSN 0280-316X, ISRN KTH/FYS/–15:09–SE

Abstract

Condensed matter systems undergoing phase transitions rarely allow exact solutions. The presence of disorder renders the situation is even worse but collective Monte Carlo methods and parallel algorithms allow numerical descriptions. This thesis considers classical phase transitions in disordered spin systems in general and in effective models of superfluids with disorder and novel interactions in particular. Quantum phase transitions are considered via a quantum to classical mapping. Central questions are if the presence of defects changes universal properties and what qualitative implications follow for experiments. Common to the cases considered is that the disorder maps out correlated structures. All results are obtained using large-scale Monte Carlo simulations of effective models capturing the relevant degrees of freedom at the transition.

Considering a model system for superflow aided by a defect network, we find that the onset properties are significantly altered compared to the λ-transition in ^{4}He. This has qualitative implications on expected experimental signatures in a defect supersolid scenario.

For the Bose glass to superfluid quantum phase transition in 2D we determine the quantum correlation time by an anisotropic finite size scaling approach. Without a priori assumptions on critical parameters, we find the critical exponent $z = 1.8 \pm 0.05$ contradicting the long standing result $z = d$.

Using a 3D effective model for multi-band type-1.5 superconductors we find that these systems possibly feature a strong first order vortex-driven phase transition. Despite its short-range nature details of the interaction are shown to play an important role.

Phase transitions in disordered spin models exposed to correlated defect structures obtained via rapid quenches of critical loop and spin models are investigated. On long length scales the correlations are shown to decay algebraically. The decay exponents are expressed through known critical exponents of the disorder generating models. For cases where the disorder correlations imply the existence of a new long-range-disorder fixed point we determine the critical exponents of the disordered systems via finite size scaling methods of Monte Carlo data and find good agreement with theoretical expectations.
keywords: condensed matter physics, phase transitions, critical phenomena, spin models, quantum phase transitions, quantum fluids, superfluidity, superconductivity, disordered systems, Bose glass, dirty bosons, vortex pinning, statistical mechanics, Monte Carlo simulation, Wolff algorithm, classical worm algorithm, Wang-Landau algorithm

Preface

The work for this thesis has been performed at the department of theoretical physics at the Royal Institute of Technology (KTH) in Stockholm. It is divided into an introductory background part and a second part featuring the scientific articles that I contributed to.

Sammanfattning

Denna avhandling studerar fasövergångar i kondenserad materia med hjälp av storskaliga datorsimuleringar. Speciellt undersöks modeller för klassiska spinnsystem och deras tillämpning på kvantvätskor. Vi definerar och använder effektiva modeller för exotiska system såsom supersolida faser, supervätskor och även för kvantfasövergånger mellan isolerande faser och supervätskefaser. De kritiska egenskaperna hos dessa system bestäms sedan genom moderna beräkningsmetoder i form av kollektiva Monte Carlo metoder. Kvalitativa implikationer för experimentellt mätbara kvantiteter ges. En central frågeställning är hur korrelationerna i oordnade system påverkar de universella egenskaperna hos fasövergången och på vilket sätt korrelationer med lång räckvidd kan genereras. Vi betraktar även hur ändringar i växelverkan i ett system av vortexlinjer påverkar fasövergångens ordning. Resultaten presenteras i fem vetenskapliga artiklar.

Artikel I syftar på att kvalitativt förklara signaturer som observerats i experiment på fast ^{4}He som ursprungligen tolkades som en övergång till ett nytt superfast tillstånd. Vi visar att om supervätskan bara transporteras på ett sammanhängande nätverk av defekter så kommer de väntade singulariteter som uppträder i supervätskeövergången i flytande ^{4}He att blir utslätade i det oordnade systemet.

I artikel II definieras en skalningskvantitet som tillåter bestämning av den dynamiska kritiska exponenten z i en exotisk kvantfasövergång mellan en isolerande Bose-glasfas och en supervärskefas genom en anisotrop skalningsansats. Utan a priori antaganden om kritiska parametrar finner vi $z = 1.8 \pm 0.05$ vilket tyder på att den teoretiska förutsägelsen $z = d$ inte gäller.

Artikel III introducerar en effektiv modell för flerkomponents typ-1.5 supraledare. I gränsen där interaktionen mellan vortexlinjerna är icke-monoton, dvs attraktiv på medellånga längdskalor och repulsiv på korta längdskalor, finner vi att modellen kan ha en stark diskontinuerlig fasövergång som drivs av vortexfluktuationer. Detta

resultat kan inte uppnås i en vanlig enkomponents Ginzburg-Landau-modell med stabila vortex excitationer. Dessa genomgår kontinuerliga övergångar. Detaljer i växelverkan verkar vara viktiga trots att denna är exponentiellt skärmad på långa avstånd.

Artikel IV och V behandlar fasövergångar i oordnade klassiska spinnmodeller där korrelerade defektstrukturer erhålls genom mappning av jämnviktskonfigurationer av kritiska loop- och spinnmodeller. Vi visar att defektkorrelationerna på långa längdskalor avtar som ett potenslag och härleder uttryck för korrelationsexponenten i termer av de kända kritiska exponenter som beskriver de loop och spinnmodeller som har använts för att skapa oordningen. I de fall där vi finner att oordningskorrelationerna avtar tillräckligt långsamt för att ge upphov till en ny oordnad fixpunkt som inte beskrivs av kända exponenter för okorrelerad oordning beräknar vi de kritiska exponenterna i det oordnade systemet via skalningsmetoder av Monte Carlo data och finner att de överensestämmer med teoretiska förväntningar.

Scientific Articles

Paper I

Superfluid Transition in a Correlated Linear Defect Network, Hannes Meier, Mats Wallin and Stephen Teitel, Physical Review B [1]

Paper II

Quantum Critical Dynamics Simulation of Dirty Boson Systems, Hannes Meier, Mats Wallin, Physical Review Letters [2].

Paper III

Fluctuation-induced first order phase transitions in type-1.5 superconductors, Physical Review B, Hannes Meier, Egor Babaev, Mats Wallin [3].

Paper IV

Phase transitions with critical loop disorder, Hannes Meier, Mats Wallin Manuscript, [4].

Paper V

Phase transitions in systems with critical cluster defects, Hannes Meier, Mats Wallin Manuscript [5].

Comments on My Contribution to the Papers

Paper I

I wrote all the simulation code, performed all data analysis, produced the figures and contributed to writing the paper.

Paper II

I wrote all the simulation code, performed the data analysis, produced the figures and contributed to writing the paper.

Paper III

I wrote all the simulation code, performed the data analysis, produced the figures and wrote a first draft of the paper.

Paper IV

I contributed with main ideas. I wrote all the simulation code, performed all analysis, produced the figures and wrote the paper. I suggested the scaling idea to determine the loop correlations via the smallest k-vector difference of the "coupling structure factor" components.

Paper V

I contributed with main ideas. I wrote all the simulation code, performed all analysis, produced the figures and wrote the first draft of the paper.

Acknowledgements

First of all, I would like to thank Mats Wallin, for offering me the opportunity to join his group as a PhD student at the Department of Theoretical Physics at KTH, triggering my interest in critical phenomena and his contributions to the articles. Sincere thanks are given to Stephen Teitel for his contributions and ideas to paperI. A big thank you also to Jack Lidmar for always keeping his door open and sharing his knowledge on Monte Carlo methods, as well as being a source of great feedback. I also want to express my gratitude towards Egor Babaev for sharing his ideas and for his contributions made during our collaboration. In particular i will miss his interesting talks given at the Alba Nova gym. I further wish to thank Edwin Langmann for answering some questions on elementary mathematics.

During my time at the department I had the pleasure to share office with a number of people. In particular Andreas, who coined the word "världsklass" and has become one of my most important guides in the cities of Stockholm, Tel-Aviv and closest friends. I want to thank Oskar, whom I have been knowing now for about four years, for his balancing influence when things got rough and for great discussions. Your presence has been very valuable. A big thank you also to Johan, for discussions covering an infinite range of topics, and for introducing me to some danish cultural heritage. Big thanks also to Richard for sharing his knowledge on structure factors and great discussions, to Linnea for discussions on music and to my newest colleague, Faezeh. It has been great to have you all around.

Deep thanks also to Erik Brandt who has been a great colleague and friend to have around despite his doubtful views on "die DFB Herren Nationalmannschaft" and his unmatched way to enforce coffee breaks. Julien Garaud is greatly acknowledged for introducing me to some great french music and for his way to explain complex subjects in a simple way. Big thanks to Farrokh for bringing some simple exactly solvable systems to my mind. Per Moosavi is acknowledged for his great musical taste.

The newly founded Stockholm branch of the Schässburger family would truly deserve a whole chapter in this thesis. But for your support i can hardly thank you enough. Kai and Marte I am incredibly happy yo have you both around.

My dear Therese, thank you for the light you bring to my life.

Finally my family, I love you.

Hannes Meier Stockholm, March , 2015

Contents

Contents **11**

I Background **1**

Introduction **3**

1 Phase Transitions **7**
1.1 Mean field theory 7
1.2 Scaling phenomenology 8
1.3 Mean field critical exponents 8
1.4 First order transitions on mean field level 10
1.5 Breakdown of mean field theory 11
1.6 Renormalization and scaling theory 11
1.7 Finite size scaling 14
1.8 Corrections to scaling 15
1.9 Above the upper critical dimension d_c 15
1.10 Quantum phase transitions 15
1.11 The $O(N)$ spin models 19
1.12 Phase transitions in the $O(N)$ models 20
1.13 Continuous global symmetry 21
1.14 Topological defects 23
1.15 Effects of disorder - Harris criterion 25
1.16 Continuous vs. discontinuous phase transitions 27

2 Superfluidity and Superconductivity **31**
2.1 Bose-Einstein condensation 31
2.2 Liquid Helium 33
2.3 Ginzburg-Landau theory of superconductivity 35
2.4 Multi component GL theory and vortex interactions 38
2.5 Supersolidity 42

3 Duality **45**
3.1 Duality transformation of the GL-model for superfluids and superconductors . . . 45
3.2 Loop representation of the Ising model . . . 49

4 Dirty Bosons **51**
4.1 The Dirty Boson Hubbard model . . . 51
4.2 Phase diagram of the pure system in the $\mu - J$ plane . . . 52
4.3 Phase diagram of the disordered system in the $\mu - J$ plane . . . 55
4.4 The equality $z = d$ . . . 56
4.5 Scaling at the Dirty Boson critical point . . . 58
4.6 Dual representation of the Josephson Lagrangian . . . 60

5 Monte Carlo Methods **63**
5.1 Classical Monte Carlo . . . 63
5.2 Warmup and convergence . . . 65
5.3 The Metropolis algorithm . . . 66
5.4 Collective updating methods . . . 67
5.5 Wang-Landau algorithm . . . 70
5.6 Replica exchange . . . 71
5.7 Replica exchange for the Wang-Landau scheme . . . 72
5.8 Reweighting methods . . . 74
5.9 Error estimation . . . 75

6 Results **77**
6.1 Paper I: Defect supersolid . . . 77
6.2 Paper II: Quantum critical dynamics in the 2D Bose glass to superfluid transition . . . 80
6.3 Paper III: Fluctuation-induced first order phase transitions in type-1.5 superconductors in zero external field . . . 82
6.4 Paper IV: Phase transitions with critical loop disorder . . . 84
6.5 Paper V: Phase transitions in systems with critical cluster defects . . . 89

7 Conclusions **93**

Bibliography **97**

II Scientific Papers **111**

Part I

Background

Introduction

This thesis focuses on transitions between different states of matter. We all are familiar with the three common states gas, liquid and solid which we encounter in everyday life. The kitchen is a good place to spot them all. Who hasn't found himself staring at the boiling water in a pasta pot and the vapor emerging from the surface. Opening the freezer one might encounter water in form of ice cubes or with a bit of luck as a wonderfully symmetric snow flake stuck to the kitchen window at a cold winter day. In all these cases one encounters a substance made up of the same molecule H_2O. So how can its properties vary so drastically?

In all these examples water is not an isolated system but embedded into a larger environment. Changes in external variables like temperature and pressure cause a substance to appear in different phases. This process of transformation is generally referred to as a *phase transition*.

Since the advent of the atomistic theory we know that matter microscopically consists of tiny building blocks called atoms. Most people are introduced to the field of physics during their high school years and maybe mostly remember it as the science subject where an attempt is made to describe the world using simple mechanical laws to predict trajectories of well defined single objects. If one were to microscopically describe all water molecules, consisting of two hydrogen and one oxygen atom, by this approach one would face a task of truly astronomical difficulty. Even a small cup filled with 1/4-liter of water contains around $8.3\times10^{24} = 8300000000000000000000000$ interacting molecules which roughly is of the same order of magnitude as the total number of stars expected to exist in the *entire universe* [6]. Even if one could describe such a system by solving Newton's laws of motion, no one could make sense of such an amount of microscopic information, let alone that the notion of temperature there is not defined.

To describe the macroscopic bulk properties of many-particle systems one therefore has to use the power of statistics. The aim is to describe the system by the average behavior reflected in observable properties such as density, magnetization, moment of inertia or conductivity under well defined external conditions. Can statistical calculations provide us with exact analytical answers? In principle, *yes*, but in practice for almost all cases, *no*. Most systems are far to complex to be studied analytically. The everyday business of a physicist therefore is to identify the important degrees of freedom expected to give rise to the properties of interest and

using symmetry arguments find a simplified *effective model* capturing the essential features. But even for most simple models as soon as one introduces interactions, again exact calculations are notoriously difficult. One thus has to apply numerical methods which using the power of modern computers, smart Monte Carlo algorithms and given enough time in principle can yield answers of arbitrary accuracy. This basically is the approach used throughout this thesis.

Here the main focus is on phases appearing under less everyday conditions, at much lower temperatures than the water example above, where the microscopic particles follow laws that seem add odds with our everyday expectation. The game changer there is *quantum mechanics*. As it turns out there are only two classes of particles called *fermions* and *bosons*. At low temperatures the microscopic constituents such as electrons and atoms even if one wanted to describe them all individually cannot be considered as independent particles but are indistinguishable.

One prime example of a low temperature state is given by the so called Bose-Einstein condensate where all bosonic atoms behave as if they where one. Like a perfectly drilled platoon, or north-korean gymnastics group. Another is found in Helium-4 (^{4}He) where at 2.17 K one observes a superfluid phase allowing it to flow with zero viscosity through tiny channels or creep up container walls. Other materials like Tin (Sn) that are rather lousy conductors at room temperature suddenly become superconductors and can carry currents without dissipation.

This thesis aims at the theoretical description of the qualitative properties of similar systems. The superfluid phase transition in ^{4}He for example exhibits the same critical behavior as the planar classical ferromagnet-paramagnet transition. This is remarkable as although the emergence of superfluidity entirely is of quantum mechanical origin the essential features of the transition can be captured by a classical system where all details of the ^{4}He interactions are reduced to classical magnetic needles sitting on the vertices of a 3D-lattice, pointing in the xy-plane and interacting only via their local magnetic moments. This usually is referred to as the 3DXY model. The surprising fact that many apparently different systems exhibit phase transitions that share similar characteristic properties lead to the classification of phase transitions in *universality classes* an idea whose theoretical origin was pioneered by Wilson [7]. Before, it had been empirically known that at the critical point of CO_2, Xe the density ρ behaves as $\rho_{\text{liquid/gas}} - \rho_c \propto (T - T_c)^\beta$ close to the critical temperature T_c on the liquid/gas side of the transition. The exponents measured are $\beta \approx 0.32-0.36$ and suspiciously close to the values obtained at the ferromagnetic paramagnetic transition in Fe, Ni and $YFeO_3$ [8, 9]. In fact these cases are examples of the 3D Ising universality class where the magnetization per spin vanishes as $m \sim |T - T_c|^{0.3265(3)}$ [10].

The spirit of identifying universality classes of simplified models is central for this thesis. Emphasis is laid on general systems with random disorder and superfluids. The research is presented in five scientific articles. Article [1] was motivated by observations made in experiments on solid ^{4}He. These showed unexpected features which were initially interpreted as a transition to a so far experimentally unob-

served superfluid-solid state, a *supersolid*. Simplified to a 3DXY model exposed to defect networks as potentially present in ^{4}He yields that such experimental signatures lacking the characteristic divergencies of the superfluid λ-transition in fact are compatible with a superfluid transition with correlated disorder. Article [2] considers the exotic case of a *quantum phase-transition* for bosons living on a two dimensional disordered substrate from a superfluid to an insulating *Bose-glass* state absent without disorder. Occurring at experimentally inaccessible temperature 0 K in two dimensions this transition can theoretically be studied by means of finite-size scaling in numerical simulations of $2+1$ dimensional classical systems. We find evidence that the relation $z = d$ of the dynamic critical exponent believed to be exact for disordered, *dirty* bosons is not obeyed.

The next paper [3] considers an effective model of a so called type-1.5 superconductor. This recently proposed state differs from ordinary superconductors which usually are classified into two types depending on how they respond to an applied magnetic field. Such a field can create vortex excitations that interact either attractively or repulsively in type-1 and type-2 materials respectively. The type 1.5 regime can occur if several superconducting components are present and coupled. Then composite vortices can be formed that under certain conditions interact via a non-monotonic potential. Simulating a 3D effective model for such a system of interacting vortex loops in zero applied field we find that in this limit the transition between the superconducting and insulating state can be different from the expected behavior of a single superconducting component with stable vortex excitations.

Articles [4] and [5] are devoted to the study of phase transitions in presence of correlated defect structures. We pursue the idea that disorder is generated from a substrate which rapidly was frozen from a critical point. Using our knowledge about this critical point we find exact expressions for the decay exponent of the disorder correlations. Our finite-size scaling analysis of Monte Carlo simulation data confirms predictions about the expected correlation length critical exponent to be found in disordered spin systems.

The remainder of this thesis is organized as follows. Chapter 1 introduces the formalism in which critical phenomena are typically studied, motivates the origin of universality and the mapping of quantum phase transitions in d-dimensional quantum systems on $(d+1)$-dimensional classical ones. It further presents the most common classical spin models that are usually exploited to effectively model much more complex systems sharing the same symmetry, the $O(N)$ spin models. Chapter 2 introduces the basic properties of superfluids and superconductors and connects them to the theoretical framework of 1. Chapter 3 shows how superfluids and type-2 superconductors can be mapped on models of interacting vortex lines via a duality transformation. A similar mapping of the Ising systems used in [4] is also presented. Chapter 4 introduces the dirty boson model studied in [2]. Chapter 5 introduces the Monte Carlo methods used in the articles. A summary of the results obtained in each article is presented in chapter 6.

Chapter 1

Phase Transitions

This chapter introduces elementary theoretical concepts used to study phase transitions. Starting from a brief overview on the milestone concept of *Landau theory* and its mean field treatment of second order phase transitions, reasons for its breakdown are discussed. This leads to the concept of the *renormalization group* and *finite-size scaling* of critical phenomena. Further the mapping of a quantum phase transition in d-dimensions on a classical phase transition in $d+1$-dimensions is discussed.

1.1 Mean field theory

At a phase transition upon varying some external set of parameters $\{g\}$ such as temperature T, pressure P, magnetic field H, a system appears in different phases on either side of the transition. Cooling a magnet through the Curie temperature the magnetization m becomes finite and points along a fixed direction. Usually the Hamiltonian of a system is symmetric under the application of some transformation group on its degrees of freedom eg. global inversion or rotation. Below the critical temperature this symmetry is therefore reduced or broken. One of the oldest attempts to theoretically study phase transitions is *Landau theory* [11]. Identifying a symmetry in the underlying Hamiltonian of the system an order parameter field $\Psi(\boldsymbol{r})$ is defined. First intended for continuous transition the general existence of a Landau free energy functional $\mathcal{L}[\Psi]$ specifying the phase by its absolute minimum with respect to the order parameter field configuration Ψ was postulated. On general grounds $\mathcal{L}$ shall only reflect the symmetries of the system under consideration and is assumed to be analytic in Ψ and $\{g\}$. The most simple and widely used model for classical thermal phase transitions is the Ψ^4-functional

$$\int d^d r \mathcal{L}\left[\Psi(\boldsymbol{r}), \mathbf{h}(\boldsymbol{r})\right] = \int d^d r \left[c\left|\nabla\Psi(\boldsymbol{r})\right|^2 + \alpha(T)\left|\Psi(\boldsymbol{r})\right|^2 + \frac{b}{2}\left|\Psi(\boldsymbol{r})\right|^4 - \mathbf{h}(\boldsymbol{r})\Psi(\boldsymbol{r})\right] \tag{1.1}$$

where $\alpha(T) = \alpha_0 (T - T_{\mathrm{c,MF}}) / T_{\mathrm{c,MF}} = \alpha_0 t$ changes from negative to positive upon increasing the temperature through the MF transition temperature $T_{\mathrm{c,MF}}$ and $\mathbf{h}$ is an external ordering field coupling to $\Psi(\boldsymbol{r})$. Although the form above originates in the ferromagnetic models where $\Psi(\boldsymbol{r}) = m(\boldsymbol{r})$ can be thought of as the local magnetization it is easily generalized to describe a large variety of phase transitions in superfluids, superconductors and other systems.

1.2 Scaling phenomenology

Empirically at continuous transitions response quantities such as the specific heat c_s or the order parameter susceptibility χ as well as the onset of the order parameter m scale as power laws in the distance to criticality $t = (T - T_{\mathrm{c}}) / T_{\mathrm{c}}$. Remarkably the set of *critical exponents* $\alpha, \beta, \gamma, \delta, \nu, \eta$ defined via

$$c_s \sim |t|^{-\alpha} \tag{1.2}$$

$$|\Psi(\boldsymbol{r})| \sim (-t)^{\beta} \tag{1.3}$$

$$\chi(t) = \left.\frac{\partial \Psi}{\partial h}\right|_{h=0} \sim |t|^{-\gamma} \tag{1.4}$$

$$|\Psi|(h)|_{t=0} \sim |h|^{1/\delta} \tag{1.5}$$

was found to agree for many systems without any obvious connection. Further the two-point correlation function has the characteristic behavior

$$G(r) = \langle \Psi(\boldsymbol{r}) \Psi(\boldsymbol{r}') \rangle - \langle \Psi(\boldsymbol{r}) \rangle \langle \Psi(\boldsymbol{r}') \rangle \sim \frac{1}{r^{d-2+\eta}} e^{-r/\xi} \tag{1.6}$$

where ξ is the correlation length, $r = |\boldsymbol{r} - \boldsymbol{r}'|$ and $\langle \ldots \rangle$ denotes ensemble averaging. If it is finite then all correlations decay exponentially fast. At a continuous phase transition ξ is found to diverge as $\xi \sim |t|^{-\nu}$ [1]. Then all correlations become long-ranged and decay algebraically $G(r) \sim r^{d-2+\eta}$. Similarly the correlation time τ diverges as $\tau \sim \xi^z = |t|^{-\nu z}$.

1.3 Mean field critical exponents

Does the Landau-functional Eq. (1.1) correctly predict these particular experimentally verifiable features at the phase transition? The central quantity in statistical mechanics is the partition function

$$Z[h(\boldsymbol{r})] = \mathrm{tr}_{\Psi(\boldsymbol{r})} \left\{ e^{-\beta \int d^d r \mathcal{L}[\Psi(\boldsymbol{r}), \mathbf{h}(\boldsymbol{r})]} \right\} \tag{1.7}$$

[1] A notable exception is the Berezinskii-Kosterlitz-Thouless phase transition [12, 13] with an essential divergence $\xi \sim e^{a/\sqrt{T - T_{\mathrm{c}}}}$ which means that $\log \xi \sim t^{-1/2}$ and effectively corresponds to $\nu \approx \infty$

from which the free energy can be obtained via

$$F = -\beta^{-1} \log [Z] \tag{1.8}$$

with $\beta = 1/k_B T$. Under the assumption behind the postulate to identify Eq. (1.1) as the free energy lies that fluctuations away from the homogenous solution minimizing $\mathcal{L}$ can be ignored. In zero field the order parameter then takes the homogeneous value

$$\psi(r) = \Psi_0 = \pm \left(\frac{-\alpha_0 t}{b} \right)^{1/2} \tag{1.9}$$

below $T_{\mathrm{c,MF}}$ and $\Psi = 0$ above. The specific heat below $T_{\mathrm{c,MF}}$ becomes

$$c_s = T \frac{\partial^2 f}{\partial T^2} = -\frac{\alpha_0^2 T}{b T_{\mathrm{c,MF}}^2} \tag{1.10}$$

and zero above. It therefore jumps discontinuously by $\Delta c = -\frac{\alpha_0^2}{b T_{\mathrm{c,MF}}}$. The susceptibility can be obtained via minimization of Eq. (1.1) w.r.t. Ψ

$$h + 2b\Psi^3 + 2\Psi\alpha_0 t \tag{1.11}$$

and differentiating with respect to h

$$\chi = \left. \frac{\partial \Psi}{\partial h} \right|_{h=0} = \frac{1}{2\alpha_0 t + 6b\Psi_0^2} = \begin{cases} (2\alpha_0 t)^{-1} \text{ if } t \geq 0 \\ (-4\alpha_0 t)^{-1} \text{ if } t < 0 \end{cases} \tag{1.12}$$

At $t = 0$ Eq. (1.11) yields the order parameter field dependence on the critical isotherm

$$\Psi(t = 0, h) \sim h^{1/3} \tag{1.13}$$

Allowing the order parameter and external field to spatially vary the two pint correlation function $G(\boldsymbol{r}, \boldsymbol{r}') = \langle \Psi(\boldsymbol{r}) \Psi(\boldsymbol{r}') \rangle - \langle \Psi(\boldsymbol{r}) \Psi(\boldsymbol{r}') \rangle$ is obtained from the partition function and can formally be related to the two-point-susceptibility and the order parameter correlations via

$$\chi(\boldsymbol{r}, \boldsymbol{r}') = -\frac{\partial^2 F}{\partial h(\boldsymbol{r}) \partial h(\boldsymbol{r}')} = \beta G(\boldsymbol{r}, \boldsymbol{r}') \tag{1.14}$$

Performing the analogous steps yielding to Eqs. (1.11) and (1.12) under the requirement of stationarity in Eq. (1.1) identifies $G(\boldsymbol{r}, \boldsymbol{r}')$ as the Green's function of

$$\left(-\nabla^2 + \xi^{-2} \right) G(r) = \frac{1}{2c\beta} \delta(r) \tag{1.15}$$

where $r = |\boldsymbol{r} - \boldsymbol{r}'|$ and $\xi = (2\alpha_0 t + 6b\Psi^2)/2c$ defines the MF correlation length

$$\xi = \begin{cases} \left(\frac{c}{\alpha_0 t} \right)^{1/2} & \text{if } t \geq 0 \\ \left(\frac{-c}{2\alpha_0 t} \right)^{1/2} & \text{if } t < 0 \end{cases} \tag{1.16}$$

assuming translational invariance. Via Eq. (1.15) $G(r)$ obeys

$$2c\beta\xi^{-2+d}G\left(r/\xi\right)=\begin{cases}e^{-r\xi}\text{ if }d=1\\(2\pi)^{-d/2}\left(r/\xi\right)^{-(d-2)/2}K_{(d-2)/2}\left(r/\xi\right)\text{i f }d\geq 2\end{cases} \tag{1.17}$$

where $K_n(r/\xi)$ are the modified spherical Bessel functions of the second kind with asymptotic behavior

$$K_n\left(r/\xi\right)\sim\left(\frac{\pi\xi}{2r}\right)^{1/2}e^{-r/\xi},\ \ r/\xi\to\infty \tag{1.18}$$

$$K_n\left(r/\xi\right)\sim\left(\frac{\Gamma\left(n\right)}{2}\right)\left(\frac{r}{2\xi}\right)^{-n},\ \ r/\xi\to 0 \tag{1.19}$$

$$K_0\left(r/\xi\right)\sim-\ln\left[r/\xi\right],\ \ r/\xi\to 0 \tag{1.20}$$

Off criticality for $d>1$ correlations considered on length scales $r\gg\xi$ vary as

$$G(r)=\frac{\pi^{(1-d)/2}}{2^{(1+d)/2}}\frac{1}{2c\beta}\frac{e^{-r/\xi}}{r^{(d-2)/2}}\xi^{(3-d)/2} \tag{1.21}$$

and thus decay exponentially. Approaching the MF transition temperature however ξ diverges and an algebraic decay given by

$$G(r)=\frac{1}{2c\beta}\frac{\Gamma\left(\frac{d-2}{2}\right)}{4\pi^{d/2}}\frac{1}{r^{d-2}} \tag{1.22}$$

is found for $d>2$. Identifying the corresponding exponents from the previous section yields the mean field critical exponents

$$\alpha=0,\qquad\beta=1/2,\qquad\gamma=1,\qquad\delta=3,\qquad\nu=1/2\qquad\eta=0 \tag{1.23}$$

1.4 First order transitions on mean field level

If the functional Eq. (1.1) is extended to include a cubic term $\epsilon\left|\Psi\right|^3$ in the order parameter then the optimal nontrivial uniform field configuration becomes

$$\Psi\left(\boldsymbol{r}\right)=-\frac{3\epsilon}{4b}\pm\sqrt{\left(\frac{3\epsilon}{4b}\right)^2-\frac{\alpha_0 t}{b}} \tag{1.24}$$

under the condition that the argument of the square root is real i.e. $t<t^*=\frac{b}{\alpha_0}\left(\frac{3\epsilon}{4b}\right)^2>0$. Thus the transition occurs at a higher temperature than the expected continuous mean field transition $T_{\mathrm{c}}>T_{\mathrm{c,MF}}$. Approaching the transition from above the order parameter discontinuously jumps to from zero to a finite value below T_{c}. A classical example is found in the superconducting phase transition in the so called type-I limit where the order parameter Ψ is a complex scalar and describes a charged condensate coupling to a gauge field. Integrating out the gauge field fluctuations the final free energy functional yields a cubic term that exhibits a first order transition [14].

1.5 Breakdown of mean field theory

The implicit assumption of Landau theory is that the partition function can be calculated by solely evaluating the functional at its optimal order parameter field configuration. This however requires the probability distribution

$$P(F) = e^{-\beta F} \tag{1.25}$$

where F is the free energy, to be sharply peaked around the field configuration minimizing $\mathcal{L}$. The normalized fluctuations averaged over a correlation volume ξ^d therefore have to be small. Landau theory itself predicts via Eqs (1.9) and (1.12)

$$\sigma_{\mathcal{L}}^2 = \frac{\int_{\xi^d} d^d r G(r)}{\int_{\xi^d} d^d r \Psi(\boldsymbol{r})^2} = \frac{\chi}{\beta_{\mathrm{c,MF}} \xi^d \Psi_0^2} = \frac{k_B}{4\Delta c \xi_0^d} |t|^{d/2-2} \tag{1.26}$$

Self consistency $\sigma_{\mathcal{L}}^2 \ll 1$ therefore implies the *Ginzburg criterion*

$$|t|^{(4-d)/2} \gg \frac{k_B}{4\Delta c \xi_0^d} \tag{1.27}$$

where the right hand side defines the relative width of the critical region. Therefore only if $d > 4$ can MF theory be self consistent. In the marginal case $d = 4$ it is strictly not correct but this will only lead to logarithmic corrections [15, 16]. For $d < 4$ it inevitably breaks down. Using the general scaling laws named in Sec. 1.2 and starting from the middle expression in Eq. (1.26) Eq. (1.27) can be rephrased as

$$d > \frac{2\beta + \gamma}{\nu} = d_c \tag{1.28}$$

where the upper critical dimension d_c marks the boundary above which MF theory becomes self consistent.

1.6 Renormalization and scaling theory

Strong correlations invalidate the mean field approach. The seemingly innocent scaling laws mentioned in Sec. 1.2 defining the correlation length critical exponent ν and the dynamic exponent z

$$\xi \propto |t|^{-\nu} \tag{1.29}$$

$$\tau_c \propto \xi^z \propto |t|^{-\nu z} \tag{1.30}$$

imply that the system exhibits highly correlated fluctuations in space and time on all possible scales. At $t = 0$ it looks the same under arbitrarily rescaling lengths and thus becomes self-similar. Thereby apart from the spatial dimensionality, fundamental symmetries of the Hamiltonian and the range of interactions microscopic

details are rendered unimportant [17]. This is at the heart of the fact that apparently unrelated systems show the same scaling laws. The theoretical framework to study phase transitions which lead to an understanding of the origins of scaling and in principle allows to calculate universal quantities is called the *renormalization group* (RG). Consider a generalization of the partition function of Eq. (1.7)

$$Z = \mathrm{tr}_X \left\{ e^{-\mathcal{S}[X]} \right\} \tag{1.31}$$

where $\mathcal{S}$ is the *Ginzburg-Landau-Wilson* (GLW) action and X symbolically denotes the degrees of freedom. Examples for $\mathcal{S}$ are $\beta \int d^d r \mathcal{L}$ in Eq. (1.1) or the rescaled Hamiltonian $\mathcal{H} = \beta H$ of a classical lattice-spin system to be introduced in Sect. 1.11. Having specified the degrees of freedom X, the GLW action in principle can be completely characterized by the set of couplings $\{g\}$ such as $\beta c, \beta\alpha\left(T\right), \beta b, \beta \mathbf{h}$ in Eq. (1.7) through which the X enter. Pioneered in the 1970's by Wilson, Fisher and Kadanoff [18, 19, 7] the RG approach basically embodies the following coarse graining procedure. One identifies and separates the short-wavelength, microscopic fluctuations from the long-wavelength, large scale fluctuations entering $\mathcal{S}$. This corresponds to changing the resolution on which changes in the degrees of freedom X are considered. If, initially, one has the resolution ΔL and decreases this resolution to considering only larger patches of linear extension $\Delta L' = l\Delta L$ the correlation length ξ', measured in units of the new coarse grained cutoff length, decreases as

$$\xi' = \xi / l \tag{1.32}$$

The system then is described by a coarse grained GLW action $\mathcal{S}'$ related to the old action via

$$e^{-\mathcal{S}'} = \mathrm{tr}_{X_{\Delta L'}} \left\{ e^{-\mathcal{S}} \right\} \tag{1.33}$$

where $\mathrm{tr}_{X_{\Delta L'}} \{\ldots\}$ indicates that fluctuations on scales shorter than $\Delta L'$ have been integrated out with the effect of *renormalizing* $\mathcal{S}$ or equivalently the couplings $\{g\}$. Equation (1.32) means that a system initially close to criticality ultimately is driven away from criticality unless ξ already has diverged and is infinite. If the system indeed is self similar $\mathcal{S}' = \mathcal{S}$ and in particular the rescaled couplings are the same as the old ones. Thus formally denoting the coarse graining procedure as a mapping R^l of the couplings $\{g\}$ at the critical point

$$R^l \left[\{g\}\right] = \left[\{g\}\right] \tag{1.34}$$

the critical couplings emerge as fixed-points of the mapping R^l, which will be denoted by $\{g^*\}$. As the correlation length transforms as $\xi\left(R^l\left[\{g^*\}\right]\right) = \xi\left(\{g^*\}\right)$, one indeed finds via Eq. (1.32) that $\xi = 0$ or $\xi = \infty$. These two cases are called *trivial fixed-points* describing the bulk phases and *critical fixed-points*. Couplings that under R^l *flow* towards a fixed point define its *basin of attraction*. The basin of attraction of a critical fixed point is called the *critical manifold*. Close to a fixed point

$$g_n = g_n^* + \delta g_n \tag{1.35}$$

which can be used to linearize R^l

$$g'_n = R^l\left[\{g^*_n + \delta g_n\}\right] \approx g^*_n + \frac{\partial g'_n}{\partial g_j}\delta g_j = g^*_n + M^l_{nj}\delta g_j \tag{1.36}$$

In a diagonal representation $\{\tilde{g}\}$ this relation becomes $\delta\tilde{g}'_n = \lambda_n\delta\tilde{g}_n$. Keep in mind that the apparent simplicity of the equations is rather misleading. The RG transformation can be quite complex such that the matrix M^l_{nj} does not need to be symmetric. In general it is complex and left and right eigenvectors have to be distinguished [17]. If, however, its right eigenvalues are real, one can exploit that a repeated application of the transformation with scales l, l' has to be equal to a single transformation to the scale $l \cdot l'$. This means that

$$\begin{aligned} M^{l'}_{nu}M^l_{uj} &= M^{l\cdot l'}_{nj} \\ \Rightarrow \lambda^l_n\lambda^{l'}_n &= \lambda^{l\cdot l'}_n \end{aligned} \tag{1.37}$$

Therefore the eigenvalues transform according to a power law $\lambda^l_n = l^{y_n}$ [17]. This is the basis for all the data analysis performed in this thesis. Depending on the value of y_n, the scaling fields $\tilde{g}_n$ are called:

1. *relevant*, if $y_n > 0$, as then the weight of the associated scaling field increases under renormalization.

2. *irrelevant*, if $y_n < 0$, as the weight of the associated scaling field decreases under renormalization.

3. *marginal*, if $y_n = 0$.

The number of relevant eigenvalues thus corresponds to the independent parameters that need to be adjusted in order to hit the critical point in experiment or simulation [17]. Due to Eq. (1.33) the RG transformation leaves the partition function invariant. The free energy density

$$f = F/Vk_BT = -V^{-1}\ln Z \tag{1.38}$$

where V is the system volume scales under the above transformation as

$$f = l^{-d}f_s\left(\{g'\}\right) + f_n\left(\{g\}\right) \tag{1.39}$$

where $f_n\left(\{g\}\right)$ is called the analytic part of the free energy density [20]. This leads to the form

$$f_s\left(g_1, g_2, \ldots\right) = l^{-d}f_s\left(l^{y_1}u_1, l^{y_2}u_2, \ldots\right) \tag{1.40}$$

The u_i are called scaling fields and depend analytically on $\{g\}$. If there only are two relevant scaling fields u_t and u_h as in the standard magnetic systems then to

lowest order $u_1 \sim t$ and $u_2 \sim h$. The homogeneity allows to eliminate l and write Eq. (1.40) in two equivalent scaling forms

$$f_s(t,h) = \begin{cases} |t|^{d/y_t}\, \Phi_\pm\left(\frac{h}{|t|^{y_h/y_t}}\right) \\ |h|^{d/y_h}\, \Sigma_\pm\left(\frac{t}{|h|^{y_t/y_h}}\right) \end{cases} \tag{1.41}$$

From these homogeneity laws basically all equilibrium scaling relations mentioned in Sec. 1.2 can be derived. According to Eq. (1.39) $f_s \sim \xi^{-d} \sim t^{d\nu}$ and thus $\nu = 1/y_t$ but Eq. (1.2) requires $f_s \sim t^{2-\alpha}$. We thus obtain a hyperscaling relation

$$d\nu = 2 - \alpha \tag{1.42}$$

called the Josephson scaling relation. Further, $m \sim \partial f_s/\partial h$ implies through Eq. (1.5) that $y_h = d\delta/(1+\delta)$. Performing the appropriate derivatives yields $\beta = (d - y_h)\,\nu$ and $\gamma = (2y_h - d)\,\nu$. Identifying the susceptibility χ with the integrated correlation function yields the Fisher scaling law

$$\gamma = (2 - \eta)\,\nu. \tag{1.43}$$

Thus by the knowledge of either ν, or equivalently α, and one other exponent from the set $\beta, \gamma, \delta, \eta$, the value of y_h and thus all other equilibrium exponents can be calculated. For the sake of completeness we state the Rushbrooke scaling law

$$\alpha + 2\beta + \gamma = 2 \tag{1.44}$$

and the Widom scaling law

$$\beta\,(\delta - 1) = \gamma \tag{1.45}$$

1.7 Finite size scaling

All systems that are studied via numerical simulation methods in this thesis necessarily need to be of finite extent. Usually confined in a hyper cubic volume L^d the correlation length in Eq. (1.29) therefore naively is expected to diverge up to $\xi \approx L$ leading to a rounded maximum in $\xi(T, L)$ at T_c. Then the system size L basically can be seen as yet another scaling field entering Eq. (1.40) scaling trivially with exponent $y_L = -1$. Choosing the rescaling factor $l = L$ yields

$$f_s(t,h,L) = \frac{1}{L^d}\tilde{f}_s\left(L^{1/\nu}t, L^{y_h}h, 1\right) \tag{1.46}$$

where Eq. (1.29) has been used. Equations (1.2)-(1.5) then imply

$$c_s|_{h=0} \sim L^{\alpha/\nu}\tilde{c_s}\left(L^{1/\nu}t\right) \tag{1.47}$$

$$m|_{h=0} \sim L^{-\beta/\nu}\tilde{m}\left(L^{1/\nu}t\right) \tag{1.48}$$

$$\chi|_{h=0} \sim L^{\gamma/\nu}\tilde{\chi}\left(L^{1/\nu}t\right) \tag{1.49}$$

$$m|_{t=0} \sim L^{y_h - d}\hat{m}\left(L^{y_h}h\right) \tag{1.50}$$

where $\tilde{c}_s, \tilde{m}, \tilde{\chi}, \hat{m}$ are scaling functions of the singular parts. Evidently any possible divergence in the response functions c_s or χ is rounded to a finite maximum for finite L. However as the finite-size form Eq. (1.46) necessarily implies hyperscaling it cannot be correct above d_c.

1.8 Corrections to scaling

The irrelevant scaling fields are associated with corrections to scaling. Assume the leading corrections to scaling field is u_3 with negative RG dimension $y_3 = -\omega$. The singular part of the free energy then reads

$$\begin{aligned} f_s\left(t, h, g_3, L\right) &= L^{-d} \tilde{f}\left(u_t L^{1/\nu}, u_h L^{y_h}, u_3 L^{-\omega}\right) \\ &\approx L^{-d} f\left(u_t L^{1\nu}, u_h L^{y_h}\right) + u_3 L^{-d-\omega} f_\omega\left(u_t L^{1/\nu}, u_h L^{y_h}\right) + \cdots \end{aligned} \tag{1.51}$$

Respecting the symmetry of f_s under $h \to -h$ they can be approximated by $u_h = h\bar{u}_h\left(t\right) + O\left(h^3\right)$ where $\bar{u}_h = a_h + a_1 t + O\left(t^2\right)$ and $u_t = c_t t + c_{02} t^2 + c_{20} h^2 + c_{21} h^2 t + O\left(t^3, h^4, h^4 t\right)$ close to the critical point $h = t = 0$. The fields u_h and u_t are independent of L. With these definitions corrections to all other quantities can be derived [21]. Implicit to the derivation above is that the free energy behaves analytic in the limit that the leading irrelevant scaling field approaches zero, which is not always the case.

1.9 Above the upper critical dimension d_c

Above d_c although all exponents are known exactly by their Landau values (1.24), the standard finite-size scaling approach from Sect. 1.7 in which the correlation length is identified with the system size L fails. In fact for models of the type Eq. (1.1) it turns out that the leading irrelevant scaling field u_b is *dangerously irrelevant* meaning that the free energy is singular in the limit $b \to 0$. It is now well established that above d_c the correct finite-size expression is $\xi \sim L^{d/d_c}$ [22, 23, 16]. This implies that the scaling variable $x = L^{1/\nu} t$ has to be replaced by $L^{d/d_c \nu} t$ above d_c instead of the naive expectation $L^2 t$. In addition precisely at d_c where the quartic coupling b is marginal one acquires logarithmic corrections $\xi\left(t\right) = t^{-1/2} \left|\log t\right|^{1/6}$ and $\xi \sim L \left(\log L\right)^{1/4}$ [15, 24]. The proper scaling variable thus becomes $x = \xi\left(t\right) / \xi\left(T_{\mathrm{c}}, L\right) = t^{-1/2} \left|\log t\right|^{1/6} / L \left|\log L\right|^{1/4}$.

1.10 Quantum phase transitions

In addition to the previously introduced classical phase transitions there is yet another class of phase transition: *Quantum phase transitions (QPT)*. At a QPT the variation of a non-thermal coupling parameter K such as chemical potential

μ, external magnetic field H or the impurity doping concentration causes a non-analyticity of the many-body ground state properties. As will be evident these QPT's are only possible at absolute zero temperature where in contrast to classical systems and due to the Heisenberg uncertainty principle a quantum mechanical system still exhibits fluctuations.

Path integral formulation of statistical mechanics

The Hamiltonian of a quantum mechanical system usually can be written as

$$\mathcal{H} = \mathcal{T} + \mathcal{V} \tag{1.52}$$

where $\mathcal{T}$ and $\mathcal{V}$ are the operators for the kinetic and potential part. In contrast to classical systems, where the partition function factorizes in $\mathcal{T}$ and $\mathcal{V}$, their general noncummutativity in a quantum description enforces a coupling between dynamics and statics. Cutting the *time scale* $\hbar\beta$ in equidistant slices $\Delta\tau = \hbar\beta/M$ the partition function $Z = \mathrm{Tr}\left\{e^{-\beta\mathcal{H}}\right\}$ can be written as the trace over a product of M *high temperature density matrices* $e^{-\beta\mathcal{H}} = \left[e^{-\frac{\Delta\tau}{\hbar}\mathcal{H}}\right]^M$. Inserting resolutions of unity and choosing an arbitrary complete set of states $\{|\alpha\rangle\}$ the partition function becomes a sum over weighted trajectories in *state-space*

$$\begin{aligned} Z &= \sum_{\alpha_0}\sum_{\alpha_1}\cdots\sum_{\alpha_{M-1}} \langle\alpha_0|e^{-\frac{\Delta\tau}{\hbar}\mathcal{H}}|\alpha_1\rangle\langle\alpha_1|e^{-\frac{\Delta\tau}{\hbar}\mathcal{H}}|\alpha_2\rangle \\ &\quad \times\ldots\times\langle\alpha_{M-1}|e^{-\frac{\Delta\tau}{\hbar}\mathcal{H}}|\alpha_0\rangle \end{aligned} \tag{1.53}$$

All these paths start and end at $|\alpha_0\rangle$. Following a trajectory the states perform intermediate transitions as in the *Feynman path integral* description of elementary quantum mechanics [25]. But with time t replaced by *imaginary time* $-i\hbar\beta$ in the time evolution operator matrix elements $\langle\alpha_i|e^{-i\frac{\Delta t}{\hbar}\mathcal{H}}|\alpha_{i+1}\rangle$. The coupling between different *time slices* can be used to express a d-dimensional quantum system as a $(d+1)$-dimensional classical one. This *quantum classical mapping* is most evident if one considers position eigenstates $|\alpha\rangle = |R\rangle = |\{\boldsymbol{r}_1\ldots\boldsymbol{r}_N\}\rangle$ as done in path integral Monte Carlo simulations to describe atoms at low temperatures such as ^{4}He . There, using $\lambda = \frac{\hbar^2}{2m}$, one has $\mathcal{T} = -\lambda\sum_i\nabla_i^2$ and $\mathcal{V} = \sum_{i<j}V(\boldsymbol{r}_i,\boldsymbol{r}_j)$ where $V(\boldsymbol{r},\boldsymbol{r}')$ is the two body potential. The partition function becomes, up to quadratic corrections in $\Delta\tau$,

$$Z = \int dR_0\int dR_1\ldots\int dR_{M-1}\prod_{i=0}^{M-1} e^{-S_{\Delta\tau}(R_{i-1},R_i)} \tag{1.54}$$

where the action $S_{\Delta\tau}$ becomes

$$S_{\Delta\tau}(R,R') = \frac{dN}{2}\log(4\pi\lambda\Delta\tau) + \frac{(R-R')^2}{4\lambda\Delta\tau} + \sum_{i<j}^{N}\Delta\tau V_R(\boldsymbol{r}_i,\boldsymbol{r}_j)$$

and couples neighboring time slices only via the kinetic term whereas atoms only interact within the same slice [26]. The d-dimensional quantum many-body problem thus has been mapped to a classical problem of polymers in $(d+1)$-dimensions. But for finite temperature T the extension in τ-direction is always limited and only for $T = 0$ the $(d + 1)$-dimensionality holds even in the thermodynamic limit. At high temperatures the corresponding *time interval* $\hbar\beta$ usually is small compared to the natural frequency scales of the system. The system then looks static in all time slices $0 \dots M-1$ and the dynamics drops out rendering the path integral description into that of an ordinary Boltzmann weight. If the underlying Hamiltonian considered is written in terms of boson field operators $\psi_i, \psi_i^\dagger$ then the usual way to evaluate Eq. (1.53) is to normal order and then use a coherent state representation. This yields the Landau-Ginzburg-Wilson functional [27, 28]

$$\mathcal{S} = \int_0^\beta d\tau \left[\sum_i \psi_i^\dagger(\tau)\partial_\tau \psi_i(\tau) + \mathcal{H}\{\psi_i^\dagger(\tau), \psi_i(\tau)\} \right] \tag{1.55}$$

with partition function Eq. (1.53)

$$Z = \mathrm{Tr}^\psi \left\{ e^{-\mathcal{S}} \right\} \tag{1.56}$$

where $\mathrm{Tr}^\psi \{\dots\} = \int \mathcal{D}\psi\mathcal{D}\psi^\dagger (\dots)$.

Scaling at quantum phase transitions

The quantum classical mapping implies the emergence of fluctuations on all length and time scales as given in Eqs. (1.29) and (1.30) at the quantum critical point (QCP). Diverging time scales directly relate to a vanishing characteristic frequency and therefore energy scale

$$\hbar\omega_c \propto |t|^{\nu z} \tag{1.57}$$

which can be applied as a measure to determine whether quantum or thermal fluctuations drive the transition. If $\hbar\omega_c \ll k_B T$ the regime is purely classical which renders quantum fluctuations irrelevant for temperatures

$$|t| < T_\mathrm{c}^{1/\nu z} \tag{1.58}$$

for any finite T_c. This, as promised above, implies that at finite temperatures the fluctuations of any physical system asymptotically close to a critical point are entirely classical. Only at zero temperature can a phase transition be entirely driven by quantum fluctuations. The presence of a QCP however leaves a signature even at finite temperatures. Figure 1.1 illustrates a general phase diagram close to a QCP. Quite generally the ordered state might persist in a large parameter range of (K, T). Then the phase diagram exhibits a classical critical line for finite T and $K < K_c$. In contrast, if order at any finite temperature is precluded, a transition is only possible at $T = 0$ between a quantum ordered and quantum disordered many

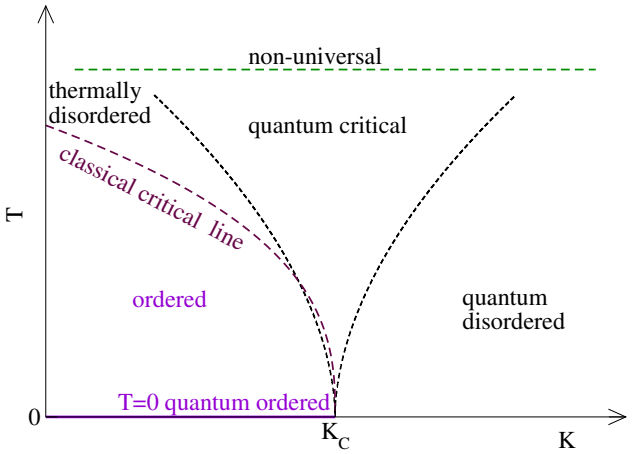

Figure 1.1: Illustration of the phase diagram close to a QCP. In general the ordered phase may exist for finite $T > 0$. The transition between thermally ordered and disordered states is entirely classical. Interestingly, below the cutoff temperature where the quantum critical region vanishes, the influence of the quantum critical point widens with respect to the distance from criticality k upon increasing T. If order is forbidden at finite T then the classical critical line vanishes and the system only exhibits a QPT at $T = 0$. The boundaries of the quantum critical region is determined by the dashed black curves $k_B T \propto |k|^{\nu z}$. Figure adapted from [29].

particle ground state. The presence of the QCP leads to a quantum critical region for determined by

$$k_B T > \hbar\omega_c \propto |k|^{\nu z} \tag{1.59}$$

where $k = K - K_c$ and the system ultimately is driven away from criticality by thermal fluctuations. This quantum critical behavior is cutoff above some system dependent temperature where microscopic energy scales are rendered irrelevant by strong thermal fluctuations. Below the behavior is to a large extend governed by excitations of the quantum critical ground state [29]. The behavior in this region is normally non-universal except in the direct vicinity of the quantum critical point itself. There the correlation length diverges as

$$\xi \propto |k|^{-\nu} \tag{1.60}$$

with a universal exponent ν. But along the extra imaginary time direction the *correlation time* diverges as

$$\tau_c \propto \xi^z \propto |k|^{-\nu z} \tag{1.61}$$

where $z \neq 1$ only if space-time symmetry is broken. Then the correlation volume grows infinite anisotropically as also observed in systems where isotropy explicitly is broken by introducing a symmetry breaking field or correlated disorder along a specified axis [30, 31]. These as evident from the quantum classical mapping introduce *columnar correlations* along the time direction. The homogeneity law Eq. (1.40) then generalizes to

$$f(k,T) = b^{-(d+z)} f\left(kb^{1/\nu}, L_\tau^{-1} b^z\right) \tag{1.62}$$

with $L_\tau = 1/T$ as effective system size along the time direction and dimensionality

$$D = d + z \tag{1.63}$$

If the critical point satisfies hyperscaling the existence of ξ, as a single length scale and ξ^z as a single timescale, apart from microscopic cutoff length scales important for anomalous scaling dimensions [17] allows the finite-size scaling ansatz

$$O(K, L, L_\tau) = L^{d_O} \tilde{O}_1\left(L^{1/\nu} k, L_\tau / L^z\right) \tag{1.64}$$

for operators with scaling dimension d_O. Again these relations are only valid below the upper critical dimension d_c of the problem at hand. Above the critical behavior is given by the mean field solution. The ratio between the inverse temperature length and the spatial system size usually is referred to as the aspect ratio $\alpha_\tau = L_\tau / L^z$.

1.11 The $O(N)$ spin models

The $O(N)$ vector models have a wide range of applicability in the study of phase transitions and critical phenomena. The Hamiltonian entering the partition function Eq. (1.31) is given by

$$\mathcal{H} = \beta H = -\beta \sum_{i,\mu} \left[J S(\boldsymbol{r}_i) \cdot S(\boldsymbol{r}_i + \hat{\mu}) - \mathbf{H}(\boldsymbol{r}_i) \cdot S(\boldsymbol{r}_i) \right] \tag{1.65}$$

where $\hat{\mu}$ shall denote the unit lattice vectors connecting the sites $i = 1 \ldots L^d$ on a simple hypercubic lattice of linear extension L. The term $O(N)$ means that the degrees of freedom $S(\boldsymbol{r})$ are given by N-component vectors or classical spins of fixed length N residing on the vertices of the lattice. J here is a uniform coupling constant. Disorder in the model can be included via defining position dependent bond couplings $J \to J^\mu(\boldsymbol{r})$ coupling $S(\boldsymbol{r})$ to $S(\boldsymbol{r} + \hat{\mu})$. $\mathbf{H}$ is an external magnetic field coupling to the magnetic moment of $S(\boldsymbol{r})$. The critical properties of many complicated systems can be captured by the properties of $O(N)$ models. In condensed matter physics the most frequently studied cases are the Ising model [32] where $N = 1$ and $S(\boldsymbol{r}) = \pm 1$, the XY model or classical planar spin model where

$N = 2$ and the Heisenberg model $N = 3$. In high energy physics the case $N = 4$ is studied to describe finite temperature transitions in the theory of strong interactions (QCD) [33]. $N = 5$ has been applied to high-T_c superconductivity [34, 35]. The large N-limit can be solved exactly [36, 37]. An extensive review of numerical and analytical calculations on the $O(N)$ vector class can be found in Ref. [10].

1.12 Phase transitions in the $O(N)$ models

From the discussion in Sec. 1.6 it is clear that the properties of any possible phase transition between an ordered and a disordered state in the models described by Eq. (1.65) in general can be expected to depend on the symmetry group and the dimensionality d of the system. In addition the range of interactions matters. Here only short-range nearest-neighbor interactions are considered. One natural order parameter is the $O(N)$ magnetization

$$M = \sum_i S(\boldsymbol{r}_i) \tag{1.66}$$

The system exhibits *long range order* if the order parameter correlation function

$$G(|\boldsymbol{r}_i - \boldsymbol{r}_j|) = \langle S(\boldsymbol{r}_i) S(\boldsymbol{r}_j) \rangle \tag{1.67}$$

is finite in the limit $|\boldsymbol{r}_i - \boldsymbol{r}_j| \to \infty$. At $T = 0$ and zero external field all spins of Eq. (1.65) are bound to point along the same direction and $G(|\boldsymbol{r}_i - \boldsymbol{r}_j|) = N^2$. To illustrate the importance of the spatial dimension on the existence of a phase transition at finite temperature consider the Ising case $N = 1$ and $d = 1$. In the thermodynamic limit fluctuations of a finite number of spins cannot destroy long range order. Assume the system has chosen all $S(\boldsymbol{r}_i) = 1$. A single *domain wall* separating a region of $S(\boldsymbol{r}_i) = 1$ from a region of $S(\boldsymbol{r}_i) = -1$ has energy cost $2J$ but entropy $S = k_B \log L$. The system can thus lower its free evergy by $\Delta F = 2J - k_B T \log L$ which tends to $-\infty$ for $L \to \infty$. Splitting the domains further lowers F and thus order is destroyed for any finite T at $N = 1$ for entropic reasons. This simple argument due to Landau and Peirls [38, 39] immediately precludes the existence of a finite temperature phase transition for *any* $N \geq 1$ in $d = 1$. For $d = 2$ domain walls have loop-like circumference. The energy cost of inserting an n bond loop scales as $2Jn$. A rough estimate of the entropy can be achieved via the assumption that having chosen the starting point of the domain wall and without backtracking the loop has 3 possibilities to choose the next lattice point from each vertex. The entropy thus roughly scales as $\Delta S \sim k_B \log(3^n)$ and the associated n-bond domain wall free energy change scales as $\Delta F_n \sim [2J - k_B T \log(3)]\, n$. There thus seems to be a temperature

$$T^* = \frac{2J}{k_B \log 3} \tag{1.68}$$

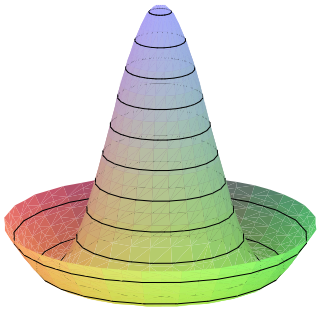

Figure 1.2: Sketch of the Mexican hat potential for the $O(2)$ model. True long range order can only appear in dimensions $d > 2$.

above which disordering the system decreases F. One therefore expects a finite temperature phase transition in the 2D Ising model. Indeed this is the case and the system is even exactly solvable [40, 37]. For continuous spins, $N > 1$, the case $d = 2$ is more tricky.

1.13 Continuous global symmetry

In the previous section, mentioning the ordered, zero temperature ground state, an important detail was swept under the rug. In all $O(N)$ models for $\mathbf{H} = 0$ the energy is left unaltered if all spins are mutually rotated by a global $O(N)$ transformation. This follows from the fact that the Hamiltonian has a *global* $O(N)$ symmetry and rotating all spins at once leaves the energy unaltered. If, hypothetically, N and d are such that there is an ordered phase, and an experimenter would cool the system deep into the ordered phase, a particular orientation is found. As in the ordered phase fluctuations have a finite correlation length, the thermodynamical averages observed, including the ground state, do therefore not display the same $O(N)$-symmetry as the Hamiltonian itself. This is referred to as *spontaneous symmetry breaking*. At the heart of it lies the fact that the limits of having an infinitesimally strong field on the one hand, and letting the number of spins go to infinity on the other hand, do not commute. For an arbitrarily small ordering field $\mathbf{H}$ letting $L^d \to \infty$ the system ends up in a symmetry-broken, ordered, *low symmetry* state. Conversely the limit $\mathbf{H} \to 0$ and subsequently $L^d \to \infty$ is not unique. In the thermodynamic limit the system thus is not ergodic. To illustrate the importance of the symmetry group for the existence of long range order consider the Hamiltonian

Eq. (1.65) in its equivalent continuum GL form [17]

$$\mathcal{S} = -\int d^d r \left[\frac{c_0}{2} \left(\partial_i S_\alpha\right)^2 + \frac{1}{2} r_0 S_\alpha^2 + \frac{1}{4} u_0 \left[S_\alpha^2\right]^2 - h_\alpha S_\alpha \right] \tag{1.69}$$

Here $\alpha = 1, \ldots, N$ denotes the spin components and $i = 1 \ldots d$ labels the spatial directions. The fixed length condition has been relaxed. For simplicity consider only $N = 2$ which yields the *Mexican hat potential* shown in Fig. 1.2. Now assume that $|S(\boldsymbol{r})| = \sqrt{|r_0/u_0|}$ minimizes the potential part with some particular orientation and the external field is zero. Then we can write $S(\boldsymbol{r}) = \sqrt{|r_0/u_0|}\left(\cos\left(\theta(\boldsymbol{r})\right), \sin\left(\theta(\boldsymbol{r})\right)\right)$ below the mean field transition temperature $T_{\mathrm{c,MF}}$ and obtain the effective action

$$\mathcal{S} = \int d^d r \frac{K}{2} \left(\nabla\theta(\boldsymbol{r})\right)^2 \tag{1.70}$$

where $K = \beta|r_0/u_0|$ is usually referred to as the *bare spin wave stiffness*. If $T \ll T_{\mathrm{c,MF}}$ one may expect only small variations in $\theta(\boldsymbol{r})$ smoothly fluctuating around a fixed direction. Then transforming $\theta(\boldsymbol{r}) = L^{-d/2} \sum_{\mathbf{q}} \theta_{\mathbf{q}} e^{i\mathbf{q}\cdot\boldsymbol{r}}$ gives

$$\mathcal{S} = \frac{K}{2} \sum_{\mathbf{q}} q^2 \left|\theta_{\mathbf{q}}\right|^2 \tag{1.71}$$

where the modes $\theta_{\mathbf{q}}$ are Gaussian variables. The q^2 dependence of the action reveals the presence of gapless *soft-mode excitations*. In momentum space $\langle\theta_{\mathbf{q}}\theta_{\mathbf{q}'}\rangle = \delta_{\mathbf{q},-\mathbf{q}'}/Kq^2$ is proportional to the Fourier transform of the unscreened Coulomb potential. The correlations can be obtained via

$$\langle S(\boldsymbol{r}) S(0)\rangle = \frac{r_0}{u_0} \langle e^{i[\theta(\boldsymbol{r})-\theta(0)]}\rangle \approx \frac{r_0}{u_0} e^{-\frac{1}{2}\langle(\theta(\boldsymbol{r})-\theta(0))^2\rangle} \tag{1.72}$$

valid in the Gaussian approximation Eq. (1.70) yielding the leading behavior

$$\langle\theta(\boldsymbol{r})\,\theta(0)\rangle = \begin{cases} \sim \text{const if } d > 2 \\ \sim r^{2-d} \text{ if } d < 2 \\ = \frac{\log r}{2\pi} \text{ if } d = 2 \end{cases} \tag{1.73}$$

In 1D as expected smooth spin wave fluctuations are thus enough to exponentially suppress correlations. In 2D however

$$\langle S(\boldsymbol{r}) S(0)\rangle \sim r^{-\eta(T)} \tag{1.74}$$

with $\eta(T) = |u_0|\,T/2\pi\,|r_0|$. Again there is no true long range order but *quasi long range order* as the correlations decay algebraically towards zero. This is the core of, and rigorously generalized in the *Mermin-Wagner-Hohenberg theorem* [41, 42, 43]. It states that there is no spontaneous symmetry breaking in systems with a continuous symmetry $N \geq 2$ and short-range interactions for $d \leq 2$. This however does

not preclude the existence of a phase transition in 2D. Obviously, the assumptions made above break down, when the temperature is increased such that the phases are allowed to fluctuate wildly, and the effective action above cannot be treated as Gaussian. Then one can expect the correlations to decay exponentially. In fact the point where the quasi-critical correlations in Eq. (1.74) change to exponentially damped marks the *Berezinskii-Kosterlitz-Thouless phase transition* [12, 13].

1.14 Topological defects

As illustrated for the 2D Ising model the gain in entropy associated with the macroscopic creation of defects above a finite temperature was shown to surmount the energy cost of their creation. Many $O(N)$ spin-systems can undergo a phase transition associated with the proliferation of defects or defect pairs with low excitation energy but high entropy gain. These can be topological in the sense that the associated field configuration, $S(\boldsymbol{r})$, is such that a removal of the defect via simple local alternation of spins is not possible but involves spins at arbitrary distances.

Domain walls

Domain walls interpolate between two different grounds states. For Ising models they therefore are the boundaries separating regions containing spins of opposite orientation. In a d-dimensional system a domain wall therefore has dimension $d-1$. In zero external field the phase transition of the Ising model is governed by the macroscopic proliferation of domain walls.

Vortices

Vortices are the natural class of topological defects emerging in the $O(2)$ or XY models in 2D. Again mapping a spin configuration to an equivalent configuration of phases $\theta(\boldsymbol{r})$ a vortex at $\boldsymbol{r}_0$ is defined by the property

$$\oint_\gamma d\boldsymbol{r}\nabla\theta = 2\pi q \tag{1.75}$$

with integer *winding number* or *charge* q for any closed path γ encircling $\boldsymbol{r}_0$. Vortices of negative q are usually referred to as *anti-vortices*. Evidently the vector field $\mathbf{v}_q = \nabla\theta \sim r^{-1}\mathbf{e}_\theta$ gives rise to a 2π winding for arbitrary paths around the origin. Using Stokes theorem this is only possible if the vortex shows up as a singularity in $\nabla \times \mathbf{v}_q = \nabla \times \nabla\theta = 2\pi q\delta(\boldsymbol{r})\,\mathbf{e}_z$. From Eq. (1.70) one obtains the cost $E_1 = K\pi\log[L/a]$ to create an isolated vortex in a finite system of radius L. Here the definition of a microscopic cutoff parameter a is a necessary. Thus in the thermodynamic limit no isolated vortex should be excited. But if a vortex configuration deliberately has been created the cost to remove it via a sequence of local distortions followed by flipping a macroscopic number of anti-aligned neighboring spins can roughly be estimated to be of the order of $\sim KL$ [44]. Returning

to the ground state from a vortex configuration via small statistical fluctuations is extremely unlikely and the vortex *topologically* and *physically stable*.

To calculate the energy for an arbitrary distribution $q(\boldsymbol{r}) = \sum_i q_i \delta(\boldsymbol{r} - \boldsymbol{r}_i)\,\mathbf{e}_z$ of vortices or charges one usually uses the following trick. The vector field $\mathbf{v} = \nabla\theta$ can be decomposed in transverse and longitudinal parts $\mathbf{v}_t, \mathbf{v}_l$ where the label has been chosen due to the analogy between a quantum mechanical phase gradient field and a velocity field. The components obey $\nabla \cdot \mathbf{v}_t = 0$ and $\nabla \times \mathbf{v}_l = 0$. Thus

$$\mathbf{v}_t = \nabla \times V_t \mathbf{e}_z \text{ and } \mathbf{v}_l = \nabla V_l \tag{1.76}$$

and by construction the vortices can only emerge from the transverse component

$$\nabla \times \mathbf{v} = \nabla \times \nabla \times V_t \mathbf{e}_z = -\nabla^2 V_t \mathbf{e}_z = q(\boldsymbol{r}) \tag{1.77}$$

Equation (1.70) then implies

$$\mathcal{S} = \frac{K}{2} \int \left[(\nabla V_l)^2 + V_t \nabla^2 V_t \right] d^2 r \tag{1.78}$$

where the longitudinal part is equivalent to Eq. (1.71). Using the Green's function $G(\boldsymbol{r}) = -\ln(|\boldsymbol{r}|)$ of the 2D laplace operator gives V_t as the convolution

$$V_t(\boldsymbol{r}) = \int G(\boldsymbol{r} - \boldsymbol{r}')\, q(\boldsymbol{r}')\, d^2 \boldsymbol{r}' \tag{1.79}$$

and therefore the vortex part of the action is described by

$$\mathcal{S}_{\mathrm{CG}} = \pi K \int \int q(\boldsymbol{r})\, G(\boldsymbol{r} - \boldsymbol{r}')\, q(\boldsymbol{r}')\, d^2 \boldsymbol{r}' d^2 \boldsymbol{r} \tag{1.80}$$

where CG stands for Coulomb gas which is motivated by the fact that the interaction between the vortices is the same as for unscreened point charges in 2D. To deal with the mathematical singularity at the center of the vortices it is required that the local order parameter $S(\boldsymbol{r})$ vanishes at the center. In a lattice theory the action then becomes

$$\mathcal{S}_{\mathrm{CG}} = \frac{1}{2} \sum_{i \neq j} q_i V(\boldsymbol{r}_i - \boldsymbol{r}_j)\, q_j + \frac{1}{2} \tilde{G}(0) \left(\sum_i q_i \right)^2 \tag{1.81}$$

where $V(\boldsymbol{r}) = \tilde{G}(\boldsymbol{r}) - \tilde{G}(0)$ and $\tilde{G}$ is the potential for vortices obtained if the delta-singularities in $q(\boldsymbol{r})$ above are smeared out to charge distribution of finite extent. As $\tilde{G}(0)$ is infinite in the thermodynamic limit, the system is restricted to be neutral i.e. $\sum_i q_i = 0$. Then the pure interaction terms between the charges asymptotically scale as $\propto -q_i q_j \log[r/a]$ which implies that the cutoff a defining the lattice constant should be of the order of the vortex core size defined by the width of the point charge distribution. Vortices with opposite charge therefore attract

and equal charges repel. As the longitudinal fluctuations of the $O(2)$ model where shown not to be able to exhibit any phase transition, the only possibility left is that it is exactly the proliferation of neutral vortex pairs which will give rise to a phase transition from a disordered state to a quasi long ranged ordered state described by the property Eq. (1.74) at low temperatures. In Ch. 3 it will become clear that in 3D order is destroyed by a similar mechanism associated with the proliferation of closed vortex loops.

1.15 Effects of disorder - Harris criterion

Defects naturally appear as impurities or can deliberately be created by thermal quenching, nuclear damage tracks [45] or by random potentials in laser traps. Spatially extended defects can show long range correlations. The effect of quenched random disorder in a system corresponds to spatial variations in $J \to J^{\mu}(\boldsymbol{r}) = J + \delta J^{\mu}(\boldsymbol{r})$ or equivalently $r_0 \to r_0 + \delta r_0(\boldsymbol{r})$ in the $O(N)$ models defined by (1.65) and (1.69) respectively. For finite temperature phase transitions it therefore leads to spatial variations in the distance to criticality $t(\boldsymbol{r}) = (T - T_{\mathrm{c}}(\boldsymbol{r}))/T_{\mathrm{c}}$.

A useful heuristic criterion for the critical behavior of disordered Ising spin systems was given by Harris for the case of uncorrelated point disorder [46]. Regarding the effects of random defects on the universal properties at a continuous phase transition a criterion for fixed point stability usually can be derived in the following way. Within a correlation volume $V_\xi = \xi^d$ the presence of disorder leads to the effective average distance to criticality

$$t_\xi \sim \frac{1}{\xi^d} \int_{V_\xi} d^d \boldsymbol{r} t(\boldsymbol{r}) \tag{1.82}$$

The fixed point should be stable, with respect to the introduction of disorder, if the spatial temperature fluctuations, $\Delta^2 = \left[t_\xi^2\right]_{\mathrm{dis}}$, due to the defects within V_ξ, are small compared to the overall distance to criticality $t = (T - T_{\mathrm{c}})/T_{\mathrm{c}}$. Here $[\ldots]_{\mathrm{dis}}$ denotes averaging over different realizations of the disorder. For correlated defects described by

$$[t(\boldsymbol{r})\, t(\boldsymbol{r}')]_{\mathrm{dis}} \sim [\delta J^{\mu}(\boldsymbol{r})\, \delta J^{\mu}(\boldsymbol{r}')]_{\mathrm{dis}} = g_{\mathrm{dis}}(\boldsymbol{r}, \boldsymbol{r}') \tag{1.83}$$

this requires

$$\frac{\Delta^2}{t^2} \sim \xi^{-2d} t^{-2} \int_{V_\xi} d^d \boldsymbol{r} \int_{V_\xi} d^d \boldsymbol{r}' g_{\mathrm{dis}}(\boldsymbol{r}, \boldsymbol{r}') \to 0 \tag{1.84}$$

for $t \to 0$. It is thus the *long distance behavior* of $g_{\mathrm{dis}}(\boldsymbol{r}, \boldsymbol{r}')$ that determines whether the critical properties are still given by the pure fixed point. Most interesting for this theses are the cases of

1. *uncorrelated random point disorder:* This is the case treated by the original Harris criterion. Here $g_{\text{dis}}(\boldsymbol{r}, \boldsymbol{r}') \sim \delta(\boldsymbol{r} - \boldsymbol{r}')$ inserted into Eq. (1.84) yields using $\xi \sim t^{-\nu}$ the requirement $t^{d\nu-2} \to 0$ and thus the original fixed point is unaltered if the Chayes inequality [47]

$$\nu > 2/d \tag{1.85}$$

is obeyed. Below the upper critical dimension this is equivalent to $\alpha < 0$.

2. *rodlike disorder along one or several symmetry axes:* Here $g(\boldsymbol{r} - \boldsymbol{r}') \propto \delta^{d-1}(\boldsymbol{r} - \boldsymbol{r}')$ forces $d-1$ components of the position vectors $\boldsymbol{r}, \boldsymbol{r}'$ to coincide for a nonzero contribution. Thus Eq. (1.84) gives $t^{2d\nu-2-(d+1)\nu} \to 0$ yielding

$$\nu > 2/(d-1) \tag{1.86}$$

3. *random planes:* Here $g(\boldsymbol{r} - \boldsymbol{r}') \propto \delta^{d-2}(\boldsymbol{r} - \boldsymbol{r}')$ forces $d-2$ components of the position vectors $\boldsymbol{r}, \boldsymbol{r}'$ to coincide for a nonzero contribution. Thus Eq. (1.84) gives $t^{2d\nu-2-(d+2)\nu} \to 0$ yielding

$$\nu > 2/(d-2) \tag{1.87}$$

4. *power law correlated disorder:* This interesting case where $g(\boldsymbol{r} - \boldsymbol{r}') \sim |\boldsymbol{r} - \boldsymbol{r}'|^{-a}$ decays with exponent $a > 0$ was treated via RG techniques in a seminal paper by Weinrib and Halperin [48]. Equation (1.84) gives, depending on the speed of the fall off,

$$\frac{\Delta^2}{t^2} \sim \begin{cases} t^{d\nu-2}, \text{ if } a > d \\ t^{d\nu-2} \ln t^{-\nu}, \text{ if } a = d \\ t^{a\nu-2}, \text{ if } a < d \end{cases} \tag{1.88}$$

Thus for $a \geq d$ the short range Harris criterion Eq. (1.85) is obtained whilst for $a < d$ one obtains

$$\nu > \frac{2}{a} \tag{1.89}$$

In fact for the case of a Gaussian disorder distribution it was argued that if the fixed point is unstable towards a new long-range-disorder fixed point then $\nu = 2/a$ should be exactly fulfilled [48].

The cases 1-3 can be seen as disorder living on $d_0 = 0, 1, 2$ dimensional, potentially interconnected, subspaces. Although the defect correlations are not power law like the stability criteria obtained correspond to $\nu > 2/a$ with $a = (d - d_0)$. In Ref. [1] the 3DXY model with disorder corresponding to the case 2 is found to flow towards a new critical fixed point in agreement with $\nu = 1$ marginally violating the extended Harris criterion Eq. (1.86) but in agreement with the marginal behavior of the last case.

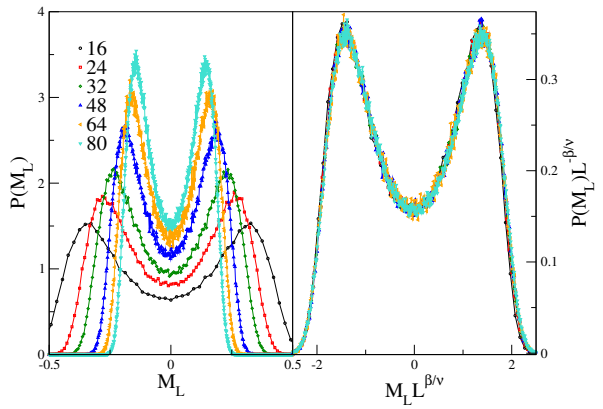

Figure 1.3: If quantities are described by universal scaling functions then their respective histograms are also universal. The magnetization per spin $M_L = L^{-d}\sum_{\boldsymbol{r}} S(\boldsymbol{r})$ for the 3D Ising model as defined via Eq. (1.66) shows a characteristic symmetric double peak structure close to T_c with constant free energy barrier ΔF.

1.16 Continuous vs. discontinuous phase transitions

At a continuous transition the correlation length ξ diverges leading to the scaling behavior described in Sec. 1.6. At a discontinuous or first order transition ξ is finite. If a system is studied numerically, without any prior knowledge, it cannot be excluded that ξ is very large but finite at the transition. Then the transition is weak first order and scaling proceeds towards a second order transition with scaling properties as $\xi \sim t^{-\nu}$ until very close to the singularity, where a first order transition occurs instead. This happens in the 2D five state Potts model where ξ is of the order of a 1000 lattice spacings which makes it difficult to determine the nature of the transition via finite-size scaling methods [49]. To distinguish between weak first order transitions and continuous transitions is generally very hard. Thermodynamic averages of quantities such as the specific heat, that are expected to show discontinuous behavior at a first order transition exhibit severe crossover effects [50]. To distinguish between discontinuous and continuous transitions using numerical simulations one usually studies energy or magnetization histograms close to T_c [51, 50, 52].

Lee-Kosterlitz method

Lee and Kosterlitz [50, 52] proposed a numerical method based on the properties of the energy histogram at T_c. In simulations of a system with size L a specific realization $X_{\mathcal{O}}$ of an observable $\mathcal{O}$ performing N_s measurements at inverse temperature

β is achieved

$$\mathcal{N}(\beta, X_{\mathcal{O}}) = \frac{N_s}{Z(\beta)} \sum_E g(E, X_{\mathcal{O}})\, e^{-\beta E} = e^{-\beta A(\beta, X_{\mathcal{O}}, L, N_s)} \tag{1.90}$$

times. Here E labels the energy levels of the underlying Hamiltonian H and $g(E, X_{\mathcal{O}})$ the joint density of states with energy $H = E$ and $\mathcal{O} = X_{\mathcal{O}}$. The quantity $A(\beta, X_{\mathcal{O}}, L, N_s)$ defined in the last step of Eq. (1.90) is, up to N_s and β dependent additive terms, the free energy $F(\beta, \mathcal{O}, L)$. Evaluating differences in $A(\beta, \mathcal{O}, L, N_s)$ at fixed L, β, N_s thus becomes equivalent to evaluating free energy differences. Calculating the probability histogram $P_L(\beta, X_{\mathcal{O}}) = \mathcal{N}(\beta, X_{\mathcal{O}})/N_s$ during a numerical simulation thus yields $A(\beta, X_{\mathcal{O}}, L, N_s) = -\frac{1}{\beta}\log[P_L(\beta, X_{\mathcal{O}})]$. Free energy differences ΔF between two values $X_{\mathcal{O}_1}$ and $X_{\mathcal{O}_2}$ can thus be simply calculated via

$$\Delta F(\beta, X_{\mathcal{O}_1}, X_{\mathcal{O}_2}, L) = F(\beta, X_{\mathcal{O}_1}, L) - F(\beta, X_{\mathcal{O}_2}, L) = \frac{1}{\beta}\log\left[\frac{P_L(\beta, X_{\mathcal{O}_2})}{P_L(\beta, X_{\mathcal{O}_1})}\right] \tag{1.91}$$

The histogram P_L has characteristically different features at first and second order transitions. For first order transitions, with finite ξ, the competing phases coexist at the transition point. Assuming now for simplicity that $\mathcal{O}$ takes the values $\mathcal{O}_{\text{dis}}$ and $\mathcal{O}_{\text{o}}$ within each respective phase this means that P_L has to have peaks of equal height $P_L = P_{\max}$ at both values. Between these two maxima P_L decays and has a minimum $P_{\min}$ at $\mathcal{O}_{\min}$ indicating the presence of a "domain wall" separating the phases. With Eq. (1.91) the interpretation is clear. The decay in the probability for the simulation to visit the region between $\mathcal{O}_{\text{o}}$ and $\mathcal{O}_{\text{dis}}$ corresponds to a free energy barrier of height

$$\Delta F(\beta, \mathcal{O}_{\text{dis}}, \mathcal{O}_{\min}, L) = \Delta F(\beta, \mathcal{O}_{\text{o}}, \mathcal{O}_{\min}, L) = \frac{1}{\beta}\log\left[\frac{P_{\max}}{P_{\min}}\right] \tag{1.92}$$

If $\xi \ll L$ then at a first order transition the free energy barrier scales as

$$\Delta F \sim L^{(d-1)} \tag{1.93}$$

but might show corrections if $\xi > L$. In general one considers temperature- and field-driven transitions. The hallmark of temperature-driven first order PT's is the presence of latent heat ΔH. The observable whose free energy dependence is of interest thus is the internal energy $\mathcal{O} = H$. The difference $\Delta H_L = |H_1 - H_2|$ between the characteristic energy values values where P_L is maximal for a fixed system size corresponds to the latent heat and needs to stay finite for $L \to \infty$. So the mere presence of a double peak in P_L is not enough. If the peaks approach each other and collapse onto a single one the transition is continuous in the thermodynamic limit. At field-driven transitions as for example in the 3D Ising model the quantity to monitor is the 3D Ising magnetization $\mathcal{O} = M$ Eq. (1.66). For temperatures below the critical point $t = h = 0$ the transition is first order with increasing

free energy barrier. Approaching the critical line from $h \to 0^-$ or $h \to 0^+$ the magnetization jumps discontinuously between M_- and M_+ in the thermodynamic limit. At T_c the transition becomes second order and as $m_L = M/L^d \sim L^{-\beta/\nu}$ and thus $P_L\left(mL^{-\beta/\nu}\right) \sim L^{\beta/\nu}$, both the magnetization and the double peak structure vanish in the thermodynamic limit whilst the free energy barrier Eq. (1.92) stays constant. In fact as according to Eq. (1.92) $L^{-\beta/\nu}m$ is described by a universal scaling function the histogram of $P_L(m)$ can be collapsed on a universal histogram as shown in Fig. 1.3. In cases where $\xi \gg L$ then the mere increase of the free energy barrier with system size might be taken as indication of a weak first order transition if at the same time the difference $\Delta\mathcal{O} = |\mathcal{O}_{\rm dis} - \mathcal{O}_{\rm o}|$ remains non-vanishing in the thermodynamic limit.

Response functions and Binder cumulant

Before the advent of the histogram reweighting methods [53, 54] and generalized ensemble methods such as replica exchange MC and Wang Landau sampling [55, 56, 57] it was close to impossible to obtain reliable histograms P_L for large system sizes. However much can be learned about the global properties of the histograms by considering simple thermodynamic response functions such as the specific heat c_s and the spin susceptibility χ as well as the expectation value of the moments $\langle\mathcal{O}^n\rangle$. Quite generally assuming that the system spends a fraction $P_{\rm o}$ of the simulation time in the ordered phase then if the double peak structure was infinitely sharp

$$\langle\mathcal{O}^n\rangle = P_{\rm o}\mathcal{O}_{\rm o}^n + (1-P_{\rm o})\,\mathcal{O}_{\rm dis}^n \tag{1.94}$$

follows. In that limit the leading contributions to the specific heat scale as

$$c_s \sim L^d\beta^2\frac{\langle H^2\rangle - \langle H\rangle^2}{L^{2d}} \sim L^d\beta^2 P_{\rm o}\,(1-P_{\rm o})\,\frac{\Delta H^2}{L^{2d}} \sim L^d \tag{1.95}$$

where a similar relation for the susceptibility can be found at a field-driven transition. Although this argument is grocely oversimplified it can be backed up by phenomenology [58, 51] and also rigorously by RG theory [59]. Binder [51] introduced the normalized fourth order cumulant

$$V_L = 1 - \frac{\langle H^4\rangle_L}{3\langle H^2\rangle_L^2} \tag{1.96}$$

which by Eq. (1.94) should show a minimum at T_c asymptotically saturating at[2]

$$V_\infty = 1 - \frac{2}{3}\frac{H_{\rm o}^4 + H_{\rm dis}^4}{\left(H_{\rm o}^2 + H_{\rm dis}^2\right)^2} \tag{1.97}$$

only in case that the double peak structure survives in the thermodynamic limit. Away from the transition it approaches a trivial limit $V_\infty^* = 2/3$. In case that the transition is continuous then the minimum converges to V_∞^* even at T_c.

[2] This value of V_∞ in general is inconsistent with simulations [52] but shall here simply illustrate the emergence of a nontrivial value in the binder ratio.

Chapter 2

Superfluidity and Superconductivity

Low temperature physics made a giant leap in 1908 when the dutch physicist Heike Kamerlingh Onnes successfully liquified ^{4}He in Leiden. Soon after that, in 1911, he discovered that the resistance of mercury drops from 0.1 Ω to essentially zero below 4.2 K within 0.01 K [60]. Achieving temperatures as low as 1.8 K he ironically did not realize that at the same day that his refrigerant went through a superfluid transition at the so called lambda temperature $T_\lambda = 2.17$ K, but only noticed that the boiling of ^{4}He suddenly stopped above the lowest temperatures [61]. Whereas the field of superconductivity took its next leap in 1933 with the discovery of the Meissner-Ochsenfeld effect [62] establishing the superconducting phase as a true thermodynamic state it took until 1937 when Kapitza [63] and Allen and Misener [64] independently discovered the frictionless flow of ^{4}He through narrow capillaries. The development on the theory side was much slower. This chapter is devoted to briefly discuss some remarkable properties of superfluids and superconductors and finally to introduce a generalization to the Landau theory of phase transitions applicable to numerically study strong fluctuations in superconductors and superfluids and to model novel superfluids the Ginzburg Landau (GL) theory [65].

2.1 Bose-Einstein condensation

The connection between superfluidity and Bose-Einstein condensation (BEC) was first made by Fritz London [66] in 1938. Bose [67] originally had derived Planck's law [68] in 1924 by considering the statistical mechanics of a quantum gas of photons with discrete energy levels without the need to invoke further assumptions and semiclassical approximations as had been necessary before. Einstein [69] subsequently generalized this idea to massive free particles with dispersion relation $\epsilon_{\boldsymbol{p}} = p^2/2m$ and average number per mode

$$\langle n_{\boldsymbol{p}} \rangle = \frac{1}{e^{\beta(\epsilon_{\boldsymbol{p}} - \mu)} - 1} \tag{2.1}$$

and found that this ideal Bose gas exhibits a phase transition at the temperature

$$T_{\mathrm{BEC}} \approx \left(\frac{2\pi\hbar^2}{mk_B}\right)\left(\frac{\langle n\rangle}{2.612}\right)^{\frac{2}{3}} \tag{2.2}$$

below which the chemical potential μ vanishes. In this limit Eq. (2.1) allows a macroscopic occupation of the zero momentum ground state in the sense that the ratio

$$\frac{\langle n_{\boldsymbol{p}=0}\rangle}{\langle n\rangle} = 1 - \left(\frac{T}{T_{\mathrm{c}}}\right)^{3/2} \tag{2.3}$$

, where n is the total particle density, becomes finite. Thus a complex many-body problem could be described in terms of a single-particle wave function

$$\Psi_0\left(\boldsymbol{r}\right) = \left.\frac{e^{i\frac{\boldsymbol{p}}{\hbar}\boldsymbol{r}}}{V^{1/2}}\right|_{\boldsymbol{p}=0} \equiv \frac{e^{i\theta}}{V^{1/2}} \tag{2.4}$$

where θ an arbitrary phase independent of $\boldsymbol{r}$. It took long, until 1995 when BEC was first experimentally realized at the extraordinarily low temperature of 170 nK, resulting in the 2001 Nobel prize for Eric Cornell, Carl Wieman and Wolfgang Ketterle [70, 71, 72]. For interacting systems the eigenvalues ϵ_i of the one-particle density matrix $\rho\left(\boldsymbol{r},\boldsymbol{r}'\right)$ determine if BEC occurs [73, 74]. If $\Psi_s\left(\boldsymbol{r}_1\ldots\boldsymbol{r}_N\right)$ denotes a set of properly symmetrized, mutually orthogonal, pure many-body states, the one-particle density matrix can be expressed as the weighted sum [74]

$$\rho\left(\boldsymbol{r},\boldsymbol{r}'\right) = N\sum_s c_s \int dr_2\ldots r_N \Psi_s^*\left(\boldsymbol{r},\boldsymbol{r}_2\ldots\boldsymbol{r}_N\right)\Psi_s\left(\boldsymbol{r}',\boldsymbol{r}_2\ldots\boldsymbol{r}_N\right) \tag{2.5}$$

If there exists a single eigenvalue ϵ_i of macroscopic order N then *simple* BEC occurs. In case that not only one, but a finite number of macroscopic eigenvalues exist the system exhibits *fragmented* BEC. If all eigenvalues are of order unity the system is *normal*. Generally the condensate fraction can be defined via

$$n_0 = \lim_{|\boldsymbol{r},\boldsymbol{r}'|\to\infty} \rho\left(\boldsymbol{r}-\boldsymbol{r}'\right) \tag{2.6}$$

meaning that the system shows off-diagonal long range order (ODLRO) [75]. Spatial variations in the phase $\theta\left(\boldsymbol{r}\right)$ imply a mass current density of

$$\mathbf{j}_s = \frac{1}{2mi}\left[\Psi_0^*\left(\boldsymbol{r}\right)\nabla\Psi_0\left(\boldsymbol{r}\right) - \Psi_0\left(\boldsymbol{r}\right)\nabla\Psi_0^*\left(\boldsymbol{r}\right)\right] = \frac{\hbar}{m}\left|\Psi_0\left(\boldsymbol{r}\right)\right|^2\nabla\theta\left(\boldsymbol{r}\right) \tag{2.7}$$

which can be used to define the superfluid velocity

$$\mathbf{v}_s\left(\boldsymbol{r}\right) = \frac{\hbar}{m}\nabla\theta\left(\boldsymbol{r}\right) \tag{2.8}$$

This has the remarkable consequence that superfluids allow for vortices, just like the $O(2)$ model discussed in Ch. 1. Due to the requirement of singlevaluedness of $\Psi(\boldsymbol{r})$ any contour integral needs to obey

$$\oint_C \nabla\theta(\boldsymbol{r}) \cdot d\boldsymbol{r} = 2\pi n \tag{2.9}$$

for any closed curve C. The circulation κ of such a vortex is *quantized* in integer multiples of h/m. Although the identification of BEC and superfluidity seems tempting the general relation is a subtle one, as shall be clarified in the next section.

2.2 Liquid Helium

Ironically there are basically only two bulk superfluids that have been realized in the laboratory. The only stable helium isotopes ^{4}He and ^{3}He. The multiple superfluid phases in the latter where discovered 35 years after those of ^{4}He at temperatures of $2-3$ mK roughly 1000 times lower than $T_\lambda \approx 2.17$ K and where first thought to be new solid phases [76, 77, 78]. In this thesis we are only concerned with ^{4}He. Helium is the second lightest and second most abundant element found in our universe. The atom ground state is $^1S_0$ and thus a boson. The pair interactions can be modeled by a Lennard-Jones potential $V_{\mathrm{LJ}}(\boldsymbol{r}) = 4\epsilon\left[(\sigma/r)^{12} - (\sigma/r)^6\right]$, with a minimum of roughly ~ 11 K at a nuclear separation of ~ 3 Å, or the more exact Aziz potential [79] which frequently is used in first principle path integral Monte Carlo (PIMC) simulations [26, 80]. The differences are small as shown in Fig. 2.1 (B). In contrast to the ideal Bose gas above ^{4}He is strongly interacting due to the hard wall for separations $r < 2.6$ Å. At temperatures below the liquification point $T \approx 4$ K the thermal de Broglie wave length $\Lambda = h^2/\left(\sqrt{2\pi m k_B T}\right)^{-1/2} \approx 4$ Å and thereby roughly matches the typical inter-particle distance reported in [26] defining ^{4}He as a quantum liquid. As shown in the phase diagram Fig. 2.1 (C) ^{4}He never freezes under its own vapor pressure. Only above 26 atm (= 26.3458 hPa) is the solid phase stable [74]. Until recently this feature was mainly attributed to the fact that the zero-point motion of ^{4}He overcompensates the weak interaction between the atoms. Recently, it has been shown that the role of Bose statistics is much more important in preventing solidification [81, 82]. Another manifestation of superfluidity apart from frictionless capillary flow is that a fraction of the fluid does not couple to moving boundaries. Andronikashvili [83] proved this experimentally by immersing a stack of rotating disks with small separation into ^{4}He showing that only a decreasing fraction was dragged along below T_λ. Later Hess and Fairbank [84] showed for bulk helium in a rotating container that the λ-transition is accompanied by the appearance of non classical rotation inertia for small rim velocities meaning only a fraction of the ^{4}He follows the motion of the container walls. This fraction usually is referred to as the normal component or He-I whereas the other component whose constituents freely move through the normal background is called superfluid or He-II.

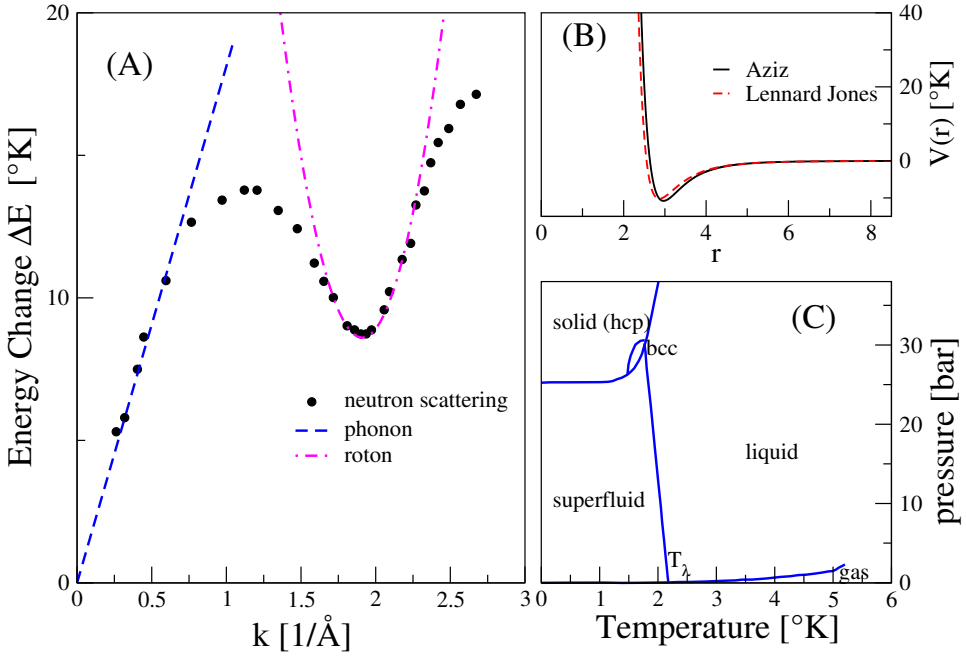

Figure 2.1: Selected properties of ^{4}He. (A) The excitation spectrum in the superfluid phase. For small scattering wave vectors the spectrum is phonon like and linear. Above 0.6 Å^{-1} it however becomes highly nonlinear and exhibits a parabolic roton-minimum (see Eq. (2.12)) around $k \approx 1.91$ Å. The experimental data has been taken from the neutron scattering measurements at 1.1K in [85]. (B) Comparison between the Aziz potential and a standard 12-6 Lennard-Jones potential with the de Boer-Michels parameters $\sigma = 2.556$ Å and $\epsilon = 10.22$ K. The minimum of the Aziz potential lies at roughly $r \approx 2.96744$ Å. Obviously ^{4}He cannot be treated as a free boson gas. (C) Sketch of the low temperature phase diagram of ^{4}He [26].

The fact that there is a critical velocity v_c below which there are no excitations was introduced as the hallmark of a superfluid by Landau. He derived a simple criterion

$$v_c = \min\left(\frac{\epsilon_{\boldsymbol{p}}}{p}\right) \tag{2.10}$$

implying $v_c = 0$ for the ideal Bose gas which hence is not regarded as a superfluid. For low momenta ^{4}He however approximately follows the linear dispersion relation

$$\epsilon_{\boldsymbol{p}} = cp \tag{2.11}$$

where $c \approx 237$ m/s [85]. This dispersion is also qualitatively obtained in the weakly interacting Bogolyubov limit of the Bose gas. However the actual ^{4}He spectrum is nonlinear. The critical velocity would roughly correspond to the location of the so called *roton minimum*. There the dispersion curve can be approximated by

$$\epsilon_{\boldsymbol{p}} = \Delta_{\text{Roton}} + \frac{(p-p_0)^2}{2m^*} \tag{2.12}$$

using $\Delta_{\text{Roton}} = 8.6$K, $m^* \approx 0.16 m_{^4\text{He}}$ and $p_0/\hbar = 1.91$ Å^{-1} [85] as shown in Fig. 2.1 (A) . Applying the relation Eq. (2.10) to the data the roton minimum corresponds to roughly $v_c = 60$ m/s at saturated vapor pressure [74]. The experimental value however is much lower due to creation of vortices as shown by Feynman [86]. The 3D superfluid transition at T_λ is continuous and the correlation length critical exponent has been determined as $\nu = 0.6709 \pm 0.0001$ in high-precision measurements in zero gravity [87]. This result corresponds to the 3DXY (or $O(2)$) universality class introduced in Ch. 1 and can be obtained as the *phase-only* or *London* limit of the 3D GL theory to be presented in the next sections. As mentioned in 2D the XY universality class goes through the Kosterlitz-Thouless transition [13] but it can be shown that there is no BEC in 2D and therefore BEC is no prerequisite of superfluidity.

2.3 Ginzburg-Landau theory of superconductivity

Against common lore the ability of some materials to sustain the flow of electric current without resistance is not the defining property of superconductivity as a thermodynamic phase. A superconductor, in contrast to a hypothetical perfect metallic conductor, in addition behaves as a perfect diamagnet in the Meissner phase below T_c [62]. There magnetic fields are shielded out completely, independently from the initial condition of whether cooling started within an applied external magnetic field or not. The first successful theoretical explanation of this effect was given 1935 by the London brothers [88]. Motivated by the two fluid model of ^{4}He and by the logical assumption that the magnetic field only could be expelled by a surface current penetrating with some finite characteristic depth λ they derived

the London equations

$$\frac{\partial \mathbf{J}_s}{\partial t} = \frac{n_e e^2}{m}\mathbf{E}, \qquad \nabla \times \mathbf{J}_s = -\frac{n_e e^2}{m}\mathbf{B}. \tag{2.13}$$

where n_e is the charge carrier number density and the latter using Ampères law $\mu_0 \mathbf{J} = \nabla \times \mathbf{B}$ can be rephrased to

$$\left(\nabla^2 - \lambda^{-2}\right)\mathbf{B} = 0 \tag{2.14}$$

Thus static magnetic fields are screened out on a length scale $\lambda = \sqrt{m/\mu_0 e^2 n_e^2}$ a relation that had been predicted already in 1925 by de Haas-Lorentz [89]. Although this was a big achievement, it could not explain why superconductivity was destroyed in strong magnetic fields. A major phenomenological breakthrough was made in the seminal paper by Ginzburg and Landau [65] who realized that the original Landau theory could be generalized to complex order parameters

$$\Psi(\boldsymbol{r}) = |\Psi(\boldsymbol{r})| e^{i\theta(\boldsymbol{r})} = \sqrt{n_s(\boldsymbol{r})} e^{i\theta(\boldsymbol{r})} \tag{2.15}$$

where n_s is the condensate density motivated by the quantum mechanical origin of the problem. If the condensate is charged it couples to a gauge field $\mathbf{A}(\boldsymbol{r})$ via its charge q. Equation (1.1) thus generalizes to

$$\mathcal{L}[\Psi, \mathbf{A}, \mathbf{H}] = \int d^d r \left[\alpha(T)|\Psi(\boldsymbol{r})|^2 + \frac{b}{2}|\Psi(\boldsymbol{r})|^4 + \frac{1}{2m^*}\left|\left(-i\hbar\nabla - q\mathbf{A}(\boldsymbol{r})\right)\Psi(\boldsymbol{r})\right|^2 + \frac{\left[\nabla \times \mathbf{A}(\boldsymbol{r})\right]^2}{2\mu_0} - \left(\nabla \times \mathbf{A}(\boldsymbol{r})\right)\mathbf{H}\right] \tag{2.16}$$

which can on a mean field level be seen as the free energy difference between the superconducting and the normal state. In absence of an external field the uniform mean field solution of Ψ below $T_{\mathrm{c,MF}}$ is again given by the right hand side of Eq. (1.9). Allowing for spatial inhomogeneities varying Eq. (2.16) with respect to $\Psi(\boldsymbol{r})$ yields the *first GL equation*

$$\alpha(T)\Psi(\boldsymbol{r}) + b|\Psi(\boldsymbol{r})|^2\Psi(\boldsymbol{r}) + \frac{1}{2m^*}\left(-i\hbar\nabla - q\mathbf{A}(\boldsymbol{r})\right)^2\Psi(\boldsymbol{r}) = 0 \tag{2.17}$$

On the other hand variation with respect to $\mathbf{A}$ gives the *second GL equation*

$$\mathbf{J}_s = \frac{q}{2m^*}\Re\left\{\Psi^*(\boldsymbol{r})\left(-i\hbar\nabla - q\mathbf{A}(\boldsymbol{r})\right)\Psi(\boldsymbol{r})\right\} = \frac{q}{m^*}|\Psi(\boldsymbol{r})|^2\left(\hbar\nabla\theta(\boldsymbol{r}) - q\mathbf{A}(\boldsymbol{r})\right) \tag{2.18}$$

defining the *supercurrent* density. In the Meissner phase, inside the superconductor, $|\Psi|^2$ is constant and no vortices appear. Taking the curl Eq. (2.18) becomes equivalent to the second equation in Eq. (2.13) retrieving the London penetration depth

$$\lambda = \sqrt{\frac{m^*}{\mu_0 q^2 |\Psi|^2}} \tag{2.19}$$

as an intrinsic length scale of the GL theory. Initially q/m^* were thought to correspond to the electron charge-mass ratio until the advent of BCS [90] who showed that an arbitrarily weak attractive interaction between electrons destabilizes the Fermi surface in such a way that electrons of opposite momenta and spin form Cooper pairs, bosonic quasi particles of mass $m^* = 2m_e$ and charge $q = (-2e)$. This leads to a gap Δ in the single particle excitation spectrum. Such an attractive mechanism was found in the interaction between the electrons and the lattice vibrations. BCS successfully predicts the Meissner effect and the upper critical field and reproduced electronic heat capacity as well as the temperature dependence of the penetration depth. Due to the accidental cancellation of the transformation $n_e \to n_e/2, e \to 2e, m \to 2m$ the London penetration depth in Eq. (2.14) is the same even if the wrong naive assumption is made that the condensate is related to single electron wave functions. The same year as BCS Gor'kov [91] showed that the GL phenomenology can be obtained as a limiting case of BCS theory and that the order parameter Ψ directly is related to the Cooper pair wave function and directly proportional to Δ.

Equations (2.9) and (2.18) together imply that the magnetic flux Φ is quantized in units of the magnetic flux quantum

$$\Phi_0 = \frac{h}{q} \tag{2.20}$$

In neutral superfluids the analog is the quantization of the angular momentum below T_c also observed in the Hess Fairbank experiment [84]. Apart from λ, Eq. (2.16) includes yet another characteristic length scale the *coherence length*

$$\xi = \sqrt{\frac{\hbar^2}{2m^* |\alpha|}} \tag{2.21}$$

which can be seen as the shortest distance on which fluctuations in the order parameter are allowed without causing a breaking of the Cooper pairs. For neutral superfluids $q \to 0$, such as ^{4}He, ξ corresponds to the characteristic vortex core radius where the superfluid density is suppressed. Actually via suitable rescaling Eq. (2.16) is entirely characterized by the ratio $\kappa = \lambda/\xi$. The mean-field phase diagram can be divided into two characteristic regions separated along the line $\kappa = 1/\sqrt{2}$ defining different regimes of vortex interaction. For $\kappa > 1/\sqrt{2}$ the surface energy becomes negative and thus was deemed unphysical by GL. Abrikosov showed that an intermediate state with magnetic flux lines penetrating the sample in an ordered lattice form (Shubnikov phase) was possible [92]. Superconductors have since then been separated into two categories characterized by their response to an externally applied magnetic field. Materials like Al and Sn with $\kappa < 1/\sqrt{2}$ are called type-I superconductors and can for small values of κ be excellently described by mean-field or BCS theory if fluctuation effects are negligible. For type-I below T_c an applied magnetic field $H < H_c$ is completely screened out of the bulk. Above H_c superconductivity is destroyed. This differs from the type-II regime $\kappa > 1/\sqrt{2}$ where

Cooper pairs are strongly bound and $\xi(T)$ is very small. For small external fields $H < H_{c1}$ again all magnetic flux is expelled from the bulk. But above the lower critical field $H_{c1} < H < H_{c2}$ the Shubnikov phase is found. Beyond the mean field approach the order of the superconducting transition in the type-I and type-II dichotomy at *finite temperatures* has been a long standing fundamental question. Since a classical work by Halperin, Lubensky and Ma [14] it has been established that gauge field fluctuations in extremely type-I superconductors generate a cubic term in the GL functional if fluctuations in the order parameter can be ignored. The transition thus is discontinuous as motivated in Ch. 1. Erroneously this was thought to apply also to the type-II limit. Dasgupta and Halperin [93] subsequently corrected this, showing that type-II superconductors undergo a continuous transition in the universality class of the inverted XY model treated in Ch. 3. The breakdown of superconductivity in the type-II limit is driven by the proliferation of vortex loops [93, 94, 95]. While the limiting cases are well investigated, the value of Ginzburg-Landau parameter $\kappa = \lambda/\xi$ at which the phase transition changes from second to first order is much harder to establish. Monte-Carlo simulations [96, 97] indicate that the correct boundary is $\kappa_{\mathrm{tri}} = (0.76 \pm 0.04)/\sqrt{2}$ slightly smaller than $\kappa_c = 1/\sqrt{2}$ in agreement with previous theoretical work [98].

Up to the 1980's the largest transition temperature observed was roughly 20 K. In 1986 Bednorz and Müller [99] at IBM Zürich discovered the high-T_{c} cuprates with T_{c} in the 30 K range as the result of a systematic research effort. All of these fall within the type-II class. Today materials have been developed leading to critical temperatures of around 133 K [100]. At such temperatures BCS theory fails and a precise theoretical understanding has still not been achieved. Interestingly the neutral superfluid ^{4}He can be seen as extreme type-II limit with $\kappa \to \infty$. This explains why the vortex transition for ^{4}He and many high-T_{c} superconductors share the same critical exponents.

After the success of BCS it was also proposed that superconducting materials even may exhibit multiple gaps [101]. But it took four decades until magnesium diboride became the first experimentally confirmed two-gap (or two band) superconductor [102, 103, 104]. Even in this case GL theory can be derived from microscopic models [105] but then is extended to contain multiple complex order parameters to describe the electrons in the different bands.

2.4 Multi component GL theory and vortex interactions

The concept of several superfluid components is not limited to the case of multi-gap superconductors. Similar behavior is expected for the multiple baryonic components found in the inner cores of neutron stars forming a proton superconductor and neutron superfluid [106]. The state of liquid metallic hydrogen projected to occur around $260-270$ GPa at room temperature is another application of the formalism [107, 108]. Equation (2.16) is easily generalized to multiple components. Using $D_{k,b} = (\hbar\nabla - iq_b\mathbf{A}(\boldsymbol{r}))_k$ and $\psi_b = |\psi_b| e^{i\theta_b(\boldsymbol{r})}$ where $k = 1, \ldots, d$ denotes the spatial

vector components and $b = 1 \ldots n$ denotes the respective n superfluid constituents gives

$$\mathcal{L}\left(\{\psi_b, \mathbf{A}\}\right) = \sum_{b,k} \frac{1}{2m_b} (D_{k,b}\psi_b)^* D_{k,b}\psi_b + \mathcal{V}\left(\{\psi_b\}\right) + \frac{1}{2\mu_0}(\nabla \times \mathbf{A})^2 \tag{2.22}$$

In the remainder only consider the case of equal charges $q_b = q$, masses $m_b = m$ and two components $n = 2$. The potential term shall be decomposed into the sum ordinary GL forms plus a problem symmetry dependent interaction $\mathcal{V}_{sym}\left(\{\psi_b\}\right)$ which has to be gauge invariant. It only can contain terms dependent on the moduli $|\psi_b|$, and on the phase differences $\theta_b - \theta_{b'}$ such as Josphson interband coupling $|\psi_b|\,|\psi_{b'}|\cos\left(\theta_b - \theta_{b'}\right)$, if the components are allowed to mix. Thus assume

$$\mathcal{V}\left(\{\psi_b\}\right) = \sum_b \alpha_b |\psi_b|^2 + \frac{\beta_b}{2}|\psi_b|^4 + \mathcal{V}_{sym}\left(\{\psi_b\}\right) \tag{2.23}$$

Negative coefficients α_b are called active bands, and positive, passive bands and as before $\beta_b > 0$. As in Sec. 1.14 isolated vortices in a single component of Eq. (2.22) have divergent energy per unit length. Only composite integer N-flux quantum vortices where both components encircling the vortex core on a contour γ obey $\oint_\gamma \left(\nabla\theta_b\right) d\boldsymbol{r} = 2\pi N$ with the same N can be produced with finite energy cost in an infinite system [109]. Allowing for spatial variations the total free energy is stationary when

$$D_{k,b}D_{k,b}\psi_b = 2m\frac{\partial \mathcal{V}}{\partial \psi_b^*} \tag{2.24}$$

$$\partial_k(\partial_k A_l - \partial_l A_k) = -\sum_{b=1}^{n} \frac{\mu_0 q}{m} \Im\left\{\psi_b^* D_l \psi_b\right\}. \tag{2.25}$$

The system has been studied intensively in 2D and for the case of $n = 2$ components.

Ground state properties of the two band superconductor in 2D

Following [110] we focus on the asymptotic solution of the field equations and the static vortex interaction potential for coinciding, composite vortices of equal phase winding. For axially symmetric, well separated, composite vortices of equal unit phase winding $N = 1$ in polar coordinates (r, θ) one can make the ansatz

$$\begin{aligned} \psi_b &= f_b(r)e^{i\theta} \\ (A_x, A_y) &= \frac{a(r)}{r}(-\sin(\theta), \cos(\theta)) \end{aligned} \tag{2.26}$$

with $\theta_1 = \theta_2 = \theta$. As $\mathbf{A} = A(r)\,\mathbf{e}_\theta$ and thus $\partial_k A_k = 0$ Eq. (2.25) becomes

$$\partial_k^2 A_l + \sum_{b=1}^{2} \frac{\hbar\mu_0 q\,|\psi_b|^2}{m}\left[(\partial_l\theta_b) - \frac{q}{\hbar}A_l\right] = 0 \tag{2.27}$$

Using the relation $(\partial_x\theta) = -y/r^2$ and $(\partial_y\theta) = x/r^2$ and transforming the Laplacian to polar coordinates the equations

$$a'' - \frac{1}{r}a' + \sum_{b=1}^{2} \frac{\hbar\mu_0 q\left|\psi_b\right|^2}{m}\left(1 - \frac{q}{\hbar}a\right) = 0 \tag{2.28}$$

$$f_b'' + \frac{1}{r}f_b' - \frac{1}{r^2}\left(1 - \frac{q}{\hbar}a\right)^2 f_b = m\frac{\partial}{\partial|\psi_b|}\mathcal{V}\left(\{|\psi_b|, \theta_b - \theta_{b'}\}\right) \tag{2.29}$$

for the gauge field and the densities of the composite vortex with axial symmetry are obtained. Far away from the vortex the amplitudes are given by the uniform values $\lim_{r\to\infty} f_b(r) = u_b = \sqrt{-\alpha_b/\beta_b}$ and the field by $\lim_{r\to\infty} a(r) = \hbar/q$. Outside the core region one assumes that the fields only slightly deviate from these boundary values by ϵ_b, α such that

$$f_b(r) = u_b + \epsilon_b(r), \qquad a(r) = \frac{\hbar}{q} + \alpha(r) \tag{2.30}$$

Then Eqs (2.28) and (2.29) can be linearized if the potential is expanded to second order in the densities

$$\mathcal{V}\left(\{|\psi_b|, \theta_b - \theta_{b'}\}\right) = \mathcal{V}\left(\{u_b\}, 0\right) + \frac{1}{2!}\epsilon_b\mathcal{H}_{bc}\epsilon_c \tag{2.31}$$

around the minimum $(\{u_1, \ldots, u_n, 0\})$. As the Hessian $\mathcal{H}_{ab}$ is a real positive definite symmetric $n \times n$ matrix the linearized equations become

$$\epsilon_b'' + \frac{1}{r}\epsilon_b' = m\sum_{c=1}^{2}\mathcal{H}_{bc}\epsilon_c \tag{2.32}$$

$$\alpha'' - \frac{1}{r}\alpha' - \alpha\sum_{b=1}^{2}\frac{\mu_0 q^2\left|\psi_b\right|^2}{m} = 0 \tag{2.33}$$

Thus in the present approximation $\alpha(r)$ is found to be

$$\alpha(r) = \frac{\tilde{m}}{r}K_1(r/\lambda) \tag{2.34}$$

with screening length λ defined through

$$\lambda^{-1} = \sqrt{\sum_{b=1}^{2}\frac{\mu_0 q^2\left|\psi_b\right|^2}{m}} \tag{2.35}$$

where K_n denotes the n-th modified Bessel's function of the second kind. The real integration constant $\tilde{m}$ can be seen as a dipole moment pointing perpendicular to the x_1x_2-plane associated with the current. Obviously the Hessian $\mathcal{H}_{bc}$ in general

is not diagonal but can be diagonalized for "physical" choices of $\mathcal{V}$. Thus the vector $\epsilon = (\epsilon_1, \ldots, \epsilon_n)$ can be rewritten as a linear superposition in the eigenbase of the Hessian $\epsilon = \sum_{b=1}^{2} \mathbf{h}_b \tilde{g}_b$. Equation (2.32) then decouples to

$$\left(\nabla^2 - \xi_b^{-2}\right) \tilde{g}_b(r) = 0 \tag{2.36}$$

where ξ_b^{-2} are the eigenvalues corresponding to $\mathbf{h}_b$. Specifically in the two component case the eigenbase can be characterized by a single real mixing angle Θ via $\mathbf{h}_1 = (\cos(\Theta), \sin(\Theta))$ and $\mathbf{h}_2 = (-\sin(\Theta), \cos(\Theta))$. The Green's function $G_b(r)$ can be found using the Fourier representation

$$G_b(r) = \frac{1}{(2\pi)^2} \int d^2k \frac{e^{ikr}}{k^2 + \xi_b^{-2}} = \frac{1}{2\pi} K_0(r/\xi_b) \tag{2.37}$$

and mediates screened Coulomb interaction. For $r \gg \xi_b$ where the linearization is applicable the *normal modes*

$$\tilde{g}_b(r) = \frac{Q_b}{2\pi} K_0(r/\xi_b) \tag{2.38}$$

are solutions to Eq. (2.36) and thus

$$\epsilon_1 = \tilde{g}_1 \cos(\Theta) - \tilde{g}_2 \sin(\Theta) \tag{2.39}$$

$$\epsilon_2 = \tilde{g}_1 \sin(\Theta) - \tilde{g}_2 \cos(\Theta) \tag{2.40}$$

to Eq. (2.32). The functions $\tilde{g}_b(r)$ resemble field configurations originating from a monopole point source of charge Q_b located at the origin. Only in some special cases, namely when Θ is an integer multiple of $\pi/2$, can the ξ_b be identified with the respective GL coherence lengths of the individual condensates ψ_b. The gauge field mediates a repulsive force between vortices whilst at the same time the densities (or cores) interact attractively. To calculate the interaction between two composite vortices, one of the pairs can be considered as sources of the field experienced by a second composite vortex brought into the system. This approach is similar to introducing an extra source term [111]

$$\mathcal{L}_{\text{source}}(\{\psi_b, \mathbf{A}\}) = \rho_b \psi_b - \mathbf{j_b} \mathbf{A}_b \tag{2.41}$$

in the free energy functional Eq. (2.22). A distance r far away from the composite vortex a second composite vortex experiences a field equivalent to that created by point particle sources $\rho_b = Q_b \delta(\boldsymbol{r})$ with monopole charge $2\pi Q_b$ and magnetic dipole moment $\tilde{m}$ perpendicular to the xy-plane originating from the current $\mathbf{j} = \tilde{m}(\partial_2, -\partial_1)\delta(\boldsymbol{r})$. The interaction energy of two monopoles with like charge Q_b at positions $\mathbf{y}, \tilde{\mathbf{y}}$ then can be approximated by

$$\begin{aligned} F_{int} &= -\int_{\mathbb{R}^2} d^d x \rho_b \psi_b \\ &= -Q_b \int_{\mathbb{R}^2} d^d x \delta(\mathbf{x} - \mathbf{y}) \frac{Q_b}{2\pi} K_0(|\mathbf{x} - \tilde{\mathbf{y}}|/\xi_b) = -\frac{Q_b^2}{2\pi} K_0(|\mathbf{y} - \tilde{\mathbf{y}}|/\xi_b) \end{aligned} \tag{2.42}$$

and is attractive. Taking all components into account and calculating the magnetic field energy in the very same way the total composite vortex interaction potential becomes [110]

$$V(r) \sim \left[\tilde{m}^2 K_0\left(r/\lambda\right) - Q_1^2 K_0\left(r/\xi_1\right) - Q_2^2 K_0\left(r/\xi_2\right)\right] \tag{2.43}$$

All terms thus correspond to the 2D screened Coulomb interaction with different signs and ranges. The first one corresponds to the current-current interaction screened by the London penetration depth and the other two stem from the densities of both components interacting attractively within the respective bands. In case that at least one of the two length scales $\xi_L = \max\left(\xi_1, \xi_2\right)$ exceeds the London penetration depth λ the resultant pair interaction between vortices can become attractive intermediate ranges. This hierarchy of length scales leads to a non-monotonic interaction which should lead to vortex clusters. This possibly gives rise to the physics of the type-1.5 superconductor which currently is is a subject of intense experimental research on materials where vortex clusters were observed [112, 113, 114, 115, 116, 117]. In Paper III a 3D vortex loop model using a generalization of this asymptotic interaction is studied.

2.5 Supersolidity

The theoretical possibility of a supersolid state was addressed by Legget in 1970 [118]. Before, Penrose and Onsager had found that perfect crystals cannot exhibit ODLRO [73] but had not used properly symmetrized wave functions [119]. In its original interpretation a supersolid would be a state of matter sharing both long-range positional order of the crystal lattice while at the same time allowing for unimpeded coherent mass flow. This supersolid remained elusive despite significant experimental efforts. A review on early experiments can be found in Ref. [120]. This changed dramatically in 2004 due to experiments performed on ^{4}He samples confined to porous vycor glass [121] as well as bulk samples [122]. There torsional oscillator (TO) experiments measured a period drop that was interpreted as the presence of non classical rotation inertia (NCRI) upon reducing the temperature below ≈ 200 mK. This was attributed to an effect of mass decoupling just as in the Hess Fairbank experiment [84] anticipated by Legett [118].

As a true phase transition to a supersolid should leave a signature in other response functions in the same temperature region, heat capacity measurements were carried out and confirmed the presence of a smooth peak close to 100 mK [123, 124, 125]. This profile of the peak was rather unexpected as the superfluid λ-transition has a sharp logarithmically diverging heat capacity peak as its key signature. With the sensation that such a discovery would display subsequent works cast doubt on whether the initial interpretation of the period drop truly was the signature of superfluid mass decoupling. First principle path integral Monte Carlo (PIMC) studies showed that ideal hcp ^{4}He crystals always are insulators [126, 127]. Independent experiments showed that TO results varied wildly with the

surface to volume ratio and that annealing could reduce NCRI below the signal to noise ratio [128, 129]. Clark and coworkers [130] pointed out the strong influence the ^{3}He concentration had on the NCRI onset.

Extended crystal defects such as grain boundaries and dislocations emerged as possible candidates for superfluid mass transport through the helium sample. Indeed grain boundaries were shown to be superfluid below 0.5 K both experimentally and via PIMC [131, 132] but their concentration was far too low to account for the total NCRI [130]. Simple order of magnitude estimates preclude a supersolid transition above the milikelvin range [133, 1]. Strong experimental indications against the dislocation supersolid had already been obtained in 2010 by Reppy whose setup allowed an in situ increase of the degree of disorder in the solid sample via plastic deformation [134]. Although the period shift increased upon deformation this effect was most prominent in the high temperature range and close to invisible for the lowest temperatures quite opposite to the expected behavior for a superfluid like signal. Interestingly simulations of ^{3}He binding to a screw dislocation showed the emergence of a peak in the right temperature interval [135].

Day and Beamish had shown in 2007 that the shear modulus of ^{4}He stiffened at low temperatures in the very same way as the NCRI increased and with the same dependence on the concentration of ^{3}He impurities [136]. As shear modulus stiffening alters the effective torsion constant of the total filled TO the period drop could be an entirely classical effect caused by the decrease in resonance frequency due to an increase in the total torsion constant.

Repeating the 2004 vycor experiment using a new oscillator design precluding any presence of bulk ^{4}He inside the TO the NCRI where shown to vanish completely [137]. Using TOs with two eigenfrequencies Mi and Reppy claim that frequency-dependent elastic signals can entirely account for the observed period shift signals for ^{4}He in vycor [138]. Also in bulk ^{4}He the major contribution was attributed to elastic defects, but also a small additional frequency-independent contribution that might actually indicate the presence of a supersolid fraction as small as 1.6×10^{-4} at 10 mK [138, 139].

Today the story of the existence of a supersolid phase in ^{4}He is not entirely settled and it can surely be seen as one of the most challenging subjects in low temperature physics.

Chapter 3

Duality

The wave particle dualism is central to quantum mechanics. For ^{4}He this dichotomy is evident by the fact that in the superfluid phase it can be treated as a delocalized, macroscopic matter wave, whereas at high pressures the crystal testifies to the presence of localized classical atoms. Similarly, as already encountered in the mapping from the 2DXY model to the 2D Coulomb gas, a proper choice of variables can vastly facilitate the identification of the collective excitations of a system. A theory described by an order parameter field in the original variables then usually can be mapped on another field theory with a disorder parameter vanishing in the ordered phase and nonzero when excitations, mostly in form of topological defects proliferate. For the purposes here a duality transformation generally shall be seen as a change of variables describing the degrees of freedom in the underlying action of the problem. Central to the articles [2, 3, 4] is the mapping of spin models and superconductors on interacting loops.

3.1 Duality transformation of the GL-model for superfluids and superconductors

Consider a general superfluid described by a complex order parameter. Ignoring amplitude fluctuations in Eq. (2.16) one arrives at the London limit

$$\mathcal{L}_{Lond}\left[\theta,\mathbf{A},\mathbf{H}\right]=J\int d^{d}r\left|\left(\nabla-i\frac{q}{\hbar}\mathbf{A}\left(\boldsymbol{r}\right)\right)e^{i\theta(\boldsymbol{r})}\right|^{2}+\lambda^{2}\left[\nabla\times\frac{q}{\hbar}\mathbf{A}\left(\boldsymbol{r}\right)\right]^{2}$$
$$-2\lambda^{2}\mu_{0}\left[\nabla\times\frac{q}{\hbar}\mathbf{A}\left(\boldsymbol{r}\right)\right]\cdot\left[\frac{q}{\hbar}\mathbf{H}\right] \tag{3.1}$$

where λ is given by Eq. (2.19) and

$$J=\frac{\left|\Psi\right|^{2}\hbar^{2}}{2m^{*}} \tag{3.2}$$

All magnetic fields naturally emerge in units of 2π times the unit flux quantum Eq. (2.20) $\Phi_0 = h/q$. Similarly to the 2D $O(2)$ model Eq. (3.1) maps on a model

of interacting topological defects. In the remainder only the case of zero external field is considered and the model is set on a cubic lattice with spacing a_μ where $\mu = \hat{x}, \hat{y}, \hat{z}$ refers to the lattice directions. Whereas ordinary gradients can straight forwardly be discretized $\partial_\mu \to \Delta_\mu$ where Δ_μ is the lattice difference operator, the gauge-invariant gradients need to be replaced by [140]

$$\left[\partial_\mu - i\frac{2\pi}{\Phi_0}A_\mu(\boldsymbol{r})\right]\Psi(\boldsymbol{r}) \to \frac{1}{a_\mu}\left[\Psi_{\boldsymbol{r}+a_\mu\hat{\mu}}e^{-i\frac{2\pi}{\Phi_0}a_\mu A_{\boldsymbol{r},\mu}} - \Psi_{\boldsymbol{r}}\right] \tag{3.3}$$

where

$$A_{\boldsymbol{r},\mu} = \int_{\boldsymbol{r}}^{\boldsymbol{r}+a_\mu\hat{\mu}} A_\mu(\boldsymbol{r})\, d\gamma \tag{3.4}$$

and γ is the curve coinciding with the bond $\boldsymbol{r} \to \boldsymbol{r} + a_\mu\hat{\mu}$. Similarly the Maxwell field energy is replaced by the plaquette sum

$$[\nabla \times \mathbf{A}(\boldsymbol{r})]_\mu \to \frac{1}{a_\mu}\left(\sum_{\nu,\sigma}\epsilon_{\mu\nu\sigma}\Delta_\nu A_{\boldsymbol{r},\sigma}\right) \tag{3.5}$$

Introducing $\mathcal{A}_{\boldsymbol{r},\mu} = \frac{2\pi}{\Phi_0}A_\mu(\boldsymbol{r})$ then ignoring effects of anisotropy and setting a_μ to unity yields

$$\mathcal{L}_{Lond}[\theta,\mathcal{A}] = -2J\sum_{\boldsymbol{r},\mu}\left[\cos(\Delta_\mu\theta_{\boldsymbol{r}} - \mathcal{A}_{\boldsymbol{r},\mu}) - \frac{\lambda^2}{2}\left(\sum_{\nu,\sigma}\epsilon_{\mu\nu\sigma}\Delta_\nu\mathcal{A}_{\boldsymbol{r},\sigma}\right)^2\right] \tag{3.6}$$

The partition function thus becomes

$$\mathcal{Z} = \int\mathcal{D}\theta\int\mathcal{D}\mathcal{A}e^{-\beta\mathcal{L}_{Lond}[\theta,\mathcal{A}]} \tag{3.7}$$

Using $K = 2\beta J$ the fields $\mathcal{A}, \theta$ can be decoupled via the Villain approximation

$$e^{K\cos(x)} \to e^K\sum_{j=-\infty}^{\infty}e^{-\frac{K}{2}(x-2\pi j)^2} \tag{3.8}$$

on each link $\boldsymbol{r}, \boldsymbol{r}+\hat{\mu}$ followed by a Hubbard-Stratonovich transformation

$$e^{-\frac{K}{2}x^2} = \frac{1}{\sqrt{2\pi K}}\int_{-\infty}^{\infty}dv e^{-\frac{v^2}{2K}+ivx} \tag{3.9}$$

where $\mathbf{v}$ is a real dummy field. The partition function then reads

$$\mathcal{Z} = \int\mathcal{D}\theta\int\mathcal{D}\mathcal{A}\int\mathcal{D}v\prod_{\boldsymbol{r}}\sum_{j_{\boldsymbol{r},\mu}=-\infty}^{\infty}e^{-\frac{v_{\boldsymbol{r},\mu}^2}{2K}+iv_{\boldsymbol{r},\mu}(\Delta_\mu\theta_{\boldsymbol{r}}-\mathcal{A}_{\boldsymbol{r},\mu}-2\pi j_{\boldsymbol{r},\mu})-K\frac{\lambda^2}{2}(\epsilon_{\mu\nu\sigma}\Delta_\nu\mathcal{A}_{\boldsymbol{r},\sigma})^2} \tag{3.10}$$

where Einstein's summation convention is implicit. Using the Poisson formula relating the infinite sum over a function to a sum over its Fourier transform

$$\sum_{j=-\infty}^{\infty} e^{2\pi i j v} = \sum_{k=-\infty}^{\infty} \delta\left(v-k\right) \tag{3.11}$$

the $j_{\boldsymbol{r},\mu}$ sum allows the v integration to be performed yielding

$$\mathcal{Z} = \int \mathcal{D}\theta \int \mathcal{D}\mathcal{A} \prod_{\boldsymbol{r}} \sum_{k_{\boldsymbol{r},\mu}=-\infty}^{\infty} e^{-\frac{k_{\boldsymbol{r},\mu}^2}{2K} + i k_{\boldsymbol{r},\mu}(\Delta_\mu \theta_{\boldsymbol{r}} - \mathcal{A}_{\boldsymbol{r},\mu}) - K\frac{\lambda^2}{2}(\epsilon_{\mu\nu\sigma}\Delta_\nu \mathcal{A}_{\boldsymbol{r},\sigma})^2} \tag{3.12}$$

Partially integrating the $\sum_{\boldsymbol{r},\mu} k_{\boldsymbol{r},\mu}\Delta_\mu\theta_{\boldsymbol{r}} = -\sum_{\boldsymbol{r},\mu}\theta_{\boldsymbol{r}}\Delta_\mu k_{\boldsymbol{r},\mu}$ term neglecting surface contributions the phases can be integrated out via

$$\int_{-\pi}^{\pi} e^{-i\theta_{\boldsymbol{r}}\sum_\mu \Delta_\mu k_{\boldsymbol{r},\mu}} = 2\pi\delta_{\nabla\cdot\mathbf{k},0} \tag{3.13}$$

leaving the zero divergence condition

$$\nabla\cdot\mathbf{k} = \Delta_\mu k_{\boldsymbol{r},\mu} = 0 \tag{3.14}$$

of the integer $\mathbf{k}$ field in each vertex of the lattice. The $\mathbf{k}$ field thus can be written as the curl of yet another auxiliary vector field $\mathbf{k} = \nabla\times\mathbf{h}$. Applying the Hubbard-Stratonovich trick also to the magnetic field energy term gives

$$\mathcal{Z} = \int \mathcal{D}\mathcal{A}\int \mathcal{D}v \prod_{\boldsymbol{r}} \sum_{k_{\boldsymbol{r},\mu}=-\infty}^{\infty} e^{-\frac{k_{\boldsymbol{r},\mu}^2}{2K} - i k_{\boldsymbol{r},\mu}\mathcal{A}_{\boldsymbol{r},\mu} - \frac{v_{\boldsymbol{r},\mu}^2}{2K\lambda^2} + i v_{\boldsymbol{r},\mu}\epsilon_{\mu\nu\sigma}\Delta_\nu\mathcal{A}_{\boldsymbol{r},\sigma}} \tag{3.15}$$

$$= \int \mathcal{D}\mathcal{A}\int \mathcal{D}v \prod_{\boldsymbol{r}} \sum_{h_{\boldsymbol{r},\mu}=-\infty}^{\infty} e^{-\frac{(\epsilon_{\mu\nu\sigma}\Delta_\nu h_{\boldsymbol{r},\sigma})^2}{2K} - \frac{v_{\boldsymbol{r},\mu}^2}{2K\lambda^2} - i\mathcal{A}_{\boldsymbol{r},\mu}\epsilon_{\mu\nu\sigma}\Delta_\nu(h_{\boldsymbol{r},\sigma}-v_{\boldsymbol{r},\sigma})} \tag{3.16}$$

Using the Poisson summation rule in reverse order lifts the $h_{\boldsymbol{r},\mu}$ to real valued variables at the cost of introducing an integer field $m_{\boldsymbol{r},\mu}$. The $\mathcal{A}$ integration then gives another constraint

$$\epsilon_{\mu\nu\sigma}\Delta_\nu\left(v_{\boldsymbol{r},\sigma} - h_{\boldsymbol{r},\sigma}\right) = 0 \tag{3.17}$$

implying that $v_{\boldsymbol{r},\mu} - h_{\boldsymbol{r},\mu}$ can be written as the gradient of a scalar potential

$$v_{\boldsymbol{r},\mu} = \Delta_\mu\Phi_{\boldsymbol{r}} + h_{\boldsymbol{r},\mu} \tag{3.18}$$

But as $\mathbf{k}$ is the curl of $\mathbf{h}$ the action Eq. (3.15) is bound to be invariant under the gauge trafo $\mathbf{h}\left(\boldsymbol{r}\right)\to\mathbf{h}\left(\boldsymbol{r}\right)+\nabla\Phi\left(\boldsymbol{r}\right)$ for any function $\Phi\left(\boldsymbol{r}\right)$. The partition function simplifies to

$$\mathcal{Z} = \int \mathcal{D}h \prod_{\boldsymbol{r}} \sum_{m_{\boldsymbol{r},\mu}=-\infty}^{\infty} e^{-\frac{(\epsilon_{\mu\nu\sigma}\Delta_\nu h_{\boldsymbol{r},\sigma})^2}{2K} - \frac{h_{\boldsymbol{r},\mu}^2}{2K\lambda^2} - 2\pi i h_{\boldsymbol{r},\mu} m_{\boldsymbol{r},\mu}} \tag{3.19}$$

$$\int \mathcal{D}h \prod_{\mathbf{q}} \sum_{m_{\mathbf{q},\mu}=-\infty}^{\infty} e^{-\frac{\left(|Q_{\mathbf{q},\mu}|^2+\lambda^{-2}\right)}{2K}|h_{\mathbf{q},\mu}|^2 - i\pi(h_{\mathbf{q},\mu}m_{-\mathbf{q},\mu} + h_{-\mathbf{q},\mu}m_{\mathbf{q},\mu})} \tag{3.20}$$

where $|Q_{\mathbf{q},\nu}|^2 = \sum_\nu (2 - \cos(q_\mu))$ is the square of the lattice difference operator in Fourier representation. Integrating out the $\mathbf{h}$ field, transforming back to real space and for cosmetic reasons replacing $m_{\boldsymbol{r}}$ by $q_{\boldsymbol{r}}$ to connect with Eq. (1.81) finally yields

$$\mathcal{Z} = \sum_{q_{\boldsymbol{r},\mu}=-\infty}^{\infty} e^{-\frac{K}{2}\sum_{\boldsymbol{r},\boldsymbol{r}',\mu} q_{\boldsymbol{r},\mu} V_{\boldsymbol{r},\boldsymbol{r}'} q_{\boldsymbol{r}',\mu}} \delta_{\nabla\mathbf{q},0}. \tag{3.21}$$

where

$$V_{\boldsymbol{r},\boldsymbol{r}'} = \frac{4\pi^2}{L^d} \sum_{\mathbf{k}} \frac{\cos(\mathbf{k}(\boldsymbol{r}-\boldsymbol{r}'))}{\lambda^{-2} + \sum_\mu (2 - \cos(k_\mu))} \tag{3.22}$$

is the Yukawa potential or Greens function of the 3D screened Poisson equation $\left(\nabla^2 - \lambda^{-2}\right) V = \delta$. Observe that in absence of the gauge field $\mathcal{A} = 0$ or by $\lambda \to \infty$ in Eq. (3.12) in principle already Eq. (3.15) provides a fully acceptable mapping on a loop model in any dimension. The phase degrees of freedom living on the lattice vertices are replaced by integer variables living on the bonds connecting the original sites required to form closed loops. In addition the coupling also has been inverted to $1/K = 1/2\beta J$. Comparing to Eq. (3.21) this corresponds a simple contact interaction and thus by the Yukawa analogy a screening length $\lambda = 0$ in Eq. (3.21). So surprisingly one finds that the limits $\lambda \to 0$ and $\lambda = \infty$ need to have the same universal equilibrium properties.

About order parameters

In contrast to global symmetries such as present in the $O(N)$ models local gauge symmetries cannot be spontaneously broken. This result is known as Elitzur's theorem [141]. Hence, in these theories no such thing as a local order parameter can be defined and nonlocal order parameters are necessary. Quite generally for systems like ^{4}He with a global $U(1)$ symmetry the superfluid density can be defined as the response of the system to an infinitesimal uniform phase twist $\Delta\theta = x\Theta/L$. Then the twisted free energy density f_Θ obtained by calculating the partition function under $\mathcal{L}_{Lond}[\theta + \Delta\theta, 0, 0]$ in Eq. (3.1) defines the helicity modulus or phase stiffness $\Upsilon = \frac{1}{2}\frac{\partial^2 f_\Theta}{\partial(\Delta\theta)^2}|_{\Delta\theta=0}$ which is directly proportional to the superfluid density ρ_s [142].

$$\Upsilon_{\hat{x}}(T) = \frac{\beta}{L^d}\left(\left\langle \sum_{\boldsymbol{r}} J^{\hat{x}}_{\boldsymbol{r}} \sin(\theta_{\boldsymbol{r}} - \theta_{\boldsymbol{r}+\hat{x}})\right\rangle^2 - \left\langle \left(\sum_{\boldsymbol{r}} J^{\hat{x}}_{\boldsymbol{r}} \sin(\theta_{\boldsymbol{r}} - \theta_{\boldsymbol{r}+\hat{x}})\right)^2 \right\rangle\right) + \frac{1}{L^d}\left\langle \sum_{\boldsymbol{r}} J^{\hat{x}}_{\boldsymbol{r}} \cos(\theta_{\boldsymbol{r}} - \theta_{\boldsymbol{r}+\hat{x}})\right\rangle \tag{3.23}$$

For charged superfluids one needs to define gauge invariant quantities associated with the proliferation of the topological defects. The helicity modulus can be associated with the dielectric tensor ϵ. In case that vortex loops proliferate or in 2D

charges unbind the medium gets polarized then the helicity modulus becomes the linear response coefficient for an external vector potential perturbation δA_μ [143]

$$\epsilon^{-1} = \lim_{\mathbf{k}\to 0}\left[1 - \frac{JV_{\mathbf{k}}}{L^d T}\langle |q_{\mathbf{k}}|^2\rangle\right] \tag{3.24}$$

For finite screening length λ there is no neutrality restriction on the vortex loops in 3D. The transition then can be detected by measuring the onset of *disorder* using the dimensionless fluctuations $W^2 = \langle W_\mu^2\rangle$ of the vortex loop winding number

$$W_\mu = L^{-d}\sum_{\boldsymbol{r}} q_{\boldsymbol{r},\mu} \tag{3.25}$$

which by construction is dimensionless and thus at a second order transition should obey the simple scaling relation $W^2(L,T) = \tilde{W}\left(L^{1/\nu}t\right)$.

3.2 Loop representation of the Ising model

Before the 2D square lattice Ising model was solved exactly by Onsager using algebraic methods [40, 144] van der Waerden noticed that it could be rewritten in terms of non-overlapping polygons [145]. This allows the partition function to be evaluated by combinatorial methods [146]. The main insight needed is that as $S(\boldsymbol{r}_i)\cdot S(\boldsymbol{r}_i+\hat{\mu}) = \pm 1$ the weight for each lattice bond $\boldsymbol{r}_i, \boldsymbol{r}_{i+\mu}$ in Eq. (1.65) using $K = \beta J$ can be rewritten as

$$e^{KS(\boldsymbol{r}_i)S(\boldsymbol{r}_i+\hat{\mu})} = \cosh(K)\left[1 + S(\boldsymbol{r}_i)\,S(\boldsymbol{r}_i+\hat{\mu})\tanh(K)\right] \tag{3.26}$$

by simply separating even and odd terms contributing to the exponential. Then in general dimension d for hypercubic lattices the partition function becomes

$$\begin{aligned} Z &= \sum_{\{S(\boldsymbol{r})\}}\prod_{\boldsymbol{r}_i,\mu}\cosh(K)\left[1 + S(\boldsymbol{r}_i)\,S(\boldsymbol{r}_i+\hat{\mu})\tanh(K)\right] \\ &= \cosh^{dL^d}(K)\sum_{\{S(\boldsymbol{r})\}}\prod_{\boldsymbol{r}_i,\mu}\left[1 + S(\boldsymbol{r}_i)\,S(\boldsymbol{r}_i+\hat{\mu})\tanh(K)\right] \\ &= \cosh^{dL^d}(K)\sum_{\{S(\boldsymbol{r})\}}\Bigg[1 + \tanh(K)\sum_{i,\mu}S(\boldsymbol{r}_i)\,S(\boldsymbol{r}_i+\hat{\mu}) \\ &\quad + \tanh^2(K)\sum_{\substack{i,j,\mu,\sigma \\ (\boldsymbol{r}_i,\boldsymbol{r}_i+\hat{\mu})\neq(\boldsymbol{r}_i,\boldsymbol{r}_j+\hat{\sigma})}} S(\boldsymbol{r}_i)\,S(\boldsymbol{r}_i+\hat{\mu})\,S(\boldsymbol{r}_j)\,S(\boldsymbol{r}_j+\hat{\sigma}) + \ldots\Bigg] \end{aligned} \tag{3.27}$$

which means that the product has been expanded to a sum over products of spin pairs or bonds. Again as $S(\boldsymbol{r}_i)$ only can take values ± 1 one finds that

$$\sum_{\{S(\boldsymbol{r})\}} S(\boldsymbol{r}_i)^{q_i}\,S(\boldsymbol{r}_j)^{q_j}\,S(\boldsymbol{r}_k)^{q_k}\,S(\boldsymbol{r}_l)^{q_l}\cdots = 2^{L^d} \tag{3.28}$$

only if all q are even $0, 2, \ldots, 2d$, and zero otherwise. Introducing new bond variables J_b where b labels the bond taking the value 1 if the bond is "active" and 0 if the bond is "incative" this translates to configurations where each site $\boldsymbol{r}_i$ is touched by an even number of $J_b = 1$. The allowed configurations thus are closed paths (CP) or loops yielding the loop representation of the Ising model

$$Z = 2^{L^d} \left[1 - e^{-2\beta_{\rm dual}}\right]^{-dL^d/2} \sum_{\{J_b=0,1\}\subset CP} \prod_b e^{-\beta_{\rm dual} J_b} \tag{3.29}$$

where $\beta_{\rm dual} = \operatorname{cotanh}(K) \leftrightarrow \tanh(\beta J) = e^{-\beta_{Dual}}$ and the identity $\cosh(x) = \left[1 - \tanh^2(x)\right]^{-1/2} = \left[1 - e^{-2\beta_{Dual}}\right]^{-1/2}$ has been used. Thus the Ising model has been rewritten in terms of a dual model where low temperatures (large β) are mapped on large temperatures in the dual model (small $\beta_{\rm dual}$). The spin-spin correlation function Eq. (1.67) now becomes

$$\begin{aligned} G(\boldsymbol{r}_\alpha, \boldsymbol{r}_\beta) &= \frac{\cosh^{dL^d}(K) \sum_{\{S(\boldsymbol{r})\}} \prod_{\boldsymbol{r}_i,\mu} S(\boldsymbol{r}_\alpha) S(\boldsymbol{r}_\beta) \left[1 + S(\boldsymbol{r}_i) S(\boldsymbol{r}_i + \hat{\mu}) \tanh(K)\right]}{Z} \\ &= 2^{L^d} \left[1 - e^{-2\beta_{\rm dual}}\right]^{-dL^d/2} \sum_{\substack{\{J_b=0,1\}\subset\mathcal{G} \\ \partial\mathcal{G}=\{\boldsymbol{r}_\alpha,\boldsymbol{r}_\beta\}}} \prod_b e^{-\beta_{\rm dual} J_b} \end{aligned} \tag{3.30}$$

where the last line is obtained using the same reasoning leading from Eq. (3.27) to (3.29). Now as there are two extra spins inserted it is exactly those graphs $\mathcal{G}$ with "open ends" or boundary $\partial\mathcal{G}$ described by the starting point $\boldsymbol{r}_\alpha$ and end point $\boldsymbol{r}_\beta$ that contribute whereas closed ones average to zero unless both ends coincide. An advantage of the worm algorithm to be introduced in Ch. 5 is that it both samples open and closed graphs. The spin correlations then map on the probability to find an open worm with "head" $\boldsymbol{r}_\alpha$ and "tail" $\boldsymbol{r}_\beta$ at any time in the simulation.

Chapter 4

Dirty Bosons

The Hubbard model was originally created to provide a simplified description for electrons in transition metals to understand their magnetic properties. Due to the sign problem the fermionic version has not been solved despite recent numerical progress in algorithms [147, 148, 149, 150]. Initially the major focus of the research around this model was on electronic transport properties. A true surprise was that in $d \leq 2$ an arbitrarily small amount of disorder is sufficient to localize the electrons [151, 152] and does not simply increases the resistivity. The bosonic version was first treated much later [153] and can serve as an effective description for a variety of systems such as Helium atoms on a substrate [154], cooper pairs of electrons tunneling between superconducting islands [31] or bosons in optical lattices [155]. Quite generally in absence of disorder one expects noninteracting bosons to always be delocalized at zero temperature. For random on-site potentials repulsive interactions between the particles are necessary in order to prevent localization. This chapter is focussed around the effects of disorder on the critical properties of the Boson Hubbard model and exploits hidden symmetries of the Josephson Hamiltonian emerging at high densities in order to arrive at a numerically tractable model.

4.1 The Dirty Boson Hubbard model

The lattice Hamiltonian $\mathcal{H} = \mathcal{H}_0 + \mathcal{H}_1$ consists of

$$\begin{aligned} \mathcal{H}_0 &= -\sum_i \left(\delta\mu_i + \mu\right) \hat{n}_i + \frac{1}{2}\sum_{i,j} V_{ij} \hat{n}_i \left(\hat{n}_j - \delta_{ij}\right) \\ \mathcal{H}_1 &= -\frac{1}{2}\sum_{i,j} J_{ij} \left(\hat{\Phi}_i^\dagger \hat{\Phi}_j + \hat{\Phi}_j^\dagger \hat{\Phi}_i\right) \end{aligned} \tag{4.1}$$

where i, j label the sites on a d-dimensional hyper cubic lattice and J_{ij} is the hopping matrix element between two sites. The zero of the chemical potential μ can be fixed by requiring $\sum_j J_{ij} = 0$, which can always be achieved by a suitable choice

of the diagonal elements J_{ii}. The random on-site potential $\delta\mu_i$ is symmetrically distributed around zero and bounded. The pair potential V_{ij} shall be translationally invariant and symmetric. The operators $\hat{\Phi}_i$ obey the usual commutation relation $\left[\hat{\Phi}_i, \hat{\Phi}_j^\dagger\right] = \delta_{ij}$ and define the particle number operator $\hat{n}_i = \hat{\Phi}_i^\dagger \hat{\Phi}_i$. For large densities one can infer the approximations $\hat{\Phi}_i^\dagger = (N_0 + \tilde{n})^{1/2} e^{i\hat{\phi}_i} \approx N_0^{\frac{1}{2}} e^{i\hat{\phi}_i}$, $\hat{\Phi}_i = e^{-i\hat{\phi}_i} (N_0 + \tilde{n})^{1/2} \approx N_0^{\frac{1}{2}} e^{-i\hat{\phi}_i}$ and $\hat{n}_i = N_0 + \tilde{n}_i$ implying $\left[\hat{\phi}_i, \tilde{n}_j\right] = i\delta_{ij}$. Equation (4.1) then reduces to the Josephson junction array Hamiltonian

$$\mathcal{H}_J = -\sum_{i,j} \tilde{J}_{ij} \cos(\hat{\phi}_i - \hat{\phi}_j) - \sum_i (\delta\tilde{\mu}_i + \tilde{\mu})\tilde{n}_i + \frac{1}{2}\sum_{i,j} U_{ij}\tilde{n}_i\tilde{n}_j \tag{4.2}$$

with redefined couplings $\tilde{J}_{ij} = N_0 J_{ij}$, $U_{ij} = V_{ij}$, $\delta\tilde{\mu}_i = \delta\mu_i$, $\tilde{\mu} = \mu - N_0\hat{V}_0 + \frac{1}{2}V_0$, $\hat{V}_0 = \sum_j V_{ij}$ and $V_0 = V_{ii}$ [28]. This transformation reveals two exact symmetries in the Hamiltonian $\mathcal{H}_J$ which the original Eq. (4.1) lacks. The shift $\tilde{n}_i \to \tilde{n}_i' = \tilde{n}_i + n_0$ only yields $f_J(\tilde{\mu}) \to f_J\left(\tilde{\mu} - n_0\hat{U}_0\right) + \epsilon^0(n_0, \tilde{\mu})$ where $\epsilon^0(n_0, \tilde{\mu}) = n_0(\frac{1}{2}n_0\hat{U}_0 - \tilde{\mu})$, and $\hat{U}_0 = \sum_j U_{ij}$ [28]. The free energy thus is simply shifted by a trivial additive term, and invariant under shifts of $\tilde{\mu}$ by kU_0 with integer k. The only difference is that the system is considered at a different density but has exactly the same properties. For the original system, this statement is generally wrong unless for zero hopping $J_{ij} = 0$. In addition $\tilde{n}_i' = -\tilde{n}_i$, $\hat{\phi}_i' = -\hat{\phi}_i$ implies $f_J(\tilde{\mu}, \{\delta\tilde{\mu}_i\}) = f_J(-\tilde{\mu}, \{-\tilde{\delta\mu}_i\})$ [28]. Together these symmetries imply, that for zero disorder the Hamiltonian is particle-hole symmetric at the points $\tilde{\mu} = \tilde{\mu}_k = \frac{1}{2}k\hat{U}_0$ for integer k as also shown in Fig. 4.1. The combined transformation $\tilde{n}' = k - \tilde{n}_i, \hat{\phi}' = -\hat{\phi}$ leaves everything unchanged. Particles and holes are equally likely to be added to the system. Strictly seen this symmetry is destroyed by the introduction of disorder but statistically conserved if the disorder distribution is chosen symmetric as above.

4.2 Phase diagram of the pure system in the $\mu - J$ plane

In absence of disorder $\delta\mu_i = 0$ the systems Eqs. (4.1) and (4.2) will exhibit two different phases. A localized insulating phase that in addition is incompressible and thus referred to as Mott insulator (MI) and a superfluid phase (SF) exhibiting coherent mass transport. In the remainder we set $V_{ij} = V_0\delta_{ij}$ to on-site and limit the hopping matrix J_{ij} to be tridiagonal and symmetric allowing only nearest-neighbor hopping with uniform strength J_0. Loosely this kinetic term favors delocalization whereas the potential term prefers to localize the particles. The existence of the incompressible Mott phase is most easily shown via the argument that in absence of hopping the total particle number n is a *good quantum number* chosen such that the energy in Eq. (4.1) is minimal. For μ in the region $n - 1 < \mu/V_0 < n$ there are

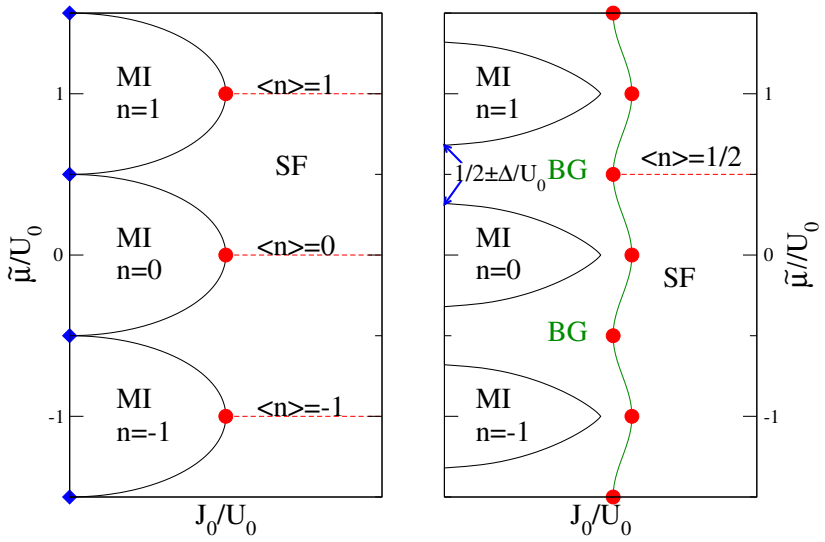

Figure 4.1: Comparison of the phase diagrams for the pure and the disordered Josephson Hamiltonian Eq. (4.2) in terms of the couplings $J_0, \tilde{\mu}$ relative to the on site repulsion $U_0 = V_0$. ***left:*** In absence of disorder the phase diagram is periodic in $\tilde{\mu} = \mu + V_0/2$ with period U_0. In each lobe the particle number per site is an integer constant n_0. The blue points $\tilde{\mu}/U_0 = k + 1/2$ with integer k are 2^N fold degenerate, as here each site independently accommodates k or $k+1$ particles. The system there is superfluid for arbitrarily small J_0. The MI to SF transitions occurring at the tips of the Mott lobes (red points) lie in the universality class of the $(d+1)$-dimensional XY-model [153, 156, 28]. ***right:*** If bounded random on-site disorder $\delta\tilde{\mu}_i$ with $\Delta \leq \tilde{\mu}_i \leq \Delta$ is introduced, a completely new phase, intervening between the MI and SF phases already shown in the left panel, appears. This is the Bose glass phase. Now the Mott lobes have shrunk and, if the disorder is sufficiently strong, might even be absent [153, 156, 28]. It has been shown that there is no direct transition between the MI and SF phase [157].

exactly n bosons per site. As any degeneracy in the energy between having n or $n-1$ particles per site immediately leads to superflow, superfluidity occurs at arbitrarily small hopping at the special points $\mu/V_0 = k$ for integer $k \geq 0$. In between these at finite J_0 the energy gained by adding or removing a single particle and allowing it to travel through the system comes at the cost of the energy δE_p (δE_h) to create a particle (hole) excitation which, for sufficiently small J_0, necessarily is finite and positive. So for each interval $k-1 < \mu/V_0 < k$ there is a region in the $J_0 - \mu$ plane where the particle number is fixed to exactly k particles per site. If a particle would be delocalized in such a region of fixed density, it would win the energy J_0 for the price of the combined energy $\delta E_{ph} = \delta E_p + \delta E_h$. Thus the probability for a

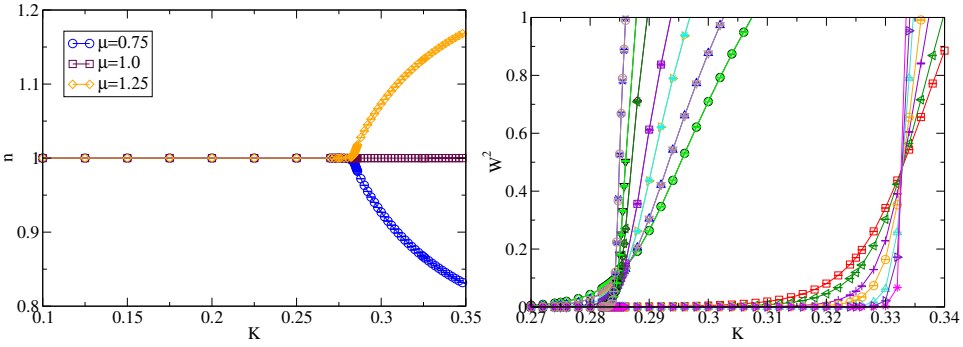

a b

Figure 4.2: Influence of particle-hole symmetry on the nature of the phase transition in the disorder-free case at different values of $\tilde{\mu}/U_0 = 3/4, 1, 5/4$. Data has been created by using the link current representation [31] of Eq. (4.2). ***left:*** If $\tilde{\mu}$ is an integer multiple of the on-site repulsion potential the pure system in the Josephson representation exhibits particle-hole symmetry. Superfluidity results from the simultaneous buildup of large scale, boson world-line, particle and hole-fluctuations within the background of the system. The particle number is fixed to an integer multiple of the number of sites. For other choices of $\tilde{\mu}$ within the same Mott lobe, the nature of the transition is different. Depending on the size of the respective excitation gap either particles or holes are added to the system. ***right:*** Onset of superfluidity for the 2D pure model. At $\tilde{\mu} = \tilde{\mu}_k$ the Mott insulator to superfluid transition lies in the universality class of the 3DXY-model (right set of curves). The curves for equal system sizes for $\tilde{\mu} = 3/4, 5/4$ collapse. Their onset is created by removing/adding particles to the system and trivial in the sense that it starts linear in density and consequently has mean field critical exponents as predicted by Bogoliubov theory [28].

boson of hopping a distance r away from its original position decays exponentially $\propto e^{r/\xi}$ with $\xi \sim [\ln(\delta E_{ph}/J_0)]^{-1}$ [153]. For fixed positive non-integer $\mu/V \neq k$ the system thus is insulating even for finite J_0 up to a threshold $J_{0,c}(\mu/V_0)$ where the kinetic gains finally overcompensate the potential energy costs leading to the lobe-like regions. As this implies a constant density for a finite range of μ the state is incompressible defining the Mott insulator. The tips of the Mott lobes lie at half integer $\mu/V_0 = k - 1/2$. Here the density approximately is fixed to an integer value for J/V_0 even in the superfluid phase in the vicinity of the tip. The phase transition there is driven by particle-hole fluctuations at constant integer density which is most easily revealed by considering the Josephson Hamiltonian Eq. (4.2) at integer $\tilde{\mu}/U_0$ exhibiting the exact particle-hole symmetry which implies a nontrivial transition in the $(d+1)$-dimensional XY universality class with a diverging correlation length

scaling as $\xi \sim (J_0 - J_{0,c})^{-\nu_{XY}}$. Although the original Hamiltonian does not possess this symmetry, it should asymptotically be restored and the same universality class obtained. The phase diagram for the Josephson limit Eq. (4.2) is illustrated in the left panel of Fig. 4.1. Leaving the Mott lobes through any other position than their tips the transition is well described by mean field critical exponents with a particle or hole gap vanishing linearly in $J - J_c$ [153].

4.3 Phase diagram of the disordered system in the $\mu - J$ plane

Adding disorder a second insulating, but yet compressible, phase the Bose-glass (BG) emerges. There particle number fluctuations occur, but no superfluid transport is possible as the bosons still are exponentially localized. In this thesis and Ref. [2] only bounded uniform weak disorder $-\Delta \leq \delta\mu_i \leq \Delta$ with $\Delta < V_0/2$ is considered. Again in absence of hopping the site occupation n_i is a good quantum number but becomes spatially dependent on the random background yielding a local energy $\epsilon(n_i) = -(\mu + \delta\mu_i)\, n_i + V_0(n_i^2 - n_i)/2$. Creating an excess particle at site i for fixed chemical potential μ now costs the potential energy of $\delta E_{p,i} = V_0 n_i - (\delta\mu_i + \mu)$ and similarly an excess hole $\delta E_{h,i} = V_0(1-n) + (\delta\mu_i + \mu)$. Therefore n_i is set to the closest integer near $\mu/V_0 + 1/2 + \delta\mu_i/V_0$. Again for $J_0 = 0$ one can expect regions around the half integer values $\mu/V_0 = (k - 1/2)$, in which the system is MI with exact particle density of k particles per site. If μ is chosen close to $k - 1/2V_0$ and increased then as soon as $\mu > kV_0 - \delta\mu_i$ it becomes favorable to accommodate one extra particle at site i. Starting in the same way for $\mu < (k-1)\, V_0 - \delta\mu_i$ the state becomes unstable towards the creation of holes. On average this means that at $J_0 = 0$ the μ axis splits up into MI intervals of width $V_0 - 2\Delta$ centered around the original half integer lobe center positions $\mu = V_0\,(k - 1/2)$. There each site is occupied *exactly* by k bosons independent of the local value of the random potential $\delta\mu_i$. But for other values of μ located within intervals of width 2Δ between these MI intervals $[(k-1)\, V_0 - \Delta] < \mu < [(k-1)\, V_0 + \Delta]$ the occupation number varies between k and $k-1$, depending on the local value of $\delta\mu_i$. Now only for $\mu < -\Delta/V_0$ the occupation number is strictly zero. If J_0 is increased to a finite positive value much smaller than V_0 the Mott insulator phase is found to survive but with the lobes partly shrunk. The transition between the insulating, incompressible Mott state and the superfluid state, now always goes via the insulating but compressible Bose-glass [157, 28]. For nonzero Δ, even in the Josephson approximation Eq. (4.2) particle-hole symmetry is locally broken *everywhere* even for $\tilde{\mu} = U_0 k/2$. Nevertheless, it is statistically conserved in these points. Tuning J_0 through the critical value at these loci the superfluid onset is in the universality class of the $(d+1)$ dimensional XY-model with columnar bond disorder [28, 31]. The phase diagram in this approximation is illustrated in Fig. 4.1.

4.4 The equality $z = d$

To derive some scaling properties of the dirty boson Hamiltonian, it is most convenient to choose a functional integral formulation [153]. As the dirty boson Hamiltonian does lack the exact particle-hole symmetries so does its GLW functional which directly can be obtained by combining Eqs (4.1), (1.55) and replacing the lattice operators $\hat{\Phi}_j, \hat{\Phi}_i^\dagger$ by their continuum counterparts $\psi(\boldsymbol{r},\tau)$, $\psi^\dagger(\boldsymbol{r},\tau)$. The strategy of reference [156] is thus to consider

$$\mathcal{L}_B = \int d^d r \int_0^\beta d\tau \left\{ -J\psi^* \nabla^2 \psi - K\psi^* [\partial_\tau - \mu(\boldsymbol{r})]^2 \psi + r_0 |\psi|^2 + u_0 |\psi|^4 \right\} \tag{4.3}$$

where only $\mu(\boldsymbol{r}) = \mu + \delta\mu\,(\boldsymbol{r})$ includes quenched random disorder and $\psi\,(\boldsymbol{r},\tau) \sim e^{i\phi(\boldsymbol{r},\tau)}$. It is a continuum approximation to the lattice Josephson Lagrangian

$$\begin{aligned} \mathcal{L}_J = -\int_0^\beta d\tau \Big\{ & \sum_{i,j} \tilde{J}_{ij} \cos[\phi_i(\tau) - \phi_j(\tau)] \\ & + \frac{1}{2} \sum_{i,j} (U^{-1})_{ij} \left[i\dot{\phi}_i(\tau) + \tilde{\mu} - \delta\tilde{\mu}_i \right] \left[i\dot{\phi}_j(\tau) + \tilde{\mu} - \delta\tilde{\mu}_j \right] \Big\} \end{aligned} \tag{4.4}$$

considered in the previous section.

Scaling arguments

Spatial phase gradients in the order parameter imply a free energy increment of

$$\Delta f_{\boldsymbol{r}} = (\Upsilon / 2\beta V) \int_0^\beta d\tau \int d^d r \, |\nabla \phi\,(\boldsymbol{r},\tau)|^2 \tag{4.5}$$

where Υ is the helicity modulus introduced in Eq. (3.23). Since $\nabla\phi$ has dimensions of inverse length it should scale as $\xi^{-1} \propto |\delta|^\nu$ where δ is the distance to the *quantum critical point*. There the universal assumption is that the free energy scales as

$$f_s \sim \xi^{-d} \xi_\tau^{-1} \sim \delta^{\nu(d+z)} \sim \delta^{2-\alpha} \sim \Upsilon \delta^{2\nu} \tag{4.6}$$

implying $\Upsilon \sim \delta^{2-\alpha-2\nu}$. The generalization $2-\alpha = (d+z)\nu$ of the Josephson scaling relation Eq. (1.42) then gives

$$\Upsilon \sim \delta^{(d+z-2)\nu} \tag{4.7}$$

Phase twists in the imaginary time direction are also punished. The coupling between changes in the chemical potential and the time derivative of ϕ can be used to define the compressibility as a helicity modulus in the imaginary time direction [31]. Temporal twists contribute

$$\Delta f_\tau = (\kappa / 2\beta V) \int_0^\beta d\tau \int d^d r \, (\partial_\tau \phi\,(\boldsymbol{r},\tau))^2 \tag{4.8}$$

to the free energy, leading to the scaling relation

$$\delta^{2-\alpha} \sim \kappa \delta^{2z\nu} \Leftrightarrow \kappa \sim \delta^{(d-z)\nu} \tag{4.9}$$

Thus if the system at the Bose glass to superfluid phase transition has finite, nonzero compressibility $\partial n/\partial \mu$ in both phases and even at $\delta = 0$ the requirement $z = d$ follows.

Weichman and Mukhopadhyay pointed out that the above argument only needs to be strictly valid if temporal or spatial phase twists each break a fundamental symmetry of the model and contribute to the singular part of the free energy [28]. One way to trigger the superfluid transition as outlined before is increasing the hopping strength J at a given $J_c(\mu)$ which makes it convenient to choose $\delta = |J - J_c(\mu)|/J_c(\mu)$. Important is that time derivatives and chemical potential in the Josephson approximation are always included in the combination $\partial_\tau - \mu$. This motivates a detailed look at how phase twists enter in different directions.

An arbitrary phase twist can be established by the boundary conditions

$$\psi(x + L_\alpha \vec{e}_\alpha) = e^{i\Theta_\alpha}\psi(x), \qquad |\Theta_\alpha| \leq \pi \tag{4.10}$$

where $x = (\boldsymbol{r}, \tau)$ is the combined space time vector. The axis $\alpha = 0$ is chosen as the temperature direction with extension $L_\tau \sim \beta$ and the remaining $\alpha = 1 \ldots d$ denote the spatial directions. Introducing $\omega_0 = \Theta_0/\beta$ and $\mathbf{k}_0 = (\Theta_1/L_1, \ldots \Theta_d/L_d)$ field

$$\bar{\psi}(x) = e^{-i\mathbf{k}_0 \boldsymbol{r} - i\omega_0 \tau}\psi(x) \tag{4.11}$$

obeys periodic boundary conditions. The *twisted* Lagrangian $\mathcal{L}^{\omega_0 \mathbf{k}_0}$ becomes equivalent to an *untwisted* Lagrangian with renormalized coupling parameters and an additional current term $\mathbf{P}\left[\bar{\psi}\right] = -iJ \int d^d x \int_0^\beta d\tau \left[\bar{\psi}^* \nabla \bar{\psi} - \bar{\psi} \nabla \bar{\psi}^*\right]$. Solving for $\psi(x)$ in Eq. (4.11) and inserting into the functional Eq. (4.3) yields

$$\mathcal{L}^{\omega_0 \mathbf{k}_0}\left[\psi, \mu, r_0\right] = \mathcal{L}\left[\bar{\psi}, \mu - i\omega_0, r_0 + J\mathbf{k}_0^2\right] + \mathbf{k}_0 \mathbf{P}\left[\bar{\psi}\right] \tag{4.12}$$

The free energy of the twisted system becomes

$$f^{\omega_0 \mathbf{k}_0} = -(\beta V)^{-1}\left[\ln\left(e^{-\mathcal{L}^{\omega_0 \mathbf{k}_0}}\right)\right]_{\mathrm{av}} \tag{4.13}$$

where $[\ldots]_{\mathrm{av}}$ denotes averaging over realizations of $\delta\mu(\mathbf{x})$ and $V = \prod_{\alpha=1}^{d} L_\alpha$. As universality classes by definition are insensitive with respect to smooth changes in the system parameters the most important feature is to consider the effects of the twisted boundary conditions on fundamental symmetries of the model. Expandig Eq. (4.13) in presence of a spatial phase twist and subtracting the corresponding

untwisted free energy yields the increments

$$\begin{aligned}\Delta f_\alpha &= f^{0,\mathbf{k}_0} - f^{0,0} \\ &\approx -\frac{1}{\beta V}\left[\log\left[\int \mathcal{D}\bar{\psi} e^{-\mathcal{L}^{0,0}}\left(1-\delta\mathcal{L}+\frac{1}{2}\delta\mathcal{L}^2\right)\right] - \log\left[\int \mathcal{D}\bar{\psi} e^{-\mathcal{L}^{0,0}}\right]\right]_{\mathrm{av}} \\ &\approx -\frac{1}{\beta V}\left[\langle\delta\mathcal{L}\rangle + \frac{1}{2}\left(\langle\delta\mathcal{L}^2\rangle - \langle\delta\mathcal{L}\rangle^2\right)\right]_{\mathrm{av}} \\ &= \frac{1}{2}\Upsilon\mathbf{k}_0^2 + O\left(\mathbf{k}_0^4\right) \end{aligned} \tag{4.14}$$

where $\delta\mathcal{L} = \mathcal{L}^{0,\mathbf{k}_0} - \mathcal{L}^{0,0}$ and $\langle\ldots\rangle = \int \mathcal{D}\bar{\psi} e^{-\mathcal{L}^{0,0}}(\ldots) / \int \mathcal{D}\bar{\psi} e^{-\mathcal{L}^{0,0}}$. By Eq. (4.12) only the term $\mathbf{k}_0\mathbf{P}\left[\bar{\psi}\right]$ can give rise to linear terms in $\mathbf{k}_0$. But as $\langle\mathbf{P}\left[\bar{\psi}\right]\rangle = 0$ these do not appear in Δf_α. For a pure temporal twist $\mathbf{k}_0 = 0$ and Eq. (4.12) directly implies

$$f^{\omega_0,0}(\mu) = f^{0,0}(\mu - i\omega_0) \tag{4.15}$$

Expanding around $\omega_0 = 0$ with $\rho = -\partial f/\partial\mu$ and $\kappa = \partial\rho/\partial\mu$ gives the increment

$$\Delta f_\tau = i\omega_0\rho + \frac{1}{2}\kappa\omega_0^2 + O\left(\omega_0^3\right) \tag{4.16}$$

The important difference pointed out in Refs. [156, 28] is that only for $\mu(\boldsymbol{r}) = 0$ does the imaginary time twist ω_0 break the initial particle-hole symmetry of the system. In any other case $\mu \neq 0$ this symmetry already has been broken and the additional twist only corresponds to a smooth variation of the chemical potential.

4.5 Scaling at the Dirty Boson critical point

For $\mu = 0$ and in absence of disorder the ψ^4 theory of the $(d+1)$-dimensional XY-model is obtained and Eq. (4.3) is invariant under both space and time inversion with all directions entering isotropically. The compressibility κ then simply is the temporal helicity modulus Υ_τ and is finite only in the ordered phase. The free energy increment then scales as [28]

$$\Delta f^{\omega_0,\mathbf{k}_0} \approx \beta^{-1}L^{-d}\tilde{\Phi}_0^{\omega_0,\mathbf{k}_0}(\mathbf{k}_0\xi, \omega_0\xi_\tau) = \beta^{-1}L^{-d}\Phi_0^{\omega_0,\mathbf{k}_0}\left(A_{\boldsymbol{r}}\delta L^{1/\nu_0}, A_\tau\delta\beta^{1/z_0\nu_0}\right) \tag{4.17}$$

where ν_0, z_0 are the critical exponents of the pure $(d+1)$-dimensional XY universality class and $\delta = (J - J_c)/J_c$ the distance to the critical point at $\mu = 0$. Due to the isotropy in space-time one requires by Eq. (4.14) leading corrections of L^{-2} and β^{-2}. Compensating for the $L^{-d}\beta^{-1}$ prefactor the scaling ansatz thus yields

$$\Phi_0^{\omega_0,\mathbf{k}_0}(x,y) \approx x^{d\nu_0}y^{z_0\nu_0}\left(Q_{\boldsymbol{r}}x^{-2\nu_0} + Q_\tau y^{-2z_0\nu_0}\right) \tag{4.18}$$

Resubstituting the above definitions and using $(\mathbf{k}_0)_\alpha = \theta_\alpha/L_\alpha$ gives

$$\Upsilon \approx A_{\boldsymbol{r}}^{(d-2)\nu_0}A_\tau^{z_0\nu_0}\left(Q_{\boldsymbol{r}}/\Theta_x^2\right)\delta^{\nu_0} \tag{4.19}$$

$$\kappa \approx A_{\boldsymbol{r}}^{d\nu_0} A_\tau^{-z_0\nu_0} \left(Q_\tau/\Theta_0^2\right) \delta^{v_{\tau 0}} \tag{4.20}$$

where $\Theta_{\boldsymbol{r}}^2 = \Theta_1^2 + \cdots + \Theta_d^2$ [28]. Thus the Josephson scaling relations

$$v_0 = (d + z_0 - 2)\,\nu_0 = 2 - \alpha_0 - 2\nu_0 \tag{4.21}$$

$$v_{\tau 0} = (d - z_0\nu_0) = 2 - \alpha_0 - 2z_0\nu_0 \tag{4.22}$$

in $D = d + z_0$ dimensions are obtained with $Q_{\boldsymbol{r}} \propto \Theta_{\boldsymbol{r}}^2$ and $Q_\tau \propto \Theta_0^2$.

At the Bose glass to superfluid transition one comes across a different situation. Both ρ and κ are smooth functions of μ in each respective phase. At finite μ a temporal twist only minimally changes the particle-hole symmetry-breaking term $\psi^* \left(\partial_\tau - \mu(\boldsymbol{r})\right)^2 \psi$ included in $\mathcal{L}$. Spatial twists however enter in the very same way as above for $\omega_0 = 0$. The scaling form of Eq. (4.17) now implies

$$\Delta f^{0,\mathbf{k}_0} \approx \beta^{-1} L^{-d} \Phi^{0,\mathbf{k}_0} \left(A_{\boldsymbol{r}} \delta L^{1/\nu}, A_\tau \delta \beta^{1/z\nu}\right) \tag{4.23}$$

where again in order to get the appropriate leading terms

$$\Phi^{0,\mathbf{k}_0}(x, y) \approx R_{\boldsymbol{r}} x^{(d-2)\nu} y^{z\nu} \tag{4.24}$$

which for large $x, y > 0$ implies the stiffness

$$\Upsilon \approx A_{\boldsymbol{r}}^{(d-2)\nu} A_\tau^{z\nu} \left(R_{\boldsymbol{r}}/\Theta_{\boldsymbol{r}}^2\right) \delta^v \tag{4.25}$$

where $v = (d+z-2)\nu = 2-\alpha-2\nu$. Again $R_{\boldsymbol{r}} \propto \Theta_{\boldsymbol{r}}^2$ and all exponents are those of the dirty Boson critical point. As there are no twisted boundary conditions imposed along the time direction, no $O\left(\beta^{-1}, \beta^{-2}\right)$ appear in the free energy increment. Finally, including a temporal phase twist ω_0 has the net effect of shifting $\mu \to \mu - i\omega_0$ and the occurrence of extra β-boundary conditions in (4.23). The free energy increment then should simply turn out to be

$$\begin{aligned} \Delta f^{\omega_0,\mathbf{k}_0} = {} & \beta^{-1} L^{-d} \Phi^{0,\mathbf{k}_0} \left(A_{\boldsymbol{r}} \delta_\Theta L^{1/\nu}, A_\tau \delta_\Theta \beta^{1/z\nu}\right) \\ & + f_a\left(J, r_0 + J\mathbf{k}_0^2, \mu - i\omega_0\right) - f_a\left(J, r_0, \mu\right) \end{aligned} \tag{4.26}$$

where $\delta_\Theta = J - J_c\left(\mu - i\omega_0\right) \approx \delta + i\omega_0 J_c'(\mu)$ has slightly been shifted and f_a denotes the analytic part of the free energy [28] . But $\Phi^{0,\mathbf{k}_0}$ is still given by Eq. (4.23) and therefore is unable to give rise to $O\left(\beta^{-1}, \beta^{-2}\right)$ corrections. Weichman *et al.* thus argue that the only ways that ρ and κ can pick up these temporal corrections are (a) through a possible ω_0 dependence of δ_Θ which has been shown in double ϵ-expansions to have dominating singular behavior $\kappa_s \propto |\delta|^{-\alpha}$ and thus for $\alpha < 0$ becomes negligible at $\delta = 0$ (b) through f_a. So far simulations of the problem including the one presented here [2] seem to be well consistent with $z > 1$ and $\nu \geq 1$ [158, 31, 159]. Thus $\alpha = 2 - (d+z)\nu < 0$ for $d \geq 2$. This then would strongly

suggest, that κ amounts from the analytic part of the free energy. Without any spatial phase twist the analytic part in the free energy therefore becomes [28]

$$f_a(J,\mu) = -\rho_c(J)\left[\mu - \mu_c(J)\right] - \frac{1}{2}\kappa_c(J)\left[\mu - \mu_c(J)\right]^2 + \dots \tag{4.27}$$

close to the transition line $\mu_c(J)$. Inserted into Eq. (4.26) at $\mathbf{k}_0 = 0$ this means that a finite κ through the transition can be obtained solely via the analytical part f_a without imposing any restrictions on z.

4.6 Dual representation of the Josephson Lagrangian

To simulate the dirty boson model and avoid complex weights naturally arising in Eq. (4.4) at non-integer densities or in presence of disorder one usually maps to the link-current model [31]. Using the same methods as in Ch. 3.1 the Josephson Lagrangian Eq. (4.4) can be mapped on a model of sterically interacting loops describing the boson world lines in a path integral formulation. Discretizing all derivatives and using the Villain approximation Eq. (3.8) of the cosine-term Eq. (4.4) reduces to the form $\mathcal{L}_{JV}[\phi,\mathbf{j}]$ by

$$e^{-\mathcal{L}_J[\phi]} = \sum_{\mathbf{j}} e^{-\mathcal{L}_{JV}[\phi,\mathbf{j}]} \tag{4.28}$$

$$\begin{aligned}\mathcal{L}_{JV}[\phi,\mathbf{j}] = {} & \frac{1}{2}\sum_{\boldsymbol{x},\alpha\neq 0} K_i^\alpha(\Delta_\alpha\phi_{\boldsymbol{x}} - 2\pi j_{\boldsymbol{x}}^\alpha)^2 \\ & + \frac{1}{2}\sum_{i,j,\tau}(\mathbf{V}^{-1})_{ij}(\Delta_\tau\phi_{(i,\tau)} - i\nu_i - 2\pi j^0_{(i,\tau)}) \\ & \times (\Delta_\tau\phi_{(j,\tau)} - i\nu_j - 2\pi j^0_{(j,\tau)})\end{aligned} \tag{4.29}$$

where $\Delta_\alpha\phi_{\boldsymbol{x}} = (\phi_{\boldsymbol{x}+\hat{\alpha}} - \phi_{\boldsymbol{x}})$ is the finite difference derivative and $\mathbf{j}_{\boldsymbol{x}} = (j^\tau_{\boldsymbol{x}}, j^1_{\boldsymbol{x}}, \dots, j^d_{\boldsymbol{x}})$ a $(d+1)$-dimensional integer vector field sitting at each lattice site $\boldsymbol{x} = (i,\tau)$ of a $L_\tau \times L^d$ space-time lattice. The index $\alpha = 0, 1, \dots, d$ denotes the $(d+1)$-unit bond directions adjacent to each site. The τ-direction corresponds to $\alpha = 0$. The coupling constants K_i^α, V_{ij} and ν_i correspond to $J_{ij}\Delta\tau$, $U_{ij}\Delta\tau$ and $(\tilde{\mu} + \delta\tilde{\mu}_i)\Delta\tau$ in Eq. (4.4). Observe that only the second term couples different "time-slices" through $\Delta_\tau\phi_{(i,\tau)}$. Straight forward multivariate generalization of the Hubbard Stratonovich decoupling Eq. (3.9) and again using the identity Eq.(3.11) and the same steps that lead from Eq. (3.7) to (3.15) one obtains the dual link-current Lagrangian

$$\tilde{\mathcal{L}}_J[\mathbf{J}] = \frac{1}{2}\sum_{i,\tau,\alpha\neq 0}\frac{(J^\alpha_{(i,\tau)})^2}{K_i^\alpha} + \frac{1}{2}\sum_{i,j} V_{ij} J^0_{(i,\tau)} J^0_{(j,\tau)} - \sum_{i\tau}\nu_i J^0_{(i,\tau)} \tag{4.30}$$

where the components $J^\alpha_{\boldsymbol{x}}$ are integer variables. The partition function becomes

$$Z = \sum_{\mathbf{J}}\prod_{\boldsymbol{x}}\delta_{\nabla\cdot\mathbf{J}_{\boldsymbol{x}},0}\, e^{-\tilde{\mathcal{L}}_J[\mathbf{J}]} \tag{4.31}$$

The divergence free condition again was obtained by integrating over the phases as in Eq. (3.14). Similar to the bond variables $\mathbf{q}$ in Eq. (3.21), describing the vortex currents in a superconductor, the space-time variables $(J^\tau_{\boldsymbol{x}}, J^x_{\boldsymbol{x}}, J^y_{\boldsymbol{x}}, \dots)$ have a neat physical interpretation. The time component $J^\tau_{\boldsymbol{x}}$ describes the density fluctuations and thus can be seen as the excess particle or hole density. If one were to include an external magnetic field minimally coupling to the kinetic hopping term then the cosine term in Eq. (4.4) transforms as $\cos[\phi_i(\tau) - \phi_{i+\alpha}(\tau)] \to \cos[\phi_i(\tau) - \phi_{i+\alpha}(\tau) + \mathcal{A}_{\boldsymbol{x},\alpha}]$. This would add a term $i\sum_{\boldsymbol{x},\alpha\neq 0} J^\alpha_{\boldsymbol{x}}\mathcal{A}_{\boldsymbol{x},\alpha}$ to $\tilde{\mathcal{L}}_J[\mathbf{J}]$ in Eq. (4.30). The expectation values of the spatial current components can therefore be written as

$$\langle J^\alpha_{\boldsymbol{x}}\rangle = -i\frac{\delta \log Z}{\delta \mathcal{A}_{\boldsymbol{x},\alpha}} \quad \alpha \neq 0 \tag{4.32}$$

and $J^\alpha_{\boldsymbol{x}}$ can be seen to describe the full physical, gauge-invariant current. Imposing a uniform phase twist along any of the spatial directions $\mu = 1 \dots d$ corresponds to the presence of a uniform vector potential $\mathcal{A}_{\boldsymbol{x},\alpha} = \delta_{\mu,\alpha}\Theta/L$ along that direction. Using the definition of the superfluid density then yields in analogy to Eq. (4.14)

$$\rho_s \sim L^2\frac{\partial^2 f_s}{\partial \Theta^2} = \frac{1}{L^{d-2}L_\tau}\left[\langle W^2_\mu\rangle\right] \tag{4.33}$$

where $W_\mu = L^{-1}\sum_{\boldsymbol{x}} J^\mu_{\boldsymbol{x}}$ is the winding number describing how many times the boson world lines wrap around the system in the spatial direction μ. Thus in contrast to the superconductor representation, where the macroscopic onset of vortex line fluctuations in the system signals the *destruction of superconductivity*, in the link-current representation the onset of macroscopic world line fluctuations signals the *onset of superfluidity*. Similarly the compressibility can be straight away calculated as

$$\kappa = \frac{\partial n}{\partial \mu} = \frac{\partial^2 f}{\partial \mu^2} = \frac{L_\tau}{L^2}\left(\langle W^2_\tau\rangle - \langle W_\tau\rangle^2\right) \tag{4.34}$$

and thus simply corresponds to the number fluctuations in the excess particle density.

Chapter 5

Monte Carlo Methods

All phase transition considered in this thesis can be mapped on equivalent classical effective models only respecting the relevant degrees of freedom and fundamental symmetries. Thus the statistical physics can be treated entirely by classical Monte Carlo methods. This chapter shall briefly outline the general properties of the Monte Carlo (MC) method starting from local algorithms over more advanced collective updating methods performing exceptionally well in the critical region of a continuous phase transition. Further generalized ensemble methods applied to the problems in this thesis are discussed. Those are particularly effective for hardly relaxing systems and for first order transitions.

5.1 Classical Monte Carlo

The need to describe classical systems of a macroscopic number of particles by statistical means arises out of the sheer impossibility and absurdity it would pose to solve the equations of motion for 10^{23} particles and describe the behavior of each of them in detail. One thus simply describes these systems in terms of their bulk properties given by averages over $\langle Q \rangle$ of some physical observable Q. For simplicity labeling all possible states by the index μ one aims to calculate

$$\langle Q \rangle = \sum_{\mu} Q_{\mu} P_{\mu} \tag{5.1}$$

where $P_{\mu} = P(X_{\mu})$ is the probability for the microscopic configuration X_{μ} to occur. The goal of MC is to generate a series of configurations $\{X_{\mu_t}\}$ that properly reproduce the statistical properties. In the same way as it is not sensible to microscopically solve for the trajectories of the individual particles, it is utterly ineffective to simply generate a random configuration of the system and accept with the proper probability P_{μ}. Usually the average is dominated by only a fraction of the theoretically accessible states. This is especially the case for the Boltzmann

distribution

$$P_\mu = \frac{e^{-\beta E_\mu}}{Z} \tag{5.2}$$

where $E_\mu = E(X_\mu)$ is the internal energy and

$$Z = \sum_\mu e^{-\beta E_\mu} = \sum_E g(E) e^{-\beta E} \tag{5.3}$$

Usually ordered low energy configurations are penalized at high temperatures by an exponentially small density of states $g(E)$ and disordered states at low temperatures by an exponentially small weight $e^{-\beta E_\mu}$. To ensure that the observables obtained from numerical simulations converge as quickly as possible and in principle to arbitrary precision the algorithm yielding the time series $\{X_{\mu_t}\}$ needs to be designed such that the state space is explored in an effective fashion. If one generates the states contributing to Eq. (5.1) according to some predetermined probability distribution $\tilde{P}_\mu$ then the average becomes

$$\langle Q \rangle = \sum_t \tilde{P}_{\mu_t}^{-1} P_{\mu_t} Q_{\mu_t} \tag{5.4}$$

The choice $\tilde{P}_\mu = P_\mu$ is known as *importance sampling*, ensuring that the algorithm automatically does not try very unlikely configurations. The average over N_s configurations generated by the MC algorithm then becomes

$$Q_{N_s} = \frac{1}{N_s} \sum_{t=1}^{N_s} Q_{\mu_t} \tag{5.5}$$

Markov processes

The quality of a MC algorithm is to a large extent determined by the speed by which all observables Q_{μ_t} approach their equilibrium distribution with increasing number N_s of configurations contributing to Eq. (5.5). To efficiently construct such a random time series X_t is highly non-trivial. An elegant way is given by Markov chains. Starting from an initial configuration X_μ one proposes random updates that eventually lead to a transition to a new configuration X_ν with conditional probability $w_{\nu\mu}$. For proper Markov chains these *transition matrix elements* need to be time independent and are allowed to "remember" the history of the process only via the current configuration X_{μ_t} with all other previously obtained configurations having no effect. The probability for being in state μ at time $t+1$ then is given by

$$P_\mu(t+1) = \sum_{\nu \neq \mu} P_\nu(t)\, w_{\mu\nu} + P_\mu(t)(1 - \sum_{\nu \neq \mu} w_{\nu\mu}) \tag{5.6}$$

where it has been used that the probability for no change at all is $w_{\mu\mu} = 1 - \sum_{\nu \neq \mu} w_{\nu\mu}$. In order to ensure that the "temporal average" of the stochastic process X_{μ_t} Eq. (5.5) is equal to the ensemble average it needs to be *ergodic*. All configurations should be reachable in a finite number of steps.

Detailed balance

In case that the Markov process has succeeded in converging towards the "true" equilibrium probability density the distribution $P_\mu(t)$ is stationary. Thus convergence can be ensured by imposing the detailed balance condition

$$P_\mu w_{\nu\mu} = P_\nu w_{\mu\nu} \tag{5.7}$$

on Eq. (5.6). This avoids the theoretical possibility of ending up in limit cycles [160]. In principle one can write the evolution of Eq. (5.6) as a matrix equation $\mathbf{P}(t+1) = \mathbf{w}\mathbf{P}(t)$. If only the weaker balance condition $\sum_\nu P_\mu w_{\nu\mu} = \sum_\nu P_\nu w_{\mu\nu}$ was imposed then Eq. (5.6) still would yield an equilibrium distribution but this equilibrium may be a dynamic one in the sense that $\mathbf{P}(\infty) = \mathbf{w}^n\mathbf{P}(\infty)$ is obtained after a finite number of steps n, where n is the length of the limit cycle. Then the temporal average obtained by taking the mean over the stochastic time series in general is different from the desired ensemble average. For the Boltzmann distribution Eq. (5.7) implies

$$\frac{w_{\nu\mu}}{w_{\mu\nu}} = \frac{P(X_\nu)}{P(X_\mu)} = e^{-\beta(E_\nu - E_\mu)} \tag{5.8}$$

Having pointed out the possible pitfalls, in fact, many widely used MC algorithms such as parallel tempering break detailed balance [161]. Under fairly mild assumptions detailed balance can be shown to be overly strict [162].

5.2 Warmup and convergence

Obviously starting from a random, or any other initial configuration, any MC algorithm will take a finite time in order to enter, sample and exit all states with their correct respective Boltzmann weights. One method to check for equilibration is given by logarithmic boxing. One calculates the expectation value

$$\langle A \rangle_{N_t} = \frac{1}{N_t} \sum_{t=N_t+1}^{2N_t} A_t \tag{5.9}$$

over increasingly large, non overlapping intervals of the MC time series. Here N_t denotes the number of MC sweeps performed. One MC sweep usually is defined as a single update attempt per degree of freedom. The equilibration time necessary can vary strongly between different quantities. The slowest quantity of interest should therefore be considered when deciding how many MC sweeps need to be run. In addition at any step in the simulation the next configuration will directly depend on the previous one. It therefore always takes a finite time to generate a completely uncorrelated new configuration. The correlations typically can be shown to approximately decay exponentially with the number of steps

$$\langle Q(t)Q_{t'} \rangle - \langle Q(t) \rangle \langle Q(t' \rangle \sim e^{-\left(t-t'\right)/\tau_Q} \tag{5.10}$$

for $t > t'$ and τ_Q again depends on the quantity Q[1]. This is important if one attempts to calculate the error bar of some quantity from a *single* MC trajectory.

Acceptance probabilities

The efficiency of a MC algorithm is to a large extent determined by the weights $w_{\mu\nu}$. In fact there is a lot of freedom to chose these weights as these only need to obey the normalization condition $\sum_\nu w_{\mu\nu} = 1$ of the transition amplitudes and the (detailed) balance condition Eq. (5.7). It proves useful to break down the transition matrix elements in two parts via defining trial probabilities $t_{\mu\nu}$ to attempt an update that given the state X_μ the system is taken to X_ν and corresponding acceptance probabilities $a_{\mu\nu}$ via

$$w_{\nu\mu} = t_{\mu\nu} \cdot a_{\mu\nu} \tag{5.11}$$

The condition (5.8) does only fix the ratio

$$\frac{w_{\nu\mu}}{w_{\mu\nu}} = \frac{t_{\mu\nu} a_{\mu\nu}}{t_{\nu\mu} a_{\nu\mu}} \tag{5.12}$$

By multiplying the larger value of $a_{\mu\nu}$ and $a_{\nu\mu}$ by a positive number in such a way that the product becomes unity and adjusting the remaining acceptance ratio by the same factor, the $a_{\mu\nu}$ are made as large as possible while still obeying all constraints. In an ideal MC algorithm the whole dependence of $w_{\mu\nu}$ would be incorporated in the trial probabilities rendering all $a_{\mu\nu}$ to unity.

5.3 The Metropolis algorithm

This is one of the first examples [163] of a successfully implemented Markov chain MC simulation. For most algorithms in the canonical ensemble the trial amplitudes are chosen symmetrically and drop out of the ratio. The ratio of the transition amplitudes then simply becomes equal to the ratio of the acceptance probabilities

$$\frac{w_{\nu\mu}}{w_{\mu\nu}} = \frac{a_{\mu\nu}}{a_{\nu\mu}} = e^{-\beta(E_\nu - E_\mu)} \tag{5.13}$$

The optimal Metropolis choice of the acceptance probabilities is

$$a_{\mu\nu} = \begin{cases} e^{-\beta(E_\nu - E_\mu)} & E_\nu - E_\mu > 0 \\ 1 & \text{else} \end{cases} \tag{5.14}$$

For the models given by Eq. (1.65) the algorithm itself then becomes

1. Start from an initial configuration $\{S(\boldsymbol{r}_i)\}$

[1] In fact this is a bit oversimplified. Writing the asymptotic probability density obtained for large times in terms of the eigenvectors of the transition matrix $\mathbf{w}$ it can be shown that there are $\mathrm{rank}(\mathbf{w}) - 1$ correlation times [160]

2. Randomly pick one spin $S(\boldsymbol{r}_i)$ and suggest a new orientation $S'(\boldsymbol{r}_i)$ uniformly distributed on the boundary of the N-dimensional sphere.
3. Calculate the energy difference ΔH
4. Accept new state $S'(\boldsymbol{r}_i)$ with probability $\min\left\{e^{-\beta\Delta H}, 1\right\}$
5. Measure all observables of interest.
6. Repeat 2-5 until the running averages of all observables have converged.

5.4 Collective updating methods

The problem for local update schemes like the Metropolis algorithm is that they suffer from *critical slowing down*, at a second order phase transition. The number of effectively sampled, independent measurements is $N_{\text{eff}} \sim N_{\text{samples}}/2\tau$ where τ is the autocorrelation time. Usually τ grows, as the transition temperature is approached, according to the power law

$$\tau \sim \xi^z \sim t^{-\nu z} \tag{5.15}$$

with the exponent $z \approx 2$ for most local methods [164]. Collective updating methods such as the Swendsen-Wang ,Wolff and Worm algorithm practically avoid critical slowing down by making *use* of the fact that the correlation length diverges at the phase transition. In single spin flip models the probability of flipping single spins let alone large clusters of spins is severely reduced at criticality, due to the local dynamics. If spin models of the $O(N)$ type Eq. (1.65) go through a phase transition the diverging correlation length leads to the emergence of cluster like regions of similarly oriented spins. Fortuin and Kastelyn [165, 166] realized that the Ising spin model can be mapped on a model for bond percolation. Swendsen and Wang [167] designed an algorithm that uses this fact in order to efficiently flip multiple clusters of spins at the same time. Their algorithm later was refined by Wolff to a single cluster algorithm [164] for arbitrary N. The dynamic exponent z for the Swendsen-Wang roughly is $z_{SW} \approx 0.25, 0.54, 0.86$ in $d = 2, 3, 4$. The Wolff algorithm performs even better with $z = 0.25(1), 0.33, 0.25$ for the same dimensions and was even found to be consistent within a logarithmic divergence scenario [168]. As much as these algorithms improve the performance of the $O(N)$ models in zero field, where the interaction along each bond can be written as a simple spin scalar product, they are useless for the London superconductor models Eq. (3.6) with fluctuating gauge field. Similarly the worm algorithm pioneered by Prokof'ev and Svistunov [169] gains from the fact that using the dual loop representation at T_{c} the loops size diverges.

Wolff algorithm

For continuos $O(N)$ models the single Ising spin flip operation is generalized towards a reflection operation, $R\left(\hat{\mathbf{S}}\right)$, with respect to a hyperplane orthogonal to some

randomly chosen vector $\hat{\mathbf{S}}$ on the respective N-dimensional unit sphere via

$$S'(\boldsymbol{r}_i) = R\left(\hat{\mathbf{S}}\right) S(\boldsymbol{r}_i) = S(\boldsymbol{r}_i) - 2\left(S(\boldsymbol{r}_i)\cdot\hat{\mathbf{S}}\right)\hat{\mathbf{S}} \tag{5.16}$$

The algorithm then can be sketched as

1. Choose a random lattice site $\boldsymbol{r}_i$ and a random reflection vector $\hat{\mathbf{S}}$.
2. The seed spin $S(\boldsymbol{r}_i)$ is flipped according to Eq. (5.16) and marked as an element of the cluster.
3. Check all bonds connecting site $\boldsymbol{r}_i$ to its nearest neighbors. The bond $\boldsymbol{r}_i \to \boldsymbol{r}_j = \boldsymbol{r}_i \pm \hat{\mu}$ is activated with probability

$$\begin{aligned} P(S(\boldsymbol{r}_i), S(\boldsymbol{r}_j)) &= 1 - \exp\left(\min\left\{0, \beta J S(\boldsymbol{r}_i)\cdot\left[1 - R\left(\hat{\mathbf{S}}\right)\right] S(\boldsymbol{r}_j)\right\}\right) \\ &= 1 - \exp\left\{\min\left\{0, 2\beta J\left(\hat{\mathbf{S}} S(\boldsymbol{r}_i)\right)\left(\hat{\mathbf{S}} S(\boldsymbol{r}_j)\right)\right\}\right\} \end{aligned} \tag{5.17}$$

   In case of activation the spin $S(\boldsymbol{r}_j)$ is flipped. All sites that have been joined to the cluster are saved in a list.
4. Consider the neighbors of the last saved element on the list and continue to consider addition of spins not marked to belong to the cluster using step 3. Remove the element from the list and continue until the list is empty.

The worm algorithm

For actions like Eqs (3.21), (4.30) and Eq. (3.29) admitting a representation whose configuration space is given by closed paths (CP), the worm algorithm is an effective tool. Its efficiency is similar to the best cluster methods with essentially logarithmic scaling $\tau \sim \ln L$ at the critical point [169]. For the classical Ising, XY and Potts models, such a representation arises by performing a high temperature expansion. As for single spin flips in the spin models, the corresponding local updates given by removing or adding elementary closed plaquette loops to the configuration, have the strong drawback that they hardly lead to loops winding around the system. Global updates, adding lines spanning over the whole system, are exponentially suppressed with increasing system size. The ingenuity of the worm algorithm was to base the generation of the loops on a local draw-and-erase procedure which can be described as follows:

1. Start from an arbitrary closed path configuration.
2. With equal probability pick a radom site on the lattice. And set the worms head and tail coordinate equal to that site.
3. With equal probability pick a random direction.

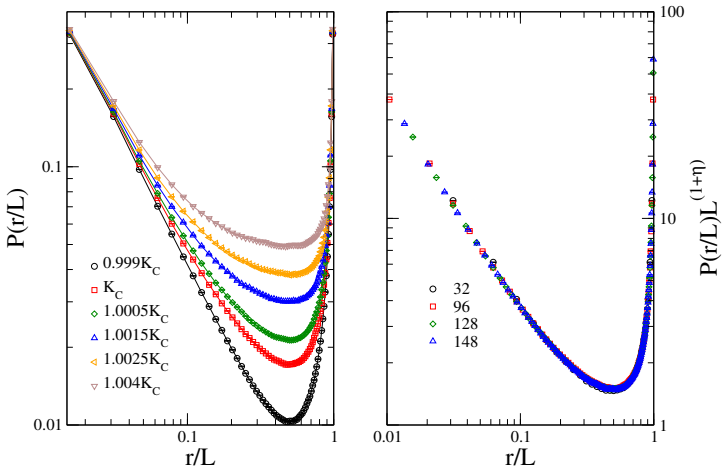

Figure 5.1: *left:* Probability amplitude $P\left(r/L\right)$, to insert an open loop segment with head and tail separated by a distance r, for the dual 3D XY model in Villain approximation at different couplings for $L = 64$. The data is normalized to $P(0) = 1$. Below K_{c} large distances are exponentially suppressed. At K_{c} the probability distribution decays as $r^{-(d-2+\eta)}$. Above K_{c} large worms become abundant. *right:* The corresponding quantity for the 3D-Ising model in loop representation at the critical coupling $\beta_{\mathrm{dual,C}} = 0.221654$ shows the same scaling properties using $\eta = 0.0366$.

4. Calculate the action difference ΔS associated with adding a worm segment along the direction.

5. Accept with probability $\min\left(1, e^{-\Delta S}\right)$ eventually creating an *open* configuration.

6. If the worms head and tail coincide stop and measure. Otherwise repeat from step 3.

7. Perform 2-6 until all running averages converged.

As due to step 5. the worm algorithm, locally for each step, is a Metropolis-like scheme, it automatically obeys detailed balance. The reason for its effectiveness is of similar origin as that of the Wolff method. The latter profits from the collective behavior of spin clusters reflected in the power law form of the spin two point correlation function $g\left(r\right) \sim r^{-(d-2+\eta)}$ at T_{c}. In the loop representation this corresponds to an open-loop length distribution, where the probability amplitude $P(r)$, to find open loops with head and tail separated by a distance r apart at any time in the simulation, scales as $P(r) \sim r^{-(d-2+\eta)}$ with the same exponent η. Thus again

precisely at the critical point where local schemes are harshly punished by critical slowing down the worm scheme is warranted by the same power law correlations, leading to the proliferation of system size spanning loops, potentially in a single MC move and to low dynamic correlation times. A plot of $P(r/L)$ is shown in the left panel of Fig. 5.1 for link-current model $S = \frac{1}{2K} \sum_{\mu,\boldsymbol{r}_i}^{\nabla\cdot\mathbf{q}=0} [q_\mu(\boldsymbol{r}_i)]^2$ for different values of the coupling $K = \beta_{\mathrm{dual}}^{-1}$ close to $K_\mathrm{c} \approx 0.33305$. Here it measures the order-parameter correlations via

$$P\left(|\boldsymbol{r}-\boldsymbol{r}'|\right) \sim \langle e^{i\theta(\boldsymbol{r})} e^{-i\theta(\boldsymbol{r}')} \rangle = \langle \prod_{\boldsymbol{r}_i \in C} \exp\left[-\frac{1}{K}\left(q_\mu(\boldsymbol{r}_i) + \frac{1}{2}\right)\right] \rangle \tag{5.18}$$

where C is an open contour connecting $\boldsymbol{r}$ and $\boldsymbol{r}'$. The right panel shows the scaling collapse of $P(r/L)$ for a 3D Ising loop model Eq. (3.29) at $\beta_{\mathrm{dual,C}}$.

5.5 Wang-Landau algorithm

Conventional Monte Carlo methods sample over phase space at a fixed temperature T according to the canonical distribution Eq. (5.2). Specifically at first order transitions this approach becomes very inefficient. There the probability to tunnel between the coexisting phases decreases exponentially with system size $\sim \exp\left(-\beta \Delta F\right)$ where $\Delta F \sim L^{d-1}$ according to Eq. (1.93). The correlation time diverges accordingly. To avoid these dynamical problems the Wang-Landau (WL) method [56, 170] directly tries to estimate the density of states $g\left(E\right)$ defined in (5.3). In principle observables $\mathcal{O}\left(\beta\right)$ that are functions $o(E)$ of the energy only and their respective probability distributions can be obtained for any temperature by simply reweighting

$$\langle \mathcal{O}\left(\beta\right) \rangle = \frac{\sum_E o\left(E\right) g\left(E\right) e^{-\beta E}}{\sum_E g\left(E\right) e^{-\beta E}} \tag{5.19}$$

according to Eq. (5.3). Of course $g(E)$ is not known initially but is estimated in the following way:

1. Set $g\left(E\right)$ to an arbitrary starting guess. Create a histogram $h(E)$ keeping track of the number of visits at the level E.

2. Attempt to update the configuration and accept proportional to the inverse of the current estimate of $g(E)$ via

$$p\left(E_\mu \to E_\nu\right) = \min\left[\frac{g\left(E_\mu\right)}{g\left(E_\nu\right)}, 1\right] \tag{5.20}$$

   using a standard elementary MC move. Update $g\left(E\right)$ for the final level according to $g\left(E\right) \to g\left(E\right) \cdot f$ where $f > 1$ and the histogram by $h(E) \to h(E) + 1$.

3. Repeat this until the energy histogram $h\left(E\right)$ is flat in the sense that the number of entries in its bins fluctuates between a fixed range (usually $\approx 20\%$) around the mean histogram entry $\langle h\left(E\right) \rangle$.

4. The density of states is now considered to be determined within the accuracy of the modification factor f. Reduce f and reset the energy histogram to $h(E) = 0$ for all entries E and repeat 2-3 with the current estimate of $g(E)$ until f is very close to unity for example $f = \exp\left(10^{-8}\right)$.

Good starting guesses for $g(E)$ can immensely increase the convergence. Further as $g(E)$ usually varies over several orders of magnitude it is numerically advantageous to solely save the logarithm $S(E) = \log[g(E)]$. Then $S(E)$ simply is updated according to $S(E) \to S(E) + F$ where $F = \log[f]$. In the original work it is suggested to modify $f \to \sqrt{f}$ after each time a flat histogram has been obtained. The density of states $g(E)$ here only is a relative estimate, but if the exact number of ground states is known then it can be normalized to truly reflect the number of states at a certain energy level. The implicit assumption in the preceding section was that the energy levels are discrete. One way to treat continuous models is to use a binning procedure but this becomes very inefficient if the bins are chosen too wide. To treat continuous cases and to efficiently calculate the joint density of states for multiple observables a generalization to the WL method has been obtained [171].

For the original WL method it can be shown that the error in the estimate of $g(E)$ saturates due to the rapidly decreasing modification factor f [172]. This can be avoided using the $1/t$ algorithm. The WL time t is defined by $t = N_{trials}/N_{bins}$ and updated at every trial move. Again the finess initially is chosen to $F_0 = 1$. Then the original WL algorithm is used until the refinement parameter F becomes smaller than $1/t$. From then on one uses $F(t) \sim 1/t$ until the desired accuracy is obtained.

5.6 Replica exchange

Some systems such as spin glasses exhibit many local energy minima out of which canonical MC algorithms can hardly escape. This implies large autocorrelation times and in some cases even leads to fundamentally wrong results if the algorithm gets stuck in the vicinity of one particular minimum. Also at first order transitions the exponentially increasing tunneling times imply that the algorithm only explores a tiny fraction of phase space, spending most of the time visiting states of the same phase. An efficient work-around for such problems is found in the replica exchange method [55]. There M replica of the same system are simulated in parallel at different temperatures β_m. A state of the system then is defined by the joint state of all independent M replica $\{\mathcal{X}\} = \left\{X_{\mu_0}, X_{\mu_1}, \ldots, X_{\mu_{M-1}}\right\}$. One is thus simulating an extended ensemble with partition function

$$\mathcal{Z} = \mathrm{Tr}_{\{\mathcal{X}\}}\left\{\exp\left(-\sum_{m=1}^{M}\beta_m E_{\mu_m}\right)\right\} = \prod_{m=1}^{M} Z(\beta_m) \tag{5.21}$$

where $Z(\beta)$ is the canonical partition function of a single system. The idea now is that in order to prevent getting stuck in metastable states one proposes to exchange

configurations between two temperatures to reduce the autocorrelations at a single temperature. In practice of course it is much easier to just assign new temperatures to the existing configurations. To assure convergence towards the Boltzmann distribution one invokes

$$\frac{W\left(X_{\mu_m},\beta_m|X_{\mu_n},\beta_n\right)}{W\left(X_{\mu_n},\beta_m|X_{\mu_m},\beta_n\right)}=\exp\left[\left(\beta_n-\beta_m\right)\left(E_{\mu_n}-E_{\mu_m}\right)\right] \tag{5.22}$$

for exchanging the replicas n and m. The acceptance probability is thus given by

$$a_{(\mu_n,\beta_n,\mu_m,\beta_m)(\mu_m,\beta_n,\mu_n,\beta_m)}=\min\left(\exp\left[\left(\beta_n-\beta_m\right)\left(E_{\mu_n}-E_{\mu_m}\right)\right],1\right) \tag{5.23}$$

The actual Monte Carlo procedure can now be summarized as:

1. Simulate all replica simultaneously and independently using any standard canonical MC method for a fixed number of sweeps.

2. Exchange two configurations with the probability given in Eq. (5.23)

From Eq. (5.23) it is obvious that the acceptance probability decays exponentially with the inverse temperature difference thereby only nearest neighbor exchanges are attempted. It is further very inefficient to choose evenly spaced temperatures. Berg [173] suggests to optimize the acceptance ratios by iterating the positions of the temperatures via the following rule. Given some initial spacing one generates a new set of temperatures β'_m by

$$\beta'_0=\beta_0 \text{ and } \beta'_m=\beta'_{m-1}+r_{a,m}\left(\beta_m-\beta_{m-1}\right) \tag{5.24}$$

where the parameter $r_{a,m}$ is determined by the weighted point to point acceptance ratios $\tilde{a}_m$ measured for the exchange move (5.22) for the replica pair $m-1\leftrightarrow m$ via

$$r_{a,m}=\tilde{a}_m\frac{\beta_{M-1}-\beta_0}{\sum_{m=1}^{M-1}\tilde{a}_m\left(\beta_m-\beta_{m-1}\right)} \tag{5.25}$$

Thus large acceptance ratios between two adjacent temperatures tend to increase their spacing in the new setting of couplings, whereas small ones lead to a shrinking distance.

5.7 Replica exchange for the Wang-Landau scheme

The above idea of simulating different replica has also been adapted to the WL scheme [57]. It can be implemented in the following way:

1. Divide the total energy range considered by the WL algorithm in N_w smaller overlapping subwindows. An overlap by around 75% between neighboring sub windows is advantageous [57].

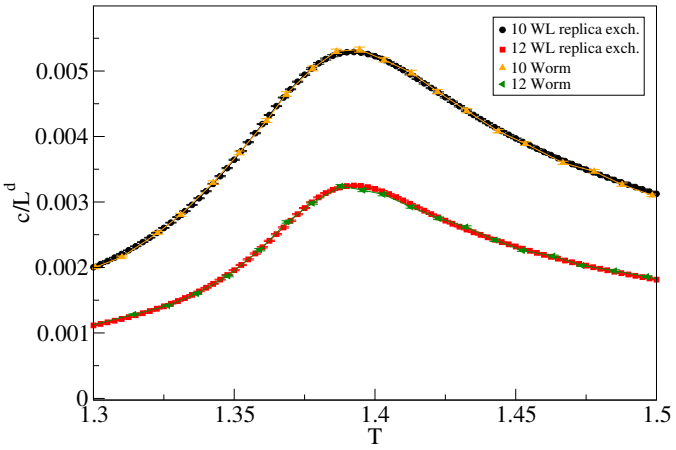

Figure 5.2: MC data for the SRM case in paper III. Specific heat results obtained via serial runs using the worm algorithm, and the WL algorithm with replica exchange using only plaquette loop and straight line updates, agree very well.

2. Now in all subwindows perform standard WL sampling for a fixed number of N_s sweeps accepting changes as in Eq. (5.20). In general one can use several "walkers" performing WL sampling within the same window.

3. All walkers within a sub-interval randomly choose an exchange partner from the neighboring interval. Let walker i be associated with configuration X_μ and walker j be associated with configuration X_ν just before the exchange. If the two are chosen for an exchange attempt then the move is accepted with probability

$$P_{acc} = \min\left[1, \frac{g_i\left(E_\mu\right) g_j\left(E_\nu\right)}{g_i\left(E_\nu\right) g_j\left(E_\mu\right)}\right] \tag{5.26}$$

   Thus in this scheme every walker i has its own density of states $g_i(E)$ and histogram $h_i(E)$ which are updated independently.

4. When multiple walkers are used within a subwindow the error can be reduced with $\sqrt{m}$ by averaging out $g(E)$ among the walkers before continuing to the next step and redistributing. The simulation then potentially moves on faster due to reduction of the effect of outliers in the simulation impeding fast advancement for the next iteration.

5. The simulation is terminated when all energy subwindows have reached the final accuracy. At the end of the simulation all $N_w \times m$ pieces of $g(E)$ fragments are used to calculate the total DOS. Two overlapping regions are joined at the point where the micrcanonical $\beta = d\log\left[g\left(E\right)\right]/dE$ do best coincide.

In paper III this method was used with single walkers in each interval. Averages where performed over independently obtained results. Test results for the SRM case treated in this article are shown in Fig. 5.2.

5.8 Reweighting methods

As for classical MC algorithms the underlying probability distribution is known, data obtained at β_0 can in principle be *reweighted* to a nearby temperature at β via [53]

$$\langle Q \rangle = \frac{\sum_{t=1}^{N_s} Q_t e^{-(\beta-\beta_0)E_t}}{\sum_{t=1}^{N_s} e^{-(\beta-\beta_0)E_{\mu_t}}} \tag{5.27}$$

The reliability of this *single histogram* procedure is however limited by the heat capacity in point β_0. Only if the corresponding temperature $T_0 = 1/\beta_0$ satisfies

$$\frac{|T - T_0|}{T_0} < \frac{T_0^2}{\mathrm{Var}\left[E\left(T_0\right)\right]} = \frac{1}{c(T_0)} \tag{5.28}$$

where c is the total, unnormalized heat capacity its data can be reweighed to T [160]. The efficiency can be boosted by joining the data of several temperatures using the technique of *multi histogram reweighting* [54]. Consider a set of N_β inverse temperatures β_i. At each temperature n_i (ideally independent) measurements shall have been performed. Then we can iteratively calculate the partition function $Z_k = e^{-f_k}$ according to

$$e^{-f_k} = \sum_{i=1}^{N_\beta} \sum_{t=1}^{n_i} \frac{1}{\sum_j n_j e^{(\beta_k-\beta_j)E_{i,t}+f_j}} \tag{5.29}$$

where $E_{i,t}$ is the t^{th} entry in the energy time series at coupling β_i. A way to solve this nonlinear equation is by just feeding a start guess to it and then reiterate until

$$\chi_s^2 = \sum_i^{N_\beta} \left[\frac{e^{-f_{\beta_i}^s} - e^{-f_{\beta_i}^{s-1}}}{e^{-f_{\beta_i}^s}} \right]^2 \tag{5.30}$$

drops below some predefined value ϵ where s denotes the step. A second possibility is given by using a stored energy histogram $h_i(E)$. Then equation (5.29) can be phrased as

$$e^{-f_k} = \sum_{i=1}^{N_\beta} \sum_E \frac{n_i h_i\left(E\right)}{\sum_j n_j e^{(\beta_k-\beta_j)E+f_j}} \tag{5.31}$$

To interpolate between temperature values to a value β we then simply can use

$$e^{-f_\beta} = \sum_{i=1}^{N_\beta} \sum_{t=1}^{n_i} \frac{1}{\sum_j n_j e^{(\beta-\beta_j)E_{i,t}+f_j}} \tag{5.32}$$

which gives us the reweighed estimators of any other operator O stored in the same set of time series

$$\langle O \rangle_\beta = \sum_{i=1}^{N_\beta} \sum_{t=1}^{n_i} \frac{O_{i,t}}{\sum_j n_j e^{(\beta-\beta_j)E_{i,t}+f_j-f_\beta}}. \tag{5.33}$$

The optimized expression for the density of states is given by

$$n(E) = \frac{\sum_{i=1}^{N_\beta} n_i h_i(E)}{\sum_j n_j e^{-\beta_j E+f_j}} \tag{5.34}$$

5.9 Error estimation

To obtain error estimates for the MC trajectories generated via the combination of temperature exchange and histogram reweighting methods in [3] we adapt to the following strategy. We calculate the longest integrated autocorrelation time at each temperature and take values once for each correlation time. Then we generate *synthetic data sets* by independently and uniformly resampling the reduced trajectories obtained. With those we again perform the reweighting procedure and calculate the variance over all estimators obtained. For the disordered systems [1, 2, 4, 5] we obtain averages for different realizations of the disorder independently. As they are uncorrelated the final disorder average can simply be calculated as the mean and variance over all independently obtained final estimators. In the Wang-Landau case we simply calculate different estimates of the density of states and average over the estimators obtained for different final results.

Chapter 6

Results

6.1 Paper I: Defect supersolid

The article considers the possibility of a superfluid onset in solid ^{4}He with signatures different from the bulk λ-transition. The approach is motivated by the peculiar disorder dependence of the NCRI and specific heat discussed in Sec. 2.5 seen in initial experiments [130, 123]. Quite generally we assume the superfluid component to be confined to the defects of the ^{4}He crystal. If the transition is driven by the breakdown of long range phase-coherence and using that ^{4}He is a neutral superfluid Eqs. (2.16) and (3.6) generalize to

$$\mathcal{L} = -\sum_{i,\mu} J_\mu(\boldsymbol{r}_i) \cos[\theta(\boldsymbol{r}_i + \hat{\mu}) - \theta(\boldsymbol{r}_i)] \tag{6.1}$$

The XY coupling parameter Eq. (3.2) is chosen spatially inhomogeneous and random in order to resemble the proportionality $J_\mu(\boldsymbol{r}_i) \propto |\Psi|^2$ where the order parameter amplitude is zero in the bulk, and nonzero on the defect. In particular there were two kinds of crystal defects shown to sustain superflow, dislocation lines and grain boundaries [133, 132, 131]. The former are effectively one dimensional defects extending throughout the whole crystal. By intersecting, these can form an interconnected network that possibly can be pinned by lattice impurities such as ^{3}He. In principle such networks then might support bulk 3D superflow. Similarly grain boundaries separating crystallites in 3D bulk crystals can effectively be seen as planar defects. Previous work on a possible phase transition signature, had mostly considered the effect of disorder with respect to uncorrelated random defects [174]. But in extended defect networks long range correlations can appear. As outlined in Sec. 1.15 this can destabilize the fixed point of the pure system towards a new disordered fixed point in particular with a new disordered critical exponent $\nu_{\rm d}$. We model dislocations in Eq. (6.1) as straight lines on a cubic lattice. The coupling parameters thus show spatial correlations $[\delta J_\mu(\boldsymbol{r})\delta J_{\mu'}(0)] \propto [\delta(x)\delta(y)+\delta(y)\delta(z)+\delta(z)\delta(x)]\delta_{\mu,\mu'}$ where $\delta J_\mu(\boldsymbol{r}_i) \equiv J_\mu(\boldsymbol{r}_i) - [J_\mu]$. As in Eq. (1.84) the integrated correlation func-

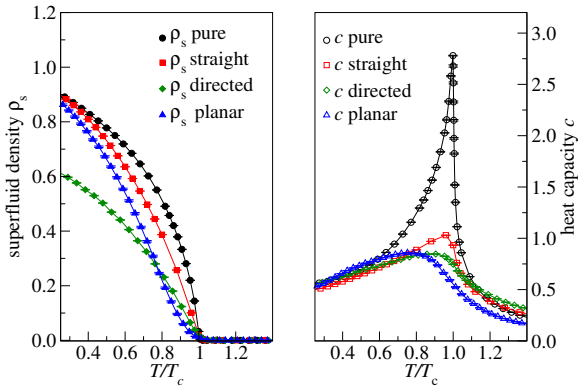

Figure 6.1: Comparison of the onset properties for a system of size $L = 40$ of the different correlated disorder cases considered in [1] compared to the pure 3DXY case. In all cases the onset features of ρ_s are considerably softened and the heat capacity maximum smoothened.

tion over the coupling constants $[(\Delta J)^2_R]$ can be rewritten in terms of the coupling correlation averaged over the sub-volume $V = R^d$,

$$[(\Delta J)^2_R] = C(R) \equiv R^{-d} \sum_{\mu,\mu'} \sum_{\boldsymbol{r}_i \in V} [\delta J_\mu(\boldsymbol{r}_i)\delta J_{\mu'}(0)] \ . \tag{6.2}$$

For straight line disorder Eq. (6.2) gives $C(\xi) \sim \xi^{-a}$ with exponent $a = d - 1 = 2$. Which is the result one would obtain for algebraic correlations with the same decay exponent a according to Eq. (1.88). In a similar way approximating grain boundaries as randomly oriented planes orthogonal to some symmetry direction of the cubic lattice gives $a = d - 2 = 1$. Using the λ-transition value $\nu_{pure} \approx 0.671$ according to the WH criterion Eq. (1.89) both dislocations and grain boundaries obey $2 > a\nu_{\rm pure}$, implying that a new disordered fixed point should appear with $\nu_{\rm d} = 2/a$ with the respective value of a. In contrast to the case of uncorrelated point disorder $[\delta J_\mu(\boldsymbol{r}_i)\delta J_{\mu'}(0)] \propto \delta_{\mu,\mu'}\delta_{\boldsymbol{r}_i,0}$ where $\nu_{\rm d} = \nu_{pure} > 2/d$. It is precisely the exponent ν that controls the onset properties of $\rho_{\rm s} \sim |T - T_{\rm c}|^\nu$ and the shape of the scaling part of the heat capacity $c \sim |T - T_{\rm c}|^{-\alpha}$ via the exponent $\alpha = 2 - d\nu$. For the correlated disorder cases considered $\nu \geq 1$ automatically implies that the derivatives $d\rho_s/dT$ and dc/dT remain finite at $T_{\rm c}$, in contrast to the pure model where both diverge. To relax the straight line condition we also consider directed random walks with enforced periodicity along the drift direction. These show a decay in the integrated correlation function that is similar to the one observed for straight lines. The upshot of this analysis is that all these disorder types should lead to onset signatures that are softened with respect to the original λ-transition as shown in Fig. 6.1. There is thus no strong reason to expect a hypothetical supersolid transition

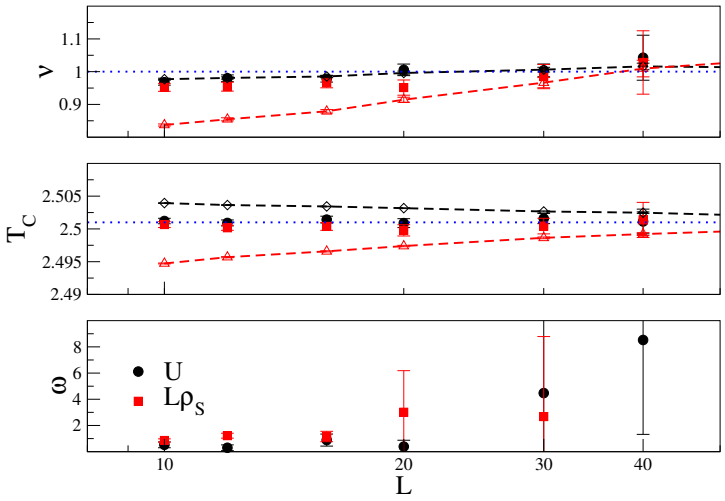

Figure 6.2: Scaling results for MC data of the Binder ratio $U(T,L) = \langle M^4\rangle / \left(\langle M^2\rangle\right)^2$ and the helicity modulus $L\rho_s(T,L)$ obtained for the defected supersolid model Eq. (6.1). Open symbols connected by dashed lines are the scaling results presented in Fig. 3 of the paper I. Filled symbols are results obtained by a corrections to scaling ansatz for $U, L\rho_s$ of the form $a_0 + a_1 x + a_2 x^2 + L^{-\omega} c_\omega$ where $x = L^{1/\nu}(T - T_c)/T_c$ using system sizes $L = 10, 12, 16, 20, 30, 40, 60, 80$ and $x < 0.2$. Invoking these corrections clearly improves the agreement if the smallest system sizes $10, 12, 16, 20$ are included. Whereas the estimate of ν obtained via U is hardly affected by the correction term, the one obtained via $L\rho_s$ is greatly improved. In addition the T_c estimates obtained for both quantities respectively are considerably improved and agree within error bars in contrast to the curves obtained without corrections. The estimate for the respective corrections to scaling exponent ω are now stable if the smallest system sizes are included but vary strongly upon using only the largest system sizes. The correction term becomes much smaller for these sizes compared to the asymptotic scaling function and thus harder to estimate. In addition the number of data points entering the scaling ansatz is much smaller. A problematic property of the correction term is that increasing c_ω can be compensated for if at the same time ω is increased.

to have the same signatures as the 3D λ-transition if the superflow is confined to extended interconnected lattice defects. For the most interesting candidate case of straight dislocation lines our results suggest that the WH conjecture $\nu_d = 2/a = 1$ is correct. For small system sizes corrections to scaling seem present but can be corrected for as shown in Fig. 6.2.

6.2 Paper II: Quantum critical dynamics in the 2D Bose glass to superfluid transition

We test the scaling prediction $z = d$ for the dynamic critical exponent at the Bose glass to superfluid quantum phase transition via Monte Carlo simulation methods. Choosing all couplings K_i^α in Eq. (4.30) isotropic and only including random on-site disorder the link-current model [31] defined by the Hamiltonian

$$H_V = \frac{1}{K}\left[\sum_{\boldsymbol{x},\hat{\alpha}}^{\nabla\cdot\mathbf{J}=0} \frac{1}{2}\left(J_{\boldsymbol{x}}^{\alpha}\right)^2 - \sum_{(i,\tau)} \left(\tilde{\mu} + \delta\tilde{\mu}_i\right) J_{(i,\tau)}^{\tau}\right] \tag{6.3}$$

emerges. Here $\boldsymbol{x} = (i, \tau)$ denotes sites on the space-time lattice $L^2 \times L_\tau$ on which the link currents reside. The chemical potential is adjusted to $\tilde{\mu} = 1/2$ and the random on-site potential is chosen at maximum strength to be uniformly distributed between $-\tilde{\Delta} < \delta\tilde{\mu}_i < \tilde{\Delta}$ where $\tilde{\Delta} = 1/2$. To extract the exponent z we construct a scaling function based on the winding number fluctuations defining the stiffness ρ_s via [175]

$$\rho_s = \frac{m}{\hbar^2}\frac{\langle W^2\rangle L^{2-d}}{\beta d} \sim L_\tau^{-1} L^{2-d}\langle W^2\rangle \tag{6.4}$$

where $\beta \sim L_\tau$ corresponds to the length of the time direction of the anisotropic space-time lattice. In the critical region, using $k = (K - K_c)/K_c$, the fluctuations $\langle W^2\rangle$ are given by a universal scaling function $\langle W^2\rangle = \mathcal{W}\left(L^{1/\nu}k, \alpha_\tau\right)$ where $\alpha_\tau = L_\tau/L^z$ is the aspect ratio. At the quantum critical point $k = 0$ and the winding number fluctuations reduce to a universal scaling function of the aspect ratio α_τ alone. At fixed L, K, $\langle W^2\rangle$ should be an increasing function of L_τ. This follows directly via rearranging Eq. (6.4) to

$$\langle W^2\rangle \sim L_\tau L^{d-2}\rho_s\left(L, L_\tau\right) \tag{6.5}$$

and by the fact that the superfluid density, at fixed L, is a monotonically increasing function of $\beta \sim L_\tau$. Then the winding number fluctuations automatically are monotonically increasing in the aspect ratio α_τ. The thermodynamic limit for the QPT corresponds to simultaneously taking $L \to \infty$ and $L_\tau \to \infty$. But care needs to be taken in the limiting procedure. Using cubic volumes, as apparently done in Ref. [159] leading to the result $z \approx 1.4$, should be invalid as then, upon increasing L, the aspect ratio is systematically reduced unless $z \leq 1$. Our approach is based on the general scaling function

$$\Phi(K, L, L_\tau) \equiv \frac{\langle W^2\rangle}{\alpha_\tau^2} = \tilde{\Phi}(L^{1/\nu}k, \alpha_\tau) \tag{6.6}$$

motivated by the fact that $\langle W^2\rangle/L_\tau^2$ at fixed K, L has a maximum at L_τ^* [2]. As the corresponding aspect ratio α_τ^* where this maximum occurs has to be the same for all L one gets

$$\alpha_\tau^* = L_\tau^*/L^z = \tilde{\gamma}(L^{1/\nu}k) \tag{6.7}$$

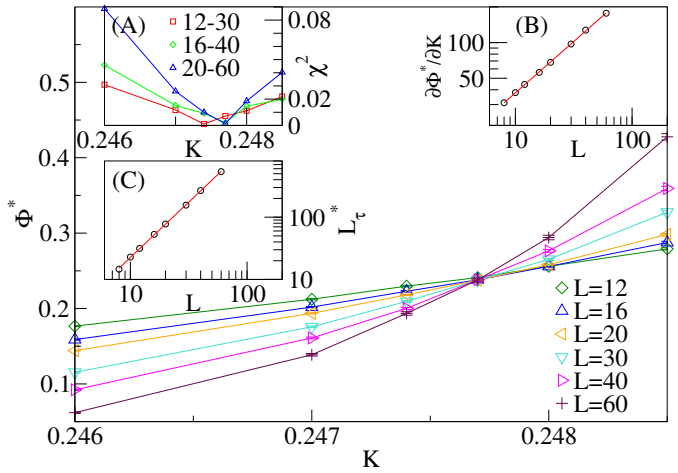

Figure 6.3: Scaling results for $\Phi\left(K, L, L_\tau\right)$ *main figure:* At all couplings K we identify the maximum $\Phi^*(K, L, L_\tau)$ of W^2/L_τ^2 for fixed L. At K_c Eq. (6.6) implies $\Phi^* \sim L^{-2z}$. Using system sizes $L \geq 16$ only, the data scales nicely with $z \approx 1.78$. *A:* Dependence of the residuals from a linear fit of $\log\left[\Phi^*(K, L, L_\tau)\right]$ vs. $\log L$ shows a clear minimum at $K = 0.2477$. *B:* The derivative with respect to K of Φ^* taken at K_c obtained via a third order polynomial fit to the data shows a power law divergence $\sim L^{1/\nu}$ where $\nu \approx 1.154$. *C:* The position L_τ^* of the maximum at $K_\mathrm{c} = 0.2477$ for different system sizes also scales $\sim L^{1.78}$.

Thus taking only the maxima at each fixed K, L the anisotropic scaling function $\tilde{\Phi}(L^{1/\nu}k, \alpha_\tau)$ reduces to a function of a single variable $L^{1/\nu}k$ and, given that the value of z is adjusted correctly, one finds a set of curves that intersect at K_c as shown in Fig. 6.3. As shown in the inset (C) at $K_\mathrm{c} \approx 0.2477$ the power-law $L_\tau \sim L^{1.78}$ is obeyed over a large range of system sizes. Further by expanding the scaling function $\mathcal{W}(L^{1/\nu}k, \alpha_\tau)$ into a third order, bivariate polynomial and fitting our data to this form for several intervals of aspect ratios, we find that our results agree well within $z = 1.8 \pm 0.05$ suggesting the relation $z = d$ is not obeyed. The values of the exponents obtained can also be tested using the scaling of the uniform order parameter susceptibility

$$\chi = \sum_{\boldsymbol{r},\tau} G(\boldsymbol{r}, \tau) \sim \int_0^L d^d r \int_0^{L^z} d\tau\, G\left(\boldsymbol{r}, \tau\right) = \tilde{G}(\mathbf{k} = 0, \omega = 0) \sim L^{2-\eta} \qquad (6.8)$$

where the generalized scaling ansatz for the propagator Eq. (5.18) in $D = d + z$ dimensions

$$G(\boldsymbol{r}, t, \boldsymbol{r}', t') = \left[\langle e^{i(\theta_{\boldsymbol{r},t} - \theta_{\boldsymbol{r}',t'})}\rangle\right] \sim r^{-(d+z-2+\eta)} g(r/\xi, \tau/\xi^z) \qquad (6.9)$$

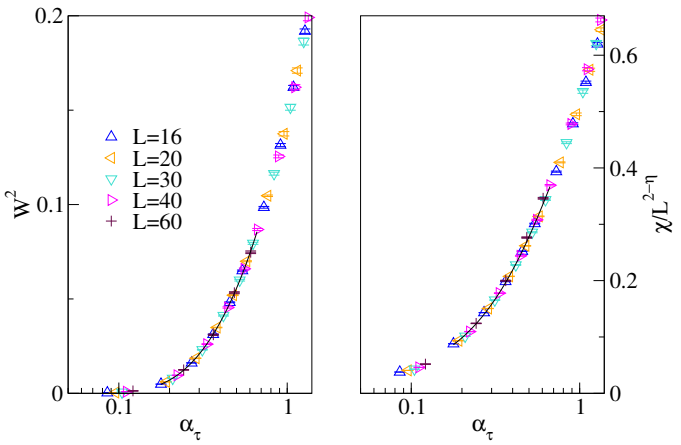

Figure 6.4: Scaling of the winding number fluctuations and the order parameter susceptibility at $K_c = 0.2477$ as functions of the aspect ratio $\alpha_\tau = L_\tau/L^z$ using $\eta = -0.29$ and $z = 1.8$. Observe that W^2 increases monotonically as a function of the aspect ratio. This invalidates using isotropic space-time volumes $L = L_\tau$ in order to extrapolate to the thermodynamic limit.

has been used. Figure 6.4 shows a combined scaling collapse of the winding number fluctuations and the susceptibility at $K_c = 0.2477$.

6.3 Paper III: Fluctuation-induced first order phase transitions in type-1.5 superconductors in zero external field

Paper III considers an effective composite vortex model for type 1.5 superconductors in 3D. Generalizing from the 2D results illustrated in Sec. 2.4 we propose a model for a two-band superconductor with strong interband coupling, made of a strongly type-II component with very short coherence length and a type-I component, with a much lower ground state density. For these systems the nature of the superconducting phase transition cannot be deduced in the same ways as for the type-I/type-II limits in Sects. 2.3 and 3.1. It is still expected that the phase transition is driven by vortex excitations. We generalize the 2D interaction Eq. (2.43) for composite vortices without fluctuating internal structure to the 3D Hamiltonian

$$H = \sum_{i,j,\sigma}^{\nabla \mathbf{q}=0} \left[\frac{1}{2} q_i^\sigma V_{ij} q_j^\sigma + \frac{1}{2} \left| q_i^\sigma \right| U_{ij} \left| q_j^\sigma \right| \right] \tag{6.10}$$

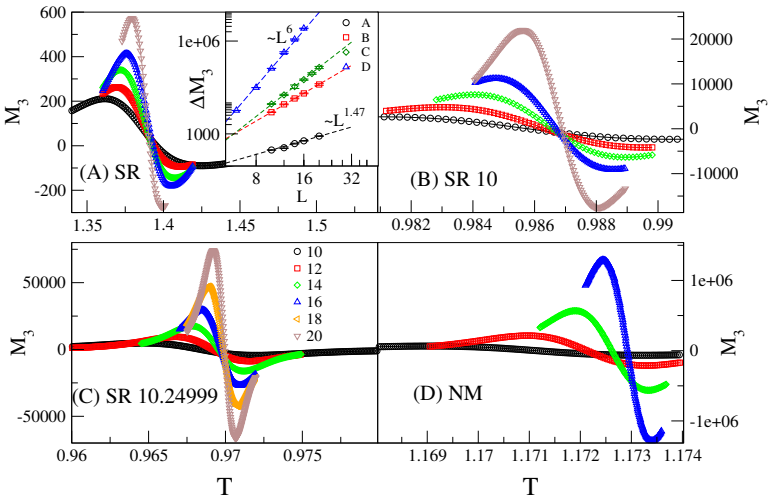

Figure 6.5: Comparison of MC results obtained for the third moment of the action M_3 for all parameter sets in article III. Inset: Scaling of the difference ΔM_3 between the extrema displayed by M_3. The short-ranged and nonmonotonic limiting cases (A),(D) scale in good agreement with the expectation of an inverted 3DXY transition and a strong first order transition respectively.

In 3D the Bessel-functions are replaced by Yukawa potentials V_{ij} and U_{ij}

$$Y_{ij} = Y\left(\frac{|\mathbf{r_i}-\mathbf{r_j}|}{\lambda_Y}\right) = \frac{c_Y}{L^d}\sum_{\mathbf{k}}\frac{\cos\left(\mathbf{k}\cdot(\mathbf{r_i}-\mathbf{r_j})\right)}{6-\sum_\sigma 2\cos\left(k_\sigma\right)+\lambda_Y^{-2}} \tag{6.11}$$

solving the 3D counterpart of Eq. (2.37). The first term corresponds to the current-current interaction $\tilde{m}^2 K_0\left(r/\lambda\right)$ in Eq. (2.43) with $\lambda_V = \lambda$. Neglecting density terms $C_U = 0$ the model is equivalent to a 3D type-II superconductor in the London-limit and the transition is expected to lie the inverted 3DXY universality class. For finite $C_U < 0$ the second term is always attractive as desired by Eq. (2.43). The range λ_U is set by the largest coherence length $\xi_L = \max\{\xi_1, \xi_2\}$ of the normal modes $\tilde{g}_{1,2}$ introduced in Sec. 2.4. As the potential U_{ij} is exponentially screened the transition is not expected to belong to a new universality class, even if C_U and range ξ_L are changed. But this might in general cause the second order phase transition to become first order.

We study this model via extensive Monte Carlo simulations. We start from a system with short-ranged, monotonic interactions (SR-case) by setting $C_V = 41$, $C_U = -2.5$ and $\xi_L = \lambda = 0.5$ measured in terms of the numerical lattice spacing. We find upon increasing the attractive range ξ_L that the heat capacity peak, signaling the transition, becomes increasingly sharp. For the choice of $\xi_L = 2\lambda = 1$,

where the vortex interaction is nonmonotonic for vortices of equal winding, we find clear finite-size signatures of a temperature-driven first order transition. In particular, the heat capacity peak scales $\sim L^d$ and the energy histogram exhibits a double peak structure with a growing free energy barrier ΔF as discussed in Sec. 1.16. In addition for the same choice of parameters, but with a truncated attractive potential U_{ij} at a range $r_c = 3$ beyond which the nonmonotonicity appears, the transition shows no sign of first order scaling for small system sizes and presumably becomes continuous. Setting the cut-off $r_c = 5$, such that the attractive tail is just included, lets the first order signatures reappear.

We also consider systems with short-ranged, repulsive interactions close to the stability boundary of the model Eq. (6.11), which is the condition of a vortex free ground state. We choose the same values of C_V, λ, ξ_L as in the SR case but larger negative values $C_U = -10, -10.24999$. We denote these as SR 10 and SR 10.24999. For these systems no unambiguous indications for a first order transition are found. The finite-size scaling properties do however significantly deviate from those expected for the inverted 3DXY transition. Figure 6.5 shows MC data for the third moment of the action [176]

$$M_3 = \langle H - \langle H \rangle \rangle^3 \sim \frac{\partial}{\partial T} \left(T^2 L^d c_L \right) \tag{6.12}$$

which exhibits two extrema around T_c whose difference ΔM_3 scales as $\sim L^{\frac{1+\alpha}{\nu}}$ for continuous- and $\sim L^{2d}$ for discontinuous transitions. The size dependence of c_L^* and ΔM_3 at a first order transition therefore corresponds to effective exponents $\alpha = 1, \nu = 1/d$. The system with a nonmonotonic interaction shows clear finite-size scaling signatures of a first order transition, and the SR system shows very good agreement with the scenario of a inverted 3DXY transition. The SR 10 and SR 10.24999 show large deviations from both scenarios.

6.4 Paper IV: Phase transitions with critical loop disorder

We consider phase transitions in disordered, ferromagnetic Ising and XY models. In this article the disordered bond couplings $J_\mu(\boldsymbol{r}_i)$ are taken from static equilibrium configurations of loop models in the Ising and inverted-XY universality class and therefore form *closed defect lines*. The aim is to determine if such *loop disorder* can give rise to a new long-range-disorder fixed point with critical exponent ν given by the lower bound of Eq. (1.89) in agreement with the Weinrib-Halperin (WH) theory [48]. The inverted XY model, or link-current model [31], can be obtained for $\mathcal{A} = 0$ from Eq. (3.12) upon integrating out the phases and is described by

$$\beta_{\text{dual}} H_{\text{D,XY}} = \frac{\beta_{\text{dual}}}{2} \sum_{\mu, \boldsymbol{r}_i}^{\nabla \cdot \mathbf{q} = 0} \left[q_\mu(\boldsymbol{r}_i) \right]^2 \tag{6.13}$$

in any dimension. The loop transformation essentially inverts the temperature scale $\beta_{\text{dual}} \sim \beta^{-1}$ and replaces the spin degrees of freedom by integer valued, directed

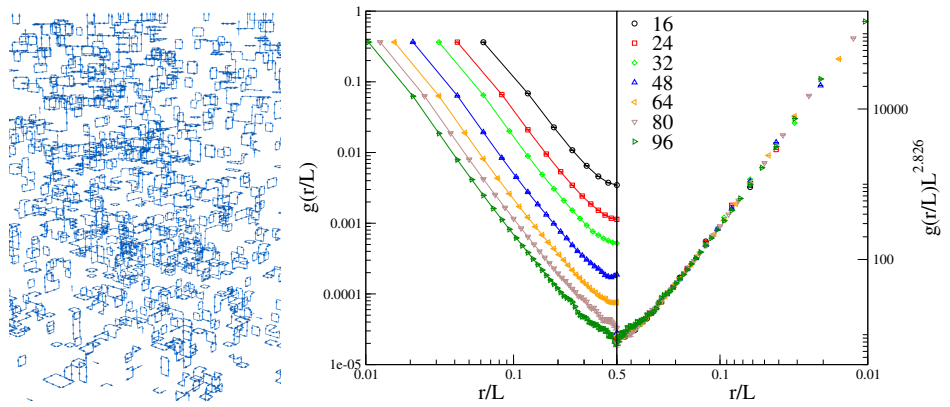

Figure 6.6: left: Snapshot of a 3D Ising loop configuration generated at $\beta_{\mathrm{dual,C}}$. The local coupling strength $J(\boldsymbol{r}_i)$ defined by Eq. (6.15) corresponds to the mean number of nonzero links attached to a site plus a uniform background term. For large separations the coupling correlations should follow a power law $\sim r^{-a}$ with $a = -\alpha_{\mathrm{loop}}/\nu_{\mathrm{loop}} + d \approx 2.826$ right: Monte Carlo results for the two-point correlations for 3D Ising critical loop disorder generated at $\beta_{\mathrm{dual,C}} \approx 1.5228$. The short-ranged part decays very quickly. Rescaling all curves by L^a where $a = 2.826$ gives a very convincing collapse for $r/L > 0.1$.

bond variables $q_\mu(\boldsymbol{r}_i)$. In the Ising case, the spin degrees of freedom are replaced by *undirected* bond variables $q_\mu(\boldsymbol{r}_i) \in \{0, 1\}$. In loop representation Eq (3.29) the Ising Hamiltonian is given by

$$\beta_{\mathrm{dual}} H_{\mathrm{D,Ising}} = \beta_{\mathrm{dual}} \sum_{\boldsymbol{r}_i,\mu}^{\{q_\mu(\boldsymbol{r}_i)=0,1\}\subset \mathrm{CP}} q_\mu(\boldsymbol{r}_i) \tag{6.14}$$

with inverted temperature scale $\beta_{\mathrm{dual}} = \log[\coth(\beta)]$. The closed path (CP) constraint means that each site $\boldsymbol{r}_i$ has an even number of nonzero q_μ attached. In the paper, using equilibrium loop configuration of these two models, the couplings in the disordered spin systems Eq. (1.65), out of which we intend to study the Ising and XY case, are set to

$$J_\mu(\boldsymbol{r}_i) = \begin{cases} 1 & \text{for } q_\mu(\boldsymbol{r}_i) = 0 \\ 2 & \text{for } q_\mu(\boldsymbol{r}_i) \neq 0 \end{cases} \tag{6.15}$$

This means that the presence of a loop increases the coupling between nearest neighbor spins connected to it.

Specifically for *critical loop disorder*, meaning quenched, disordered coupling configurations obtained from simulations at the critical couplings $\beta_{\mathrm{dual,C}}$, one ex-

pects long-range correlations in the bond variables $J_\mu(\boldsymbol{r})$. At $\beta_{\mathrm{dual,C}}$ the probability amplitude Eq. (5.18) to insert an open loop configuration with head and tail separated by a distance r scales as $P(r) \sim r^{-(d-2+\eta_{\mathrm{loop}})}$ for both loop models resembling algebraic spin correlations in the original spin models. Therefore the natural expectation is, that by mapping such configurations on the couplings $J_\mu(\boldsymbol{r}_i)$ of lattice spin models via Eq. (6.15), the average local couplings $J(\boldsymbol{r}_i) = \frac{1}{2}\sum_\mu (J_\mu(\boldsymbol{r}_i) + J_\mu(\boldsymbol{r}_i - \mu))$ show similar power law correlations.

Via simple scaling arguments and numerical simulations in 3D this is shown not to be the case. The approach we use to calculate the defect correlations in the paper is illustrated in detail in the next section and applied to a more general case. The disorder correlations $g(|\boldsymbol{r}|) = L^{-d}\sum_{\boldsymbol{r}_i}\left([J(\boldsymbol{r}_i)J(\boldsymbol{r}_i+\boldsymbol{r})] - [J]^2\right)$ turn out to be not entirely algebraic. Here $[\ldots]$ means disorder average over quenched equilibrium loop configurations which is equivalent to a *thermal average* for the loop model studied. As the loop model Hamiltonian, at criticality, basically is proportional to the total number of segments q_μ present in the system one finds

$$c(\beta_{\mathrm{dual}}, L) = c_a(\beta_{\mathrm{dual}}) + c_s(\beta_{\mathrm{dual}}, L) \propto \sum_{\boldsymbol{r}\in V} g(|\boldsymbol{r}|) \tag{6.16}$$

where c_s is the singular part of the heat capacity per lattice site and c_a the analytic part. For *critical loop disorder* one expects $g(r) = g_{\mathrm{short}}(r) + g_{\mathrm{scale}}(r)$ where

$$g_{\mathrm{scale}}(r) \sim r^{-a} \tag{6.17}$$

decays with exponent $a = -\alpha_{\mathrm{loop}}/\nu_{\mathrm{loop}} + d$, determined by the known exponents of the generating loop model. The function g_{short} is short-ranged and does not contribute to scaling. In particular a is independent of η_{loop} and, as long as the hyperscaling law Eq. (1.42) is obeyed, essentially only determined by the heat capacity exponent α_{loop} and d.

For the universal properties of the phase transitions in 3D Ising and 3DXY spin models with loop defects the WH extension of the Harris criterion then gives rise to the following expectation. Loop disorder generated by bond variable configurations of Eqs. (6.13) and (6.14) only yields a fixed point stability criterion different from the standard case of uncorrelated point disorder $\nu > 2/d$, if the generating loop model obeys $\alpha_{\mathrm{loop}} > 0$ e.g. a heat capacity peak that diverges with system size faster than $\log(L)$. For the mechanisms considered this only applies to the case of Ising loops in 3D $\alpha_{\,\mathrm{loop}} \approx 0.11$ and $\nu_{\,\mathrm{loop}} \approx 0.63$ [10]. In MC simulations of 3D Ising and 3DXY models exposed to this particular kind of disorder we find good agreement with the WH value $\nu_{\mathrm{d}} = 2/a \approx 0.71$. Figure 6.6 shows a snapshot of a 3D Ising loop model at criticality and the scaling of the resulting *critical loop disorder* coupling correlation function.

The "heat capacity sum rule" applied to spin systems

With the same approach used to determine the loop correlations in paper IV we attempt to construct a scaling function which can be used to determine the critical

exponent ν and the ratio α/ν also in other cases. For an arbitrary Hamiltonian which can be expressed in terms of local variables $q(\boldsymbol{r}_i)$ via

$$H = \sum_i q(\boldsymbol{r}_i) \tag{6.18}$$

such as $q(\boldsymbol{r}_i) = \sum_\mu J_\mu(\boldsymbol{r}_i) S(\boldsymbol{r}_i) S(\boldsymbol{r}_i + \hat{\mu})$ for the standard $O(N)$ models, or $q(\boldsymbol{r}_i) = S(\boldsymbol{r}_i) E(\boldsymbol{r}_i)$ using the field $E(\boldsymbol{r}_i) = \sum_j V(\boldsymbol{r}_i - \boldsymbol{r}_j) S(\boldsymbol{r}_j)$ for models with pair interactions, the heat capacity can be expressed as the integral over a correlation function $g(\boldsymbol{r})$ via

$$\begin{aligned} c &= L^{-d}\beta^2 \left(\langle H^2 \rangle - \langle H \rangle^2 \right) && (6.19)\\ &= L^{-d}\beta^2 \sum_{i,j} \left[\langle q(\boldsymbol{r}_i) q(\boldsymbol{r}_j) \rangle - \langle q(\boldsymbol{r}_i) \rangle \langle q(\boldsymbol{r}_j) \rangle \right] && (6.20)\\ &= \beta^2 \sum_i g(\boldsymbol{r}_i) && (6.21) \end{aligned}$$

Assuming rotational invariance the Fourier transform $g^*(k)$ of the correlation function $g(|\boldsymbol{r}|)$

$$g^*(k) = L^{-d} \langle |q(\mathbf{k})|^2 \rangle - \langle q \rangle^2 \delta_{\mathbf{k},0} \tag{6.22}$$

yields a similar "sum rule" as in Eq. (6.8)

$$c = \beta^2 \sum_i g(\boldsymbol{r}_i) = \beta^2 \lim_{\mathbf{k}\to 0} g^*(\mathbf{k}) = \beta^2 g^*(\mathbf{k})\,|_{\mathbf{k}=0} \tag{6.23}$$

At criticality it should be possible to decompose $g(|\boldsymbol{r}|)$ in a short-ranged part, giving rise to the analytic contribution to c, and a long-ranged part, $g_{\text{scale}}(r) \sim r^{\alpha/\nu - d}$, yielding the scaling contribution $\sim L^{\alpha/\nu}$. If the leading contribution to the Fourier transform of the short ranged part at small k can be approximated by a constant the ansatz

$$\beta^2 g_L^*(k) \sim w k^{-\alpha/\nu} + v \tag{6.24}$$

where v and w are real can be made. Taking the difference between the two smallest wave vector components gives

$$\Delta g(T, L) = T^{-2} \left[g^*(2\pi/L) - g^*(4\pi/L) \right] \approx c^* L^{\alpha/\nu} \tag{6.25}$$

where $c^* = \beta^2 w (2\pi)^{-\alpha/\nu} \left(1 - 2^{-\alpha/\nu}\right)$. This defines an operator with scaling dimension α/ν and allows the finite-size scaling ansatz

$$L^{-\alpha/\nu} \Delta g(T, L) = \Delta \tilde{g}\left(L^{1/\nu} t \right) \tag{6.26}$$

where $t = (T - T_c)/T_c$. Equation (6.26) might also provide a direct test of the hyperscaling relation Eq. (1.42). Replacing α/ν by $2/\nu - d$ a collapse on a universal

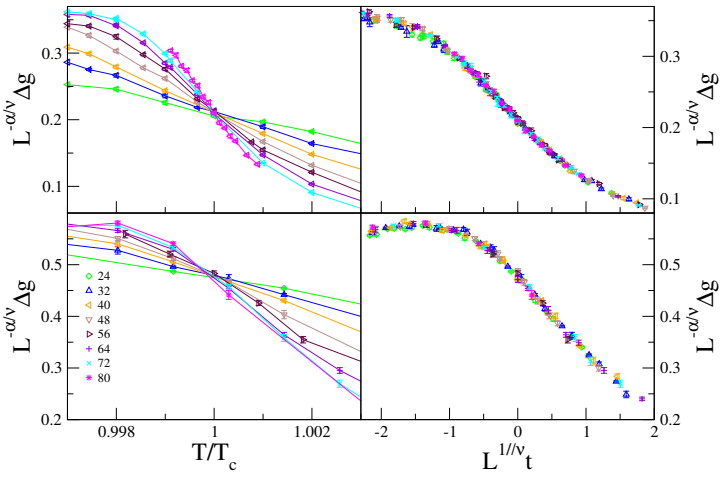

Figure 6.7: The quantity Δg can be used to determine the exponent ν and the exponent ratio α/ν independently. The upper panel shows results for the 3D Ising model using $\nu = 0.63$, $T_\mathrm{c} = 4.5115$ and $\alpha = 0.11$. The lower panel shows results for the 3DXY model in spin representation using $T_\mathrm{c} = 2.2018$, $\nu = 0.671$ and $\alpha = -0.0146$. For these models $q(\boldsymbol{r}_i) = \sum_\mu S(\boldsymbol{r}_i)\, S(\boldsymbol{r}_i + \hat{\mu})$.

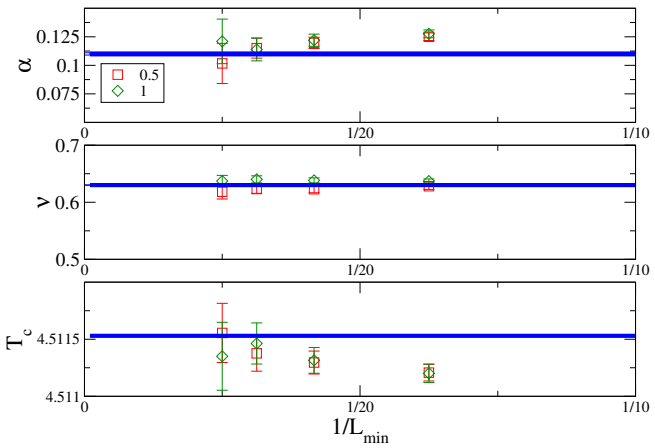

Figure 6.8: Scaling results for the 3D Ising MC data of Δg shown in the upper row of Fig. 6.7. A second order polynomial ansatz to Eq. (6.26) within the intervals $\left|L^{1/0.63}\,(T/4.5115 - 1)\right| < 0.5, 1$ was used. Here α, ν and T_c are free parameters. The agreement with the numerical estimates $\nu = 0.6301(4), \alpha = 0.110(1)$ from Refs. [177, 10] (thick blue lines) is good. In all cases system sizes in the range $L = L_\mathrm{min}$ to $L = 80$ have been considered.

scaling function $\Delta\tilde{g}$ can only be expected if Eq. (1.42) holds. Figure 6.7 illustrates the method using MC data for Δg obtained for the 3D Ising and 3DXY models. For both cases curves for $L^{\alpha/\nu}\Delta g$ show nice intersections and collapse on universal scaling functions. Figure 6.8 shows scaling results obtained for the 3D Ising model using a second order polynomial ansatz for $\Delta\tilde{g}$ and compares them to numerical estimates [177, 10].

6.5 Paper V: Phase transitions in systems with critical cluster defects

Another natural way to create long-range correlated, disordered coupling constants with the help of a critical point is using the *active bonds* of spin clusters at criticality. Specifically we study a model of quenched disorder given by frozen-in configurations of a 3D Ising model

$$\mathcal{H}_{\mathrm{Ising}} = \beta H_{\mathrm{Ising}} = -\beta \sum_{i,\mu} S\left(\boldsymbol{r}_i\right) \cdot S\left(\boldsymbol{r}_i + \hat{\mu}\right) \tag{6.27}$$

coupling to the phase fluctuations of a 3DXY model described by the Hamiltonian

$$\mathcal{H}_{\mathrm{XY}} = \beta H_{\mathrm{XY}} = -\beta \sum_{i,\mu} J_\mu(\boldsymbol{r}_i) \cos\left(\theta\left(\boldsymbol{r}_i\right) - \theta\left(\boldsymbol{r}_i + \hat{\mu}\right)\right) \tag{6.28}$$

The random bond couplings are set to

$$J_\mu\left(\boldsymbol{r}_i\right) = 1 + (\Delta - 1)\delta J_\mu\left(\boldsymbol{r}_i\right)) \tag{6.29}$$

with local disorder $\delta J_\mu\left(\boldsymbol{r}_i\right)$ determined by the frozen-in Ising configuration

$$\delta J_\mu\left(\boldsymbol{r}_i\right) = \frac{\left(S\left(\boldsymbol{r}_i\right) + 1\right)\left(S\left(\boldsymbol{r}_i\right) + S\left(\boldsymbol{r}_i + \hat{\mu}\right)\right)}{4} \tag{6.30}$$

As $S\left(\boldsymbol{r}_i\right) = \pm 1$ this automatically yields a bimodal distribution $J_\mu\left(\boldsymbol{r}_i\right) = 1, \Delta$ with all bonds connecting neighbors $S\left(\boldsymbol{r}_i\right) = +1$ set to Δ. As in paper IV we choose $\Delta = 2$ for our numerical simulations. The coupling correlations are expected to be dominated by the Ising spin-correlation function and should, to leading order, decay algebraically as $g(r) \sim r^{-a}$ with exponent $a = d - 2 + \eta_{\mathrm{g}}$. This implies $a < d$ for all relevant dimensions. The subscript "g" refers to the 3D Ising critical exponents $\nu_{\mathrm{g}} = 0.6301(4), \eta_{\mathrm{g}} = 0.0364(5)$, and $\beta_{\mathrm{g}} = 0.3265(3)$ of the disorder generating mechanism [10]. Below the upper critical dimension this is equivalent to $a = 2\beta_{\mathrm{g}}/\nu_{\mathrm{g}}$ and thus in 3D to $a \approx 1.037$.

In large scale MC simulations of the 3DXY Hamiltonian Eq. (6.28) double peak signatures in the disorder averages of the XY spin-susceptibility and shoulders in the heat capacity appear. One might be tempted to interpret these as indications for either two subsequent phase transitions or as evidence for algebraic finite-size

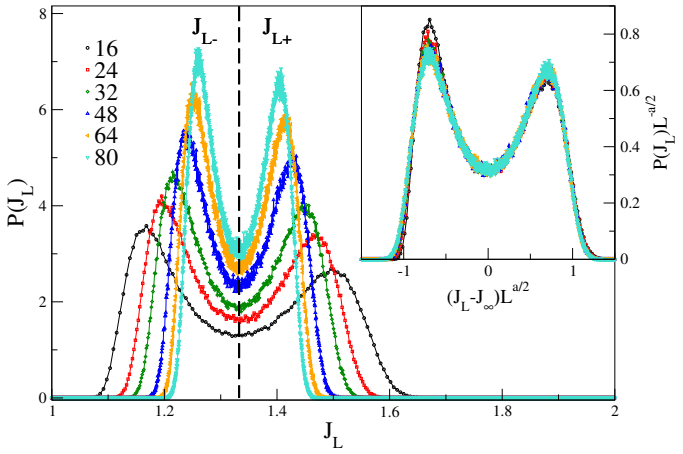

Figure 6.9: The probability density of the mean coupling strength exhibits a double peak structure. As in our disorder mechanism Eq. (6.30), for antiparallel Ising spin neighbors $S(\boldsymbol{r})\,S(\boldsymbol{r}+\hat{\mu}) = -1$, the coupling always is set to $J_\mu(\boldsymbol{r}) = 1$, the resulting histogram is asymmetric. *inset:* To leading order, the coupling distribution scales as the magnetization distribution of a classical 3D Ising model with peak height $\sim L^{\beta_g/\nu_g} = L^{a/2} \sim L^{0.52}$ and a peak width scaling inversely to the height. This gives rise to the apparent double peak signatures found in the disorder averages of the XY spin susceptibility Fig. 6.10.

scaling, in a finite range of temperatures such as recently reported for 2D Potts models with long-range correlated disorder [178]. Taking a closer look at the distribution for the average coupling strength J_L within the system the mechanism behind this feature is revealed. For a random coupling configuration averaged over the whole volume L^d, J_L can be seen as a random variable determined by the joint distribution of the Ising magnetization and energy via

$$J_L = \frac{1}{dL^d}\sum_{\boldsymbol{r},\mu} J_\mu(\boldsymbol{r}) = 1 + \frac{(\Delta-1)}{4}\left(1 + 2m_L - \frac{1}{d}e_L\right) \tag{6.31}$$

Due to the double peak structure of the Ising magnetization-histogram shown in Fig. 1.3, the mean coupling J_L in Fig. 6.9 exhibits a similar structure. This has dramatic consequences, Fig. 6.10 illustrates that the ordinary disorder average does not capture the properties of the "infinite" system within a broad region of temperatures. The system is non self-averaging within this region [179]. An important fact is, that none of the single disorder realizations shows any double peak signature, which the disorder average apparently displays.

In the paper, we use the sample to sample fluctuations of different scaling quantities and show that those collapse well on a scaling function within the region

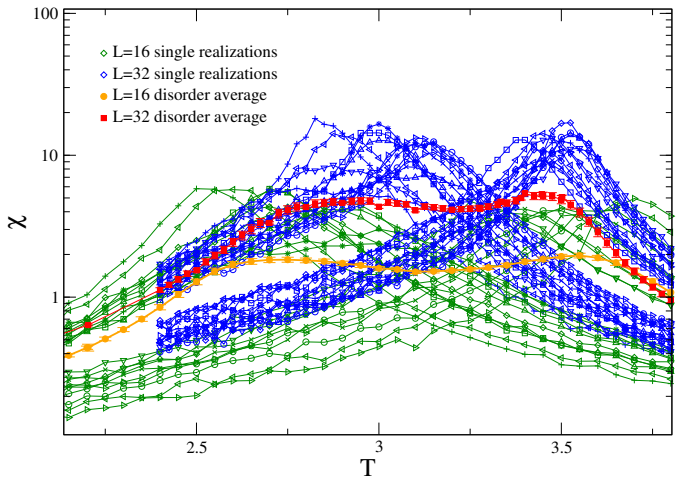

Figure 6.10: MC data for the spin susceptibility χ of the 3DXY model with cluster defects Eq. (6.28). Disorder average vs. averages for single disorder realizations for sizes $L = 16, 32$. This region where the system is non self-averaging decays however slowly towards a single transition temperature.

where the system is non self averaging. The width of this regions is found to decay slowly as $\sim L^{-a/2} = L^{-0.52}$, where a again is the exponent describing the disorder correlations. This can be understood by the fact that the exponent a at the same time determines the width of the distribution for the average coupling per realization, as can be seen from the variance

$$\mathrm{Var}\,(J_L) \sim \left(\langle m_L^2 \rangle + \frac{L^{-d} T_c^2}{4d^2} c_{s,L} \right) \sim c_{m_L} L^{-2\beta_g/\nu_g} + c_1 L^{-d} + c_2 L^{\alpha_g/\nu_g - d} \quad (6.32)$$

and $a = 2\nu_g/\beta_g$ in 3D. Although the effect shown in Fig. 6.10 largely prevents a proper scaling analysis of our data using ordinary disorder averages we find good agreement with the assumption that the WH result $\nu = 2/a = 1.037$ holds for the disordered system Eq. (6.28).

Chapter 7

Conclusions

The majority of the work presented in this thesis was concerned with the effects imposed by correlated defects on second order phase transitions with well known properties in the disorder-free case by means of numerical simulation. A central question was if and potentially how the universality class and thereby the critical exponents are changed by the presence of disorder. In some cases also what qualitative implications this has on the experimentally measurable quantities.

The defected supersolid scenario of paper I, where simple 3D XY models are exposed to one and two dimensional randomly intersecting defects, suggests that given the same knowledge there was at the height of the supersolid dilemma around 2009, there was in principle no a priori reason to expect a possible supersolid transition to show the same λ-like signature as liquid ^{4}He. The onset of superflow carried on interconnected correlated defect networks can in contrast be expected to show smoothened onset features. As today the existence of a supersolid phase in ^{4}He seems to be ruled out for temperatures above the 1mK range. Possible future work, building on the scenario presented, could aim at investigating whether or not the heat capacity maximum observed around 100 mK can be explained in an interconnected defect network without the need to invoke a phase transition. This potentially can be done by PIMC simulations of ^{4}He confined to tube like dimensional geometries or actual dislocations as done by Boninsegni and coworkers [133]. Even simpler methods such as one dimensional Ginzburg-Landau theories that are known to exhibit a heat capacity maximum [180, 181] could serve as effective models.

Dirty bosons have been a central problem to localization physics in the last 20 years. The finite-size scaling analysis performed in paper II for the 2+1 dimensional dirty boson model showed, without any a priori assumption on the dynamic critical exponent z, that our data is best described by $z \approx 1.8 \pm 0.05$ [2]. To achieve this we defined a new finite-size scaling quantity expected to display a universal maximum at the quantum critical point. Our result is in accordance with recent theoretical work by Weichman et. al. [156] predicting that, at finite chemical potential, the

compressibility can arise out of the analytic contribution to the free energy alone. As of today the exact value of z is still debated. Recent work found $z = 1.85 \pm 0.15$ [182] using a quantum Monte Carlo algorithm [183]. Other groups found $z = 1.88 \pm 0.08$ for hard core bosons, but disagree for the soft core case where $z = 1.99 \pm 0.05$ was reported, very close to the original, theoretically predicted value $z = d = 2$ [184, 153]. This discrepancy shows that this problem is very hard to tackle numerically. As illustrated in Sec. 6.2 the recently presented value $z \approx 1.4$ [159] probably can be ruled out by scaling arguments as the extrapolation to the infinite correlation volume limit was done using isotropic space-time volumes.

The results from paper III suggest that the fluctuation-driven superconducting phase transition in type-1.5 superconductors, where vortices interact nonmonotonically, can be first order. This result is nontrivial as it cannot appear in ordinary single band type-II superconductors with stable vortex excitations. As our simulations were limited to an effective, phenomenologically motivated composite vortex loop description of 3D type-1.5 superconductors we cannot answer the question if the transition *generically* is discontinuous. This will require and motivates future studies of two-band Ginzburg-Landau models including amplitude fluctuations.

The papers IV, V considered phase transitions in more complex defect networks than obtained from random straight lines or planar defects studied in paper I. The interesting feature we exploited was that extended, correlated defect structures can be expected to result from critical configurations of $O(N)$ spin models in various representations. Naturally the anomalous scaling dimension η can be seen as the exponent characterizing the power-law decay of the critical order parameter correlations. Therefore one might expect that it also describes other equilibrium correlations between the degrees of freedom in the loop models or clusters. Whereas this trivially holds true for critical cluster disorder we showed that it certainly is not the case for the disorder generated via the Ising loop model and the XY loop model in link current representation. Instead the bond variable correlations for large separations decay $\sim r^{-a}$ with an exponent $a = -\alpha_{\text{loop}}/\nu_{\text{loop}} + d$ which is given in terms of the known loop-model critical exponents α_{loop} and ν_{loop} and the spatial dimensionality alone. Generally the disorder correlations arising from the loop configurations, even if quenched from criticality, decay much faster than random straight line correlations considered in paper I. For the XY link-currents $\alpha_{\text{loop}} \leq 0$ and one therefore expects in all dimensions that the resulting critical loop disorder fixed point stability criterion is ultimately described by the standard Harris criterion. Interestingly, the same probably holds true if one would have used a vortex representation for 3D type-II superconductors. There the interaction between vortices is exponentially screened. It is then still plausible to assume that the number of segments in each configuration scales similarly to the energy. The long-range correlations then should decay with the same exponent a as obtained for the link current model in paper IV. A case that lies outside this treatment is the neutral superfluid or extreme type-II case $\lambda \to \infty$ which is much harder to study numerically due to the long-range, unscreened Coulomb interactions.

In paper V, where the disordered, ferromagnetic bond couplings are directly

obtained from fully connected Ising spin clusters, the disorder correlations obey the power-law decay $\sim r^{-a} = r^{-d+2-\eta}$ for large r. Although we are able to show that the critical cluster disorder is a relevant perturbation to the 3DXY phase transition, an accurate estimate of the correlation length critical exponent could not be obtained due to the broad double peak distribution found in the average couplings for the system sizes we studied. Nevertheless we found that the data for large system sizes together with the sample to sample fluctuations can be well described under the assumption that the critical exponent ν as in papers I and IV is given by the Weinrib-Halperin theory $\nu = 2/a$. We find similar signatures such as a broad plateau in the order parameter susceptibility as recently found in 2D Potts models with related disorder distributions [178]. There they were interpreted as a Griffiths phase in the disordered system. In our case these signatures are likely to be artifacts of the disorder averaging procedure used in our simulations and should vanish in the thermodynamic limit. For models with such broad disorder distributions it could prove advantageous to perform large parallel simulations over single disorder realizations and extract thermodynamic signatures by different methods as suggested in [185].

Bibliography

[1] H. Meier, M. Wallin, and S. Teitel, "Superfluid transition in a correlated defect network," *Phys. Rev. B*, vol. 87, p. 214520, Jun 2013.

[2] H. Meier and M. Wallin, "Quantum critical dynamics simulation of dirty boson systems," *Phys. Rev. Lett.*, vol. 108, p. 055701, Jan 2012.

[3] H. Meier, E. Babaev, and M. Wallin, "Fluctuation-induced first-order phase transitions in type-1.5 superconductors in zero external field," *accepted in Phys. Rev. B*, 2015.

[4] H. Meier and M. Wallin, "Phase transitions with critical loop disorder," *Manuscript*, 2015.

[5] H. Meier and M. Wallin, "Phase transitions in systems with critical cluster defects," *Manuscript*, 2015.

[6] "How many stars are there in the universe." `http://www.esa.int/Our_Activities/Space_Science/Herschel/How_many_stars_are_there_in_the_Universe`.

[7] K. G. Wilson, "Renormalization group and critical phenomena. I. renormalization group and the kadanoff scaling picture," *Phys. Rev. B*, vol. 4, pp. 3174–3183, Nov 1971.

[8] D. Beysens, J. Straub, and D. Turner, "Phase transitions and near-critical phenomena," in *Fluid Sciences and Materials Science in Space* (H. Walter, ed.), pp. 221–256, Springer Berlin Heidelberg, 1987.

[9] S. Ma, *Modern Theory of Critical Phenomena*. Advanced book classics, Perseus, 2000.

[10] A. Pelissetto and E. Vicari, "Critical phenomena and renormalization-group theory," *Physics Reports*, vol. 368, no. 6, pp. 549 – 727, 2002.

[11] L. Landau and E. Lifshitz, *Statistical Physics*. No. v. 5, Elsevier Science, 1996.

[12] V. L. Berezinskiĭ, "Destruction of Long-range Order in One-dimensional and Two-dimensional Systems having a Continuous Symmetry Group I. Classical Systems," *Soviet Journal of Experimental and Theoretical Physics*, vol. 32, p. 493, 1971.

[13] J. M. Kosterlitz and D. J. Thouless, "Ordering, metastability and phase transitions in two-dimensional systems," *Journal of Physics C: Solid State Physics*, vol. 6, no. 7, p. 1181, 1973.

[14] B. I. Halperin, T. C. Lubensky, and S.-K. Ma, "First-order phase transitions in superconductors and smectic-*a* liquid crystals," *Phys. Rev. Lett.*, vol. 32, pp. 292–295, Feb 1974.

[15] E. Brézin, "An investigation of finite size scaling," *Journal de Physique*, Jan 1982.

[16] J. L. Jones and A. P. Young, "Finite-size scaling of the correlation length above the upper critical dimension in the five-dimensional ising model," *Phys. Rev. B*, vol. 71, p. 174438, May 2005.

[17] N. Goldenfeld, *Lectures on Phase Transitions and the Renormalization Group*. Addison-Wesley Publishing Company, 1992.

[18] K. G. Wilson and M. E. Fisher, "Critical exponents in 3.99 dimensions," *Phys. Rev. Lett.*, vol. 28, pp. 240–243, Jan 1972.

[19] K. G. Wilson and J. Kogut, "The renormalization group and the ϵ expansion," *Physics Reports*, vol. 12, no. 2, pp. 75 – 199, 1974.

[20] J. Cardy, *Scaling and Renormalization in Statistical Physics*. Cambridge university press, 1996.

[21] M. Hasenbusch, A. Pelissetto, and E. Vicari, "The critical behavior of 3d ising spin glass models: universality and scaling corrections," *Journal of Statistical Mechanics: Theory and Experiment*, vol. 2008, no. 02, p. L02001, 2008.

[22] K. Binder and E. Luijten, "Monte carlo tests of renormalization-group predictions for critical phenomena in ising models," *Physics Reports*, vol. 344, no. 4–6, pp. 179 – 253, 2001. Renormalization group theory in the new millennium.

[23] B. Berche, R. Kenna, and J.-C. Walter, "Hyperscaling above the upper critical dimension," *Nuclear Physics B*, vol. 865, no. 1, pp. 115 – 132, 2012.

[24] R. Kenna and C. Lang, "Finite size scaling and the zeroes of the partition function in the ϕ^4 model," *Physics Letters B*, vol. 264, no. 3–4, pp. 396 – 400, 1991.

[25] R. P. Feynman and A. R. Hibbs, *Quantum Mechanics and Path Integrals.* McGraw-Hill, 1965.

[26] D. M. Ceperley, "Path integrals in the theory of condensed helium," *Rev. Mod. Phys.*, vol. 67, pp. 279–355, Apr 1995.

[27] I. Herbut, *A Modern Approach to Critical Phenomena.* Cambridge University Press, 2007.

[28] P. Weichman and R. Mukhopadhyay, "Particle-hole symmetry and the dirty boson problem," *Physical Review B*, Jan 2008.

[29] M. Vojta, "Quantum phase transitions," *Reports on Progress in Physics*, vol. 66, no. 12, p. 2069, 2003.

[30] A. Vestergren, J. Lidmar, and M. Wallin, "Generalized anisotropic scaling theory and the transverse meissner transition," *Phys. Rev. Lett.*, vol. 94, p. 087002, Mar 2005.

[31] M. Wallin, E. S. Sørensen, S. M. Girvin, and A. P. Young, "Superconductor-insulator transition in two-dimensional dirty boson systems," *Phys. Rev. B*, vol. 49, pp. 12115–12139, May 1994.

[32] E. Ising, "Beitrag zur theorie des ferromagnetismus," *Zeitschrift für Physik*, vol. 31, no. 1, pp. 253–258, 1925.

[33] H. G. Ballesteros, L. A. Fernández, V. Martín-Mayor, and A. Muñoz Sudupe, "Finite size effects on measures of critical exponents in d = 3 o(n) models," *Physics Letters B*, vol. 387, no. 1, pp. 125 – 131, 1996.

[34] X. Hu, "Bicritical and tetracritical phenomena and scaling properties of the so(5) theory," *Phys. Rev. Lett.*, vol. 87, p. 057004, Jul 2001.

[35] M. Hasenbusch, A. Pelissetto, and E. Vicari, "Instability of o(5) multicritical behavior in so(5) theory of high-T_c superconductors," *Phys. Rev. B*, vol. 72, p. 014532, Jul 2005.

[36] T. H. Berlin and M. Kac, "The spherical model of a ferromagnet," *Phys. Rev.*, vol. 86, pp. 821–835, Jun 1952.

[37] R. Baxter, *Exactly Solved Models in Statistical Mechanics.* Academic Press, 1982.

[38] R. Peierls, "On ising's model of ferromagnetism," *Mathematical Proceedings of the Cambridge Philosophical Society*, vol. 32, pp. 477–481, 10 1936.

[39] R. B. Griffiths, "Peierls proof of spontaneous magnetization in a two-dimensional ising ferromagnet," *Phys. Rev.*, vol. 136, pp. A437–A439, Oct 1964.

[40] L. Onsager, "Crystal statistics. I. a two-dimensional model with an order-disorder transition," *Phys. Rev.*, vol. 65, pp. 117–149, Feb 1944.

[41] N. D. Mermin and H. Wagner, "Absence of ferromagnetism or antiferromagnetism in one- or two-dimensional isotropic heisenberg models," *Phys. Rev. Lett.*, vol. 17, pp. 1133–1136, Nov 1966.

[42] P. C. Hohenberg, "Existence of long-range order in one and two dimensions," *Phys. Rev.*, vol. 158, pp. 383–386, Jun 1967.

[43] S. Coleman, "There are no goldstone bosons in two dimensions," *Communications in Mathematical Physics*, vol. 31, no. 4, pp. 259–264, 1973.

[44] P. Chaikin and T. Lubensky, *Principles of condensed matter physics*. Cambridge university press, 1995.

[45] D. R. Nelson and V. M. Vinokur, "Boson localization and pinning by correlated disorder in high-temperature superconductors," *Phys. Rev. Lett.*, vol. 68, pp. 2398–2401, Apr 1992.

[46] A. Harris, "Effect of random defects on the critical behaviour of ising models," *Journal of Physics C: Solid State Physics*, Jan 1974.

[47] J. T. Chayes, L. Chayes, D. S. Fisher, and T. Spencer, "Finite-size scaling and correlation lengths for disordered systems," *Phys. Rev. Lett.*, vol. 57, pp. 2999–3002, Dec 1986.

[48] A. Weinrib and B. I. Halperin, "Critical phenomena in systems with long-range-correlated quenched disorder," *Phys. Rev. B*, vol. 27, pp. 413–427, Jan 1983.

[49] P. Peczak and D. P. Landau, "Monte carlo study of finite-size effects at a weakly first-order phase transition," *Phys. Rev. B*, vol. 39, pp. 11932–11942, Jun 1989.

[50] J. Lee and J. M. Kosterlitz, "New numerical method to study phase transitions," *Phys. Rev. Lett.*, vol. 65, pp. 137–140, Jul 1990.

[51] M. S. S. Challa, D. P. Landau, and K. Binder, "Finite-size effects at temperature-driven first-order transitions," *Phys. Rev. B*, vol. 34, pp. 1841–1852, Aug 1986.

[52] J. Lee and J. M. Kosterlitz, "Finite-size scaling and monte carlo simulations of first-order phase transitions," *Phys. Rev. B*, vol. 43, pp. 3265–3277, Feb 1991.

[53] A. M. Ferrenberg and R. H. Swendsen, "New monte carlo technique for studying phase transitions," *Phys. Rev. Lett.*, vol. 61, pp. 2635–2638, Dec 1988.

[54] A. M. Ferrenberg and R. H. Swendsen, "Optimized monte carlo data analysis," *Phys. Rev. Lett.*, vol. 63, pp. 1195–1198, Sep 1989.

[55] K. Hukushima and K. Nemoto, "Exchange monte carlo method and application to spin glass simulations," *Journal of the Physical Society of Japan*, vol. 65, no. 6, pp. 1604–1608, 1996.

[56] F. Wang and D. P. Landau, "Efficient, multiple-range random walk algorithm to calculate the density of states," *Phys. Rev. Lett.*, vol. 86, pp. 2050–2053, Mar 2001.

[57] T. Vogel, Y. W. Li, T. Wüst, and D. P. Landau, "Generic, hierarchical framework for massively parallel wang-landau sampling," *Phys. Rev. Lett.*, vol. 110, p. 210603, May 2013.

[58] K. Binder and D. P. Landau, "Finite-size scaling at first-order phase transitions," *Phys. Rev. B*, vol. 30, pp. 1477–1485, Aug 1984.

[59] M. E. Fisher and A. N. Berker, "Scaling for first-order phase transitions in thermodynamic and finite systems," *Phys. Rev. B*, vol. 26, pp. 2507–2513, Sep 1982.

[60] H. K. Onnes, "The resistance of pure mercury at helium temperatures," *Commun. Phys. Lab. Univ. Leiden*, vol. 12, pp. 120+, 1911.

[61] D. V. Delft and P. Kes, "The discovery of superconductivity," *Physics Today*, Jan 2010.

[62] W. Meissner and R. Ochsenfeld, "Ein neuer effekt bei eintritt der supraleitfähigkeit," *Naturwissenschaften*, vol. 21, no. 44, pp. 787–788, 1933.

[63] P. Kapitza, "Viscosity of liquid helium below the λ-point," *Nature*, vol. 141, no. 3558, p. 74, 1938.

[64] J. Allen and A. Misener, "Flow of liquid helium II," *Nature*, vol. 141, no. 3558, p. 75, 1938.

[65] V. Ginzburg and L. Landau, "On the theory of superconductivity," *Zh. Eksp. Teor. Fiz.*, vol. 20, pp. 1064–1082, 1950.

[66] F. London, "The λ-phenomenon of liquid helium and the bose-einstein degeneracy," *Nature*, vol. 141, no. 3571, pp. 643–644, 1938.

[67] Bose, "Plancks gesetz und lichtquantenhypothese," *Zeitschrift für Physik*, vol. 26, no. 1, pp. 178–181, 1924.

[68] M. Planck, "Ueber das gesetz der energieverteilung im normalspectrum," *Annalen der Physik*, vol. 309, no. 3, pp. 553–563, 1901.

[69] A. Einstein, "Quantentheorie des einatomigen idealen gases." Sitzungsberichte der Preussischen Akademie der Wissenschaften 1: 3., 1925.

[70] T. N. Foundation, "The nobel prize in physics 2001." `http://www.nobelprize.org/nobel_prizes/physics/laureates/2001/`.

[71] M. H. Anderson, J. R. Ensher, M. R. Matthews, C. E. Wieman, and E. A. Cornell, "Observation of bose-einstein condensation in a dilute atomic vapor," *Science*, vol. 269, no. 5221, pp. 198–201, 1995.

[72] K. B. Davis, M. O. Mewes, M. R. Andrews, N. J. van Druten, D. S. Durfee, D. M. Kurn, and W. Ketterle, "Bose-einstein condensation in a gas of sodium atoms," *Phys. Rev. Lett.*, vol. 75, pp. 3969–3973, Nov 1995.

[73] O. Penrose and L. Onsager, "Bose-einstein condensation and liquid helium," *Phys. Rev.*, vol. 104, no. 3, pp. 576–584, 1956.

[74] A. Leggett, *Quantum liquids*. Oxford Graduate Texts, 2006.

[75] C. N. Yang, "Concept of off-diagonal long-range order and the quantum phases of liquid He and of superconductors," *Rev. Mod. Phys.*, vol. 34, pp. 694–704, Oct 1962.

[76] D. D. Osheroff, R. C. Richardson, and D. M. Lee, "Evidence for a new phase of solid he^3," *Phys. Rev. Lett.*, vol. 28, pp. 885–888, Apr 1972.

[77] D. D. Osheroff, W. J. Gully, R. C. Richardson, and D. M. Lee, "New magnetic phenomena in liquid he^3 below 3 mk," *Phys. Rev. Lett.*, vol. 29, pp. 920–923, Oct 1972.

[78] A. J. Leggett, "Interpretation of recent results on he^3 below 3 mk: A new liquid phase?," *Phys. Rev. Lett.*, vol. 29, pp. 1227–1230, Oct 1972.

[79] R. A. Aziz, V. P. S. Nain, J. S. Carley, W. L. Taylor, and G. T. McConville, "An accurate intermolecular potential for helium," *The Journal of Chemical Physics*, vol. 70, no. 9, pp. 4330–4342, 1979.

[80] M. Boninsegni, N. Prokof'ev, and B. Svistunov, "Worm algorithm for continuous-space path integral monte carlo simulations," *Physical review letters*, Jan 2006.

[81] H. Rieger, "The twisted paths of bosons," *Physics*, vol. 5, p. 75, Jul 2012.

[82] M. Boninsegni, L. Pollet, N. Prokof'ev, and B. Svistunov, "Role of bose statistics in crystallization and quantum jamming," *Phys. Rev. Lett.*, vol. 109, p. 025302, Jul 2012.

[83] E. L. Andronikashvili *J. Phys. USSR*, vol. 10, p. 201, 1946.

[84] G. B. Hess and W. M. Fairbank, "Measurements of angular momentum in superfluid helium," *Phys. Rev. Lett.*, vol. 19, pp. 216–218, Jul 1967.

[85] D. G. Henshaw and A. D. B. Woods, "Modes of atomic motions in liquid helium by inelastic scattering of neutrons," *Phys. Rev.*, vol. 121, no. 5, pp. 1266–1274, 1961.

[86] R. Feynman, *Progress in Low Temperature Physics*. No. v. 1, North Holland, 1955.

[87] J. A. Lipa, J. A. Nissen, D. A. Stricker, D. R. Swanson, and T. C. P. Chui, "Specific heat of liquid helium in zero gravity very near the lambda point," *Phys. Rev. B*, vol. 68, p. 174518, Nov 2003.

[88] F. London and H. London, "The electromagnetic equations of the supraconductor," *Proceedings of the Royal Society of London. Series A, Mathematical and Physical Sciences*, vol. 149, no. 866, pp. pp. 71–88, 1935.

[89] G. L. deHaas Lorentz *Lorentz Jubileenumber of Physica*, vol. 5, p. 384, 1925.

[90] J. Bardeen, L. N. Cooper, and J. R. Schrieffer, "Theory of superconductivity," *Phys. Rev.*, vol. 108, pp. 1175–1204, Dec 1957.

[91] L. Gor'kov, "Microscopic derivation of the ginzburg-landau equations in the theory of superconductivity," *Zh. Eksp. Teor. Fiz.*, vol. 36, pp. 1918–1923, 1959.

[92] A. Abrikosov *Zh. Eksp. i Teor. Fiz.*, vol. 32, p. 1442, 1957.

[93] C. Dasgupta and B. I. Halperin, "Phase transition in a lattice model of superconductivity," *Phys. Rev. Lett.*, vol. 47, pp. 1556–1560, Nov 1981.

[94] M. E. Peskin, "Mandelstam-'t hooft duality in abelian lattice models," *Annals of Physics*, vol. 113, no. 1, pp. 122 – 152, 1978.

[95] P. R. Thomas and M. Stone, "Nature of the phase transition in a non-linear o(2)3 model," *Nuclear Physics B*, vol. 144, no. 2–3, pp. 513 – 524, 1978.

[96] S. Mo, J. Hove, and A. Sudbø, "Order of the metal-to-superconductor transition," *Phys. Rev. B*, vol. 65, p. 104501, Jan 2002.

[97] J. Hove, S. Mo, and A. Sudbø, "Vortex interactions and thermally induced crossover from type-I to type-II superconductivity," *Phys. Rev. B*, vol. 66, p. 064524, Aug 2002.

[98] H. Kleinert, "Disorder version of the abelian higgs model and the order of the superconductive phase transition," *Lettere Al Nuovo Cimento Series 2*, vol. 35, no. 13, pp. 405–412, 1982.

[99] J. Bednorz and K. Müller, "Possible high-Tc superconductivity in the ba-la-cu-o system," *Zeitschrift für Physik B Condensed Matter*, vol. 64, no. 2, pp. 189–193, 1986.

[100] A. Schilling, M. Cantoni, J. D. Guo, and H. R. Ott, "Superconductivity above 130 k in the hg-ba-ca-cu-o system," *Nature*, vol. 363, pp. 56–58, 1993.

[101] H. Suhl, B. T. Matthias, and L. R. Walker, "Bardeen-cooper-schrieffer theory of superconductivity in the case of overlapping bands," *Phys. Rev. Lett.*, vol. 3, pp. 552–554, Dec 1959.

[102] T. Yildirim, O. Gülseren, J. W. Lynn, C. M. Brown, T. J. Udovic, Q. Huang, N. Rogado, K. A. Regan, M. A. Hayward, J. S. Slusky, T. He, M. K. Haas, P. Khalifah, K. Inumaru, and R. J. Cava, "Giant anharmonicity and nonlinear electron-phonon coupling in mgb_2: A combined first-principles calculation and neutron scattering study," *Phys. Rev. Lett.*, vol. 87, p. 037001, Jun 2001.

[103] A. Y. Liu, I. I. Mazin, and J. Kortus, "Beyond eliashberg superconductivity in mgb_2: Anharmonicity, two-phonon scattering, and multiple gaps," *Phys. Rev. Lett.*, vol. 87, p. 087005, Aug 2001.

[104] S. Souma, Y. Machida, T. Sato, T. Takahashi, H. Matsui, S.-C. Wang, H. Ding, A. Kaminski, J. C. Campuzano, S. Sasaki, and K. Kadowaki, "The origin of multiple superconducting gaps in mgb2," *Nature*, vol. 423, pp. 65–67, 2003.

[105] M. Silaev and E. Babaev, "Microscopic theory of type-1.5 superconductivity in multiband systems," *Phys. Rev. B*, vol. 84, p. 094515, Sep 2011.

[106] P. B. Jones, "Type-I and two-gap superconductivity in neutron star magnetism," *Monthly Notices of the Royal Astronomical Society*, vol. 371, no. 3, pp. 1327–1333, 2006.

[107] E. Babaev, A. Sudbo, and N. W. Ashcroft, "A superconductor to superfluid phase transition in liquid metallic hydrogen," *Nature*, vol. 431, pp. 666–668, 10 2004.

[108] M. I. Eremets and I. A. Troyan, "Conductive dense hydrogen," *Nat Mater*, vol. 10, pp. 927–931, Dec 2011.

[109] E. Babaev, "Vortices with fractional flux in two-gap superconductors and in extended faddeev model," *Phys. Rev. Lett.*, vol. 89, p. 067001, Jul 2002.

[110] J. Carlström, E. Babaev, and M. Speight, "Type-1.5 superconductivity in multiband systems: Effects of interband couplings," *Phys. Rev. B*, vol. 83, p. 174509, May 2011.

[111] J. M. Speight, "Static intervortex forces," *Phys. Rev. D*, vol. 55, pp. 3830–3835, Mar 1997.

[112] V. Moshchalkov, M. Menghini, T. Nishio, Q. H. Chen, A. V. Silhanek, V. H. Dao, L. F. Chibotaru, N. D. Zhigadlo, and J. Karpinski, "Type-1.5 superconductivity," *Phys. Rev. Lett.*, vol. 102, p. 117001, Mar 2009.

[113] S. J. Ray, A. S. Gibbs, S. J. Bending, P. J. Curran, E. Babaev, C. Baines, A. P. Mackenzie, and S. L. Lee, "Muon-spin rotation measurements of the vortex state in sr_2Ruo_4: Type-1.5 superconductivity, vortex clustering, and a crossover from a triangular to a square vortex lattice," *Phys. Rev. B*, vol. 89, p. 094504, Mar 2014.

[114] L. J. Li, T. Nishio, Z. A. Xu, and V. V. Moshchalkov, "Low-field vortex patterns in the multiband $bafe_{2-x}ni_xas_2$ superconductor (x = 0.1, 0.16)," *Phys. Rev. B*, vol. 83, p. 224522, Jun 2011.

[115] J. Gutierrez, B. Raes, A. V. Silhanek, L. J. Li, N. D. Zhigadlo, J. Karpinski, J. Tempere, and V. V. Moshchalkov, "Scanning hall probe microscopy of unconventional vortex patterns in the two-gap mgb_2 superconductor," *Phys. Rev. B*, vol. 85, p. 094511, Mar 2012.

[116] T. Nishio, V. H. Dao, Q. Chen, L. F. Chibotaru, K. Kadowaki, and V. V. Moshchalkov, "Scanning squid microscopy of vortex clusters in multiband superconductors," *Phys. Rev. B*, vol. 81, p. 020506, Jan 2010.

[117] C. W. Hicks, J. R. Kirtley, T. M. Lippman, N. C. Koshnick, M. E. Huber, Y. Maeno, W. M. Yuhasz, M. B. Maple, and K. A. Moler, "Limits on superconductivity-related magnetization in sr_2ruo_4 and $pros_4sb_{12}$ from scanning squid microscopy," *Phys. Rev. B*, vol. 81, p. 214501, Jun 2010.

[118] A. J. Leggett, "Can a solid be "superfluid"?," *Phys. Rev. Lett.*, vol. 25, pp. 1543–1546, Nov 1970.

[119] S. Balibar and F. Caupin, "Supersolidity and disorder," *Journal of Physics: Condensed Matter*, vol. 20, no. 17, p. 173201 (19pp), 2008.

[120] D. E. Galli and L. Reatto, "Solid ^{4}he and the supersolid phase: from theoretical speculation to the discovery of a new state of matter? —a review of the past and present status of research—," *Journal of the Physical Society of Japan*, vol. 77, no. 11, p. 111010, 2008.

[121] E.Kim and M. H. W. Chan, "Probable Observation of a Supersolid Helium Phase," *Nature*, vol. 427, 2004.

[122] E. Kim and M. H. W. Chan, "Observation of superflow in solid helium," *Science*, vol. 305, no. 5692, pp. 1941–1944, 2004.

[123] X.Lin, M. Chan, and C. A.C., "Probable heat capacity signature of the supersolid transition," *Nature*, vol. 449, pp. 1025–1028, 2007.

[124] X. Lin, A. C. Clark, Z. G. Cheng, and M. H. W. Chan, "Heat capacity peak in solid ^{4}He: Effects of disorder and ^{3}He impurities," *Phys. Rev. Lett.*, vol. 102, p. 125302, Mar 2009.

[125] X. Lin, A. C. Clark, Z. G. Cheng, and M. H. W. Chan, "Erratum: Heat capacity peak in solid ^{4}He: Effects of disorder and ^{3}He impurities [phys. rev. lett. 102, 125302 (2009)]," *Phys. Rev. Lett.*, vol. 103, p. 259903, Dec 2009.

[126] B. K. Clark and D. M. Ceperley, "Off-diagonal long-range order in solid ^{4}He," *Physical Review Letters*, vol. 96, no. 10, p. 105302, 2006.

[127] M. Boninsegni, N. Prokof'ev, and B. Svistunov, "Superglass phase of ^{4}He," *Phys. Rev. Lett.*, vol. 96, p. 105301, Mar 2006.

[128] A. S. C. Rittner and J. D. Reppy, "Observation of classical rotational inertia and nonclassical supersolid signals in solid ^{4}He below 250 mk," *Physical Review Letters*, vol. 97, no. 16, p. 165301, 2006.

[129] A. S. C. Rittner and J. D. Reppy, "Disorder and the supersolid state of solid ^{4}He," *Physical Review Letters*, vol. 98, p. 175302, 2007.

[130] A. C. Clark, J. T. West, and M. W. Chan, "Nonclassical rotational inertia in helium crystals," *Physical Review Letters*, vol. 99, no. 13, p. 135302, 2007.

[131] S. Sasaki, R. Ishiguro, F. Caupin, H. J. Maris, and S. Balibar, "Superfluidity of grain boundaries and supersolid behavior," *Science*, vol. 313, no. 5790, pp. 1098–1100, 2006.

[132] L. Pollet, M. Boninsegni, A. B. Kuklov, N. V. Prokof'ev, B. V. Svistunov, and M. Troyer, "Superfluidity of grain boundaries in solid," *Phys. Rev. Lett.*, vol. 98, p. 135301, Mar 2007.

[133] M. Boninsegni, A. B. Kuklov, L. Pollet, N. V. Prokof'ev, B. V. Svistunov, and M. Troyer, "Luttinger liquid in the core of a screw dislocation in helium-4," *Phys. Rev. Lett.*, vol. 99, p. 035301, Jul 2007.

[134] J. D. Reppy, "Nonsuperfluid origin of the nonclassical rotational inertia in a bulk sample of solid ^{4}He," *Phys. Rev. Lett.*, vol. 104, p. 255301, Jun 2010.

[135] P. Corboz, L. Pollet, N. V. Prokof'ev, and M. Troyer, "Binding of a ^{3}He impurity to a screw dislocation in solid ^{4}He," *Phys. Rev. Lett.*, vol. 101, p. 155302, Oct 2008.

[136] J. Day and J. Beamish, " Low-temperature shear modulus changes in solid ^{4}He and connection to supersolidity," *Nature*, vol. 450, 2007.

[137] D. Y. Kim and M. H. W. Chan, "Absence of supersolidity in solid helium in porous vycor glass," *Phys. Rev. Lett.*, vol. 109, p. 155301, Oct 2012.

[138] X. Mi and J. Reppy, "In pursuit of the elusive supersolid," *Journal of Low Temperature Physics*, pp. 1–9, 2013.

[139] X. Mi, A. Eyal, A. V. Talanov, and J. D. Reppy, "Evidence for supersolidity in bulk solid ^{4}He," 2014.

[140] A. K. Nguyen and A. Sudbø, "Topological phase fluctuations, amplitude fluctuations, and criticality in extreme type-II superconductors," *Phys. Rev. B*, vol. 60, pp. 15307–15331, Dec 1999.

[141] S. Elitzur, "Impossibility of spontaneously breaking local symmetries," *Phys. Rev. D*, vol. 12, pp. 3978–3982, Dec 1975.

[142] M. E. Fisher, M. N. Barber, and D. Jasnow, "Helicity modulus, superfluidity, and scaling in isotropic systems," *Phys. Rev. A*, vol. 8, pp. 1111–1124, Aug 1973.

[143] T. Chen and S. Teitel, "Helicity modulus and fluctuating type-II superconductors: Elastic approximation and numerical simulations," *Phys. Rev. B*, vol. 55, pp. 15197–15222, Jun 1997.

[144] B. Kaufman, "Crystal statistics. II. partition function evaluated by spinor analysis," *Phys. Rev.*, vol. 76, pp. 1232–1243, Oct 1949.

[145] B. van der Waerden, "Die lange reichweite der regelmäßigen atomanordnung in mischkristallen," *Zeitschrift für Physik*, vol. 118, no. 7-8, pp. 473–488, 1941.

[146] M. Kac and J. C. Ward, "A combinatorial solution of the two-dimensional ising model," *Phys. Rev.*, vol. 88, pp. 1332–1337, Dec 1952.

[147] N. Prokof'ev and B. Svistunov, "Bold diagrammatic monte carlo technique: When the sign problem is welcome," *Phys. Rev. Lett.*, vol. 99, p. 250201, Dec 2007.

[148] K. V. Houcke, F. Werner, E. Kozik, and N. Prokof'ev. . . , "Feynman diagrams versus fermi-gas feynman emulator," *Nature Physics*, Jan 2012.

[149] Y. Deng, E. Kozik, N. Prokof'ev, and B. Svistunov, "Emergent bcs regime of the two-dimensional fermionic hubbard model: ground-state phase diagram," *arXiv:1408.2088*, Jan 2014.

[150] J. Gukelberger, E. Kozik, L. Pollet, N. Prokof'ev, M. Sigrist, B. Svistunov, and M. Troyer, "p-wave superfluidity by spin-nematic fermi surface deformation," *Phys. Rev. Lett.*, vol. 113, p. 195301, Nov 2014.

[151] P. W. Anderson, "Absence of diffusion in certain random lattices," *Phys. Rev.*, vol. 109, pp. 1492–1505, Mar 1958.

[152] E. Abrahams, P. W. Anderson, D. C. Licciardello, and T. V. Ramakrishnan, "Scaling theory of localization: Absence of quantum diffusion in two dimensions," *Phys. Rev. Lett.*, vol. 42, pp. 673–676, Mar 1979.

[153] M. P. A. Fisher, P. B. Weichman, G. Grinstein, and D. S. Fisher, "Boson localization and the superfluid-insulator transition," *Phys. Rev. B*, vol. 40, pp. 546–570, Jul 1989.

[154] B. C. Crooker, B. Hebral, E. N. Smith, Y. Takano, and J. D. Reppy, "Superfluidity in a dilute bose gas," *Phys. Rev. Lett.*, vol. 51, pp. 666–669, Aug 1983.

[155] M. Greiner, O. Mandel, T. Esslinger, and T. Hänsch. . . , "Quantum phase transition from a superfluid to a mott insulator in a gas of ultracold atoms," *Nature*, Jan 2002.

[156] P. Weichman and R. Mukhopadhyay, "Critical dynamics of the dirty boson problem: Revisiting the equality z= d," *Physical review letters*, Jan 2007.

[157] L. Pollet, N. V. Prokof'ev, B. V. Svistunov, and M. Troyer, "Absence of a direct superfluid to mott insulator transition in disordered bose systems," *Phys. Rev. Lett.*, vol. 103, p. 140402, Sep 2009.

[158] F. Alet and E. S. Sørensen, "Cluster monte carlo algorithm for the quantum rotor model," *Phys. Rev. E*, vol. 67, p. 015701, Jan 2003.

[159] A. Priyadarshee, S. Chandrasekharan, J.-W. Lee, and H. Baranger, "Quantum phase transitions of hard-core bosons in background potentials," *Physical review letters*, vol. 97, p. 115703, Sep 2006.

[160] M. Newman and G. Barkema, *Monte Carlo Methods in Statistical Physics*. Oxford University Press, 1999.

[161] D. J. Earl and M. W. Deem, "Parallel tempering: Theory, applications, and new perspectives," *Phys. Chem. Chem. Phys.*, vol. 7, pp. 3910–3916, 2005.

[162] V. I. Manousiouthakis and M. W. Deem, "Strict detailed balance is unnecessary in monte carlo simulation," *The Journal of Chemical Physics*, vol. 110, no. 6, pp. 2753–2756, 1999.

[163] N. Metropolis, A. W. Rosenbluth, M. N. Rosenbluth, A. H. Teller, and E. Teller, "Equation of State Calculations by Fast Computing Machines," *Journal of Chemical Physics*, vol. 21, pp. 1087–1092, 1953.

[164] U. Wolff, "Collective Monte Carlo Updating for Spin Systems," *Phys. Rev. Lett.*, vol. 62, pp. 361–364, Jan 1989.

[165] P. W. Kasteleyn and C. M. Fortuin *J. Phys. Soc. Jpn. Suppl.*, vol. 26s, p. 11, 1969.

[166] C. M. Fortuin and P. W. Kasteleyn *Physica (Utrecht)*, vol. 57, p. 536, 1972.

[167] R. H. Swendsen and J.-S. Wang, "Nonuniversal critical dynamics in monte carlo simulations," *Phys. Rev. Lett.*, vol. 58, pp. 86–88, Jan 1987.

[168] P. D. Coddington and C. F. Baillie, "Empirical relations between static and dynamic exponents for ising model cluster algorithms," *Phys. Rev. Lett.*, vol. 68, pp. 962–965, Feb 1992.

[169] N. Prokof'ev and B. Svistunov, "Worm algorithms for classical statistical models," *Phys. Rev. Lett.*, vol. 87, p. 160601, Sep 2001.

[170] F. Wang and D. Landau, "Determining the density of states for classical statistical models: A random walk algorithm to produce a flat histogram," *Phys. Rev. E*, vol. 64, p. 056101, Oct 2001.

[171] C. Zhou, T. Schulthess, S. Torbrügge, and D. Landau, "Wang-landau algorithm for continuous models and joint density of states," *Phys. Rev. Lett.*, vol. 96, p. 120201, Mar 2006.

[172] R. E. Belardinelli and V. D. Pereyra, "Wang-landau algorithm: A theoretical analysis of the saturation of the error," *The Journal of Chemical Physics*, vol. 127, no. 18, pp. –, 2007.

[173] B. Berg, *Markov Chain Monte Carlo Simulations and Their Statistical Analysis*. World Scientific, 2004.

[174] D. Goswami, K. Dasbiswas, C.-D. Yoo, and A. T. Dorsey, "Dislocation-induced superfluidity in a model supersolid," *Phys. Rev. B*, vol. 84, p. 054523, Aug 2011.

[175] E. L. Pollock and D. M. Ceperley, "Path-integral computation of superfluid densities," *Phys. Rev. B*, vol. 36, pp. 8343–8352, Dec 1987.

[176] J. Smiseth, E. Smørgrav, F. S. Nogueira, J. Hove, and A. Sudbø, "Phase structure of (2+1)-dimensional compact lattice gauge theories and the transition from mott insulator to fractionalized insulator," *Phys. Rev. B*, vol. 67, p. 205104, May 2003.

[177] M. Hasenbusch, K. Pinn, and S. Vinti, "Critical exponents of the three-dimensional ising universality class from finite-size scaling with standard and improved actions," *Phys. Rev. B*, vol. 59, pp. 11471–11483, May 1999.

[178] C. Chatelain, "Griffiths phase and critical behavior of the two-dimensional potts models with long-range correlated disorder," *Phys. Rev. E*, vol. 89, p. 032105, Mar 2014.

[179] A. Aharony and A. B. Harris, "Absence of self-averaging and universal fluctuations in random systems near critical points," *Phys. Rev. Lett.*, vol. 77, pp. 3700–3703, Oct 1996.

[180] D. J. Scalapino, M. Sears, and R. A. Ferrell, "Statistical mechanics of one-dimensional ginzburg-landau fields," *Phys. Rev. B*, vol. 6, pp. 3409–3416, Nov 1972.

[181] R. H. McKenzie, "Ginzburg-landau theory of phase transitions in quasi-one-dimensional systems," *Phys. Rev. B*, vol. 51, pp. 6249–6260, Mar 1995.

[182] J. Zúñiga, D. Luitz, G. Lemarié, and N. Laflorencie, "Critical properties of the superfluid - bose glass transition in two dimensions," *Preprint arXiv:1412.5595*, Jan 2014.

[183] O. F. Syljuåsen and A. W. Sandvik, "Quantum monte carlo with directed loops," *Phys. Rev. E*, vol. 66, p. 046701, Oct 2002.

[184] R. Ng and E. Sorensen, "Quantum critical scaling of dirty bosons in two dimensions," *Preprint arXiv:1501.05981*, Jan 2015.

[185] S. Wiseman and E. Domany, "Finite-size scaling and lack of self-averaging in critical disordered systems," *Phys. Rev. Lett.*, vol. 81, p. 22, Jul 1998.

Part II

Scientific Papers